

# FOLIA VETERINARIA

PUBLISHED BY  
THE UNIVERSITY OF VETERINARY MEDICINE AND PHARMACY IN KOŠICE  
SLOVAKIA



Folia Veterinaria  
Vol. 61, 2017

VYDÁVA  
UNIVERZITA VETERINÁRSKEHO LEKÁRSTVA A FARMÁCIE V KOŠICIACH  
2017

# FOLIA VETERINARIA, 61, 4, 2017

## CONTENTS

IBE, C. S., SALAMI, S. O., WANMI, N.: BRAIN SIZE OF THE AFRICAN GRASSCUTTER ( <i>THRYONOMYS SWINDERIANUS</i> , TEMMINCK, 1827) AT DEFINED POSTNATAL PERIODS .....	5
FLEŠÁROVÁ, S., MAŽENSKÝ, D.: ANATOMICAL COMPARISON OF THE RENAL ARTERIES IN THE RABBIT AND EUROPEAN HARE .....	12
SOLHEIM T. N., TARABOVÁ L., FAIXOVÁ Z.: CHANGES IN TEMPERATURE OF THE EQUINE SKIN SURFACE UNDER BOOTS AFTER EXERCISE.....	17
MAŽENSKÝ, D., FLEŠÁROVÁ, S.: ANATOMICAL ARRANGEMENT OF THE SUBCLAVIAN ARTERY BRANCHES IN THE RABBIT AND EUROPEAN HARE .....	22
GRAJCIAROVÁ, M., HOLEČKOVÁ, B.: EVALUATION OF THE GENOTOXIC EFFECT OF THE COMMERCIAL FUNGICIDE TANGO® SUPER ON BOVINE LYMPHOCYTES .....	28
BÓNA, G., ŠIVIKOVÁ, K.: DETECTION OF MUTATIONS IN SELECTED PROTO-ONCOGENES OF CANINE LYMPHOMA .....	34
MRAVCOVÁ, K., FERKO, M., ŠTRKOLCOVÁ, G., GOLDOVÁ, M.: OPPORTUNISTIC PROTOZOAN INFECTIONS OF CARNIVORES .....	40
FIGUROVÁ, M., KULINOVÁ, V.: ULTRASONOGRAPHIC EXAMINATION OF SOME VESSELS IN DOGS AND THE CHARACTERISTICS OF BLOOD FLOW IN THESE VESSELS.....	44
STRAPÁČ, I., KURUC, M., BARANOVÁ, M.: DETERMINATION OF ANTIOXIDANT PARAMETERS OF PLEUROTUS MUSHROOMS GROWING ON DIFFERENT WOOD SUBSTRATES.....	53
ZIGO, F., VASIL, M., ELEČKO, J., FARKAŠOVÁ, Z., ZIGOVÁ, M.: OCCURENCE OF MASTITIS IN DAIRY COWS SITUATED IN MARGINAL PARTS OF SLOVAKIA.....	59



## BRAIN SIZE OF THE AFRICAN GRASSCUTTER (*Thryonomys swinderianus*, TEMMINCK, 1827) AT DEFINED POSTNATAL PERIODS

Ibe, C. S.<sup>1</sup>, Salami, S. O.<sup>2</sup>, Wanmi, N.<sup>3</sup>

<sup>1</sup>Department of Veterinary Anatomy, Michael Okpara University of Agriculture, Umudike

<sup>2</sup>University of Ilorin, Ilorin

<sup>3</sup>University of Agriculture, Markurdi  
Nigeria

writechikera@yahoo.com

### ABSTRACT

As a sequel to the current advancement in ethology, this study was designed to provide information on the brain size of the African grasscutter at specific postnatal periods and to extrapolate these findings to the behaviour of the rodent in its natural habitat. Brain samples were extracted from African grasscutter neonates on postnatal day 6, juveniles on postnatal day 72 and adults on postnatal day 450 by basic neuro-anatomical techniques. The weight, volume and dimensions of the brain samples were determined in absolute and relative terms. Their encephalisation quotient was also computed. There was a very strong positive correlation between nose-rump length and brain length in the neonates. The relative brain weight of neonates, juveniles and adults were  $3.84 \pm 0.12\%$ ,  $2.49 \pm 0.07\%$  and  $0.44 \pm 0.03\%$ , respectively. The differences were significant ( $P < 0.05$ ). The encephalisation quotient of juveniles was  $1.62 \pm 0.03$  while that of the adult was  $0.49 \pm 0.02$ . The difference was significant ( $P < 0.05$ ). The results were extrapolated to the animal's cognitive ability, and compared with other

rodents. It was concluded that the juvenile African grasscutter may have higher cognitive ability than the adult rodent, thus, juveniles should be preferred in physiological studies of memory and cognition.

**Key words:** African grasscutter; brain; cognition; Encephalisation Quotient

### INTRODUCTION

The qualification of intelligence in animals does not have a specific yard-stick. It can be explained as the extent to which an animal is able to acquire cues to solve complex problems posed by the environment including interspecies communication, threat detection and response. Simon ton [30] stated that intelligence is a set of cognitive capacities such as memory and retrieval or problem solving that enable an individual to adapt and thrive in any given environment. Deary [6] proposed that the environment and its interaction with genes play a vital role with regards to cognition. However, as environmental challenges vary

with animals of the same class, the measure of cognition may not be taxa-specific, but closely related to the animal's environment. In their review, Roth and Dicke [28] explained that cognition is not orthogenetic but has evolved independently in different classes of vertebrates, such that in each class, some animals are considered most intelligent. For example, parrots and owls are considered most intelligent in avian class [15] and primates in mammalian [16].

Brain size is a measure of its dimension, volume and weight. It varies with species, breed, sex and age. According to Sahin et al. [29], changes in brain size are due to changes in the number of neuronal and neuroglial cells in the brain, which is dependent on the extent or rate of neurogenesis. There is a fierce debate on the relationship between brain size and cognition. While some authors [18, 21] agree to a strong correlation between the two, others [8, 32] emphasize that the neuronal connectivity and internal complexity of the neuronal network defines cognition, and not just the size of the brain. The debatable brain markers for cognitive ability are the absolute or relative size of the brain, cortical gray matter thickness, encephalisation quotient and cortical neurone number [9, 18, 21, 28,]. However, encephalisation quotient and cortical neurone number are more reliable markers than absolute or relative brain size. Rieke [27] attributed encephalisation quotient as a rough estimate of the cognitive ability of an animal. Herculano-Houzel [9] observed that more encephalised rodents have larger number of neurones than expected for their body size, and proposed that the excess neurones may be responsible for the improved associative functions and cognitive advantage observed in them.

Encephalisation quotient is a useful measure which provides the information of how much bigger or smaller an animal's brain is, after the effect of body size has been corrected. Encephalisation quotient was developed for mammals, and may not yield relevant results when applied to non-mammals [20]. It is hypothesized to be a rough estimate of the intelligence of an animal [27], and varies among animals of even the same genus. No wonder Krubitzer et al. [14] reported that encephalisation quotient of tree squirrels is higher than that of ground squirrels and attributed it to the need for a higher cognitive ability for climbing.

The subject is a rodent of the sub-order *Hystricomorpha*. The family (*Thryomyidae*) is represented by a single genus, *Thryonomys*; and two species, *Thryonomys swin-*

*derianus*, known as the greater cane rat and *Thryonomys gregorianus*, known as the lesser cane rat [4]. The generic name *Thryonomys* was coined from the Greek word "thryon" which means reed and "mys" which means mouse. They are known to rapidly destroy reeds with their incisors [2]. Thus, the name cane rat, due to their destructive effects on sugar-cane plantations, and their preference for cane grass (*Eragrostis infecunda*). The rodent is found in virtually all African countries, including Nigeria [31]. They reside in grassland or in wooded savannah, along riverbanks [3]. They are rare in the arid Horn of Africa [23]. They are not common in rainforest, and do not inhabit dry shrub or desert [19]. Genetically, they are more closely related to the porcupine than to the house rat [19].

Over time, researchers have compared the cognitive ability of adult rodents of different species [5, 9, 10]; no attention is geared towards depicting the variation in the cognitive ability of rodents of same species, but of different ages. It may be a general notion that adult animals are more intelligent than juveniles and neonates, but, a recent neuro-anatomical study [22] has shown that juvenile animals may have higher cognitive potentials than their adult counterparts.

To determine the cognitive ability of different age groups of the African grasscutter, the brain sizes were determined and compared in the present study.

## MATERIALS AND METHODS

### Experimental Animals and Management

A total of 27 apparently healthy African grasscutters, comprising of 9 neonates of 6 days old, 9 juveniles of 72 days old and 9 adults of 450 days old were used for the study. They were purchased from a commercial grasscutter farm in Elele, Rivers state, Nigeria. The ages of the animals were confirmed from the farm records. There were transported by road in locally made wooden cages with adequate ventilation, and measuring 1.5 m × 1.5 m × 1.5 m, to the Veterinary Histology Laboratory of the Michael Okpara University of Agriculture, Umudike, Abia state, Nigeria, for the study. In the laboratory, there were transferred to standard laboratory animal cages and kept for a pre-experimental period of 1 month. They were fed twice daily, 8.00 a. m. and 6.00 p. m. They were fed with fresh guinea grass (*Panicum maximum*), fresh cane grass (*Eragrostis infecunda*) and

commercial rodent pelleted concentrates. Drinking water was provided ad libitum. The feeding troughs and drinkers were sterilized daily using Milton® (Laboratoire Riva-dis, Louzy, France; active ingredient: sodium hypochlorite 2% w/w). The cages were also swept and disinfected daily using Milton®, as well as a broad spectrum bactericidal, fungicidal and veridical agents.

The experimental protocol was approved by the Ethical Committee of Ahmadu Bello University, Zaria, Nigeria. The management of the experimental animals was as stipulated in the Guide for the Care and Use of Laboratory Animals, 8th Edition, National Research Council, USA (National Academic Press, Washington D.C.: www.nap.edu.).

### Brain Extraction

Each animal was sedated by an intraperitoneal injection of 20 mg.kg<sup>-1</sup> thiopental sodium (Rotexmedica, Trittau, Germany) and immediately weighed using a digital electronic balance [Citizen Scales (1) PVT Ltd., sensitivity: 0.01 kg] and converted into grams. The nose-rump and tail lengths were also obtained with a centimetre measuring tape and converted into millimetres. The anogenital distance was obtained using a vernier caliper MG6001DC (General Tools and Instruments Co., New York; sensitivity of 0.01 cm) and converted to millimetres. Thereafter, each animal was placed on a dorsal recumbency on a dissection table, and perfused with 4% paraformaldehyde fixative, through the left ventricle, using a modification of the method of Gage et al. [7]. Immediately after the perfusion fixation, the head was separated from the rest of the body at the atlanto-occipital joint, using a pair of scissors and knife. Thereafter, each skull containing the brain was obtained after skinning and stripping off all the facial muscles; then, craniotomy preceded the brain extraction. Specifically, brain extraction was performed in a caudo-rostral and dorso-ventral direction, using scalpel blades, thumb forceps, rongeur and a pair of scissors. The meninges and underlying blood vessels were gently removed to expose the intact brain.

### Determination of Brain Size

The absolute brain weight was obtained using the Mettler balance P 1261 (Mettler instrument AG., Greifensee, Switzerland; sensitivity: 0.01 g). The absolute brain length was obtained using a vernier caliper MG6001DC (General Tools and Instruments Co., New York; sensitivity of

0.01 cm) and then converted into millimetres. The landmark for the absolute brain length was the rostro-caudal extent of the intact brain, from the tip of the olfactory bulb to the caudal end of the medulla oblongata. The volume measurement was obtained by the water displacement method. Each brain specimen was totally submerged into a known volume of bi-distilled water at 20°C in a graduated cylinder. The volume difference in the cylinder equalled the brain volume in millilitres. The relative brain weight was calculated by dividing the absolute brain weight by the body weight, expressed in percentages. The relative brain length was calculated by dividing the absolute brain length by the nose-rump length, expressed in percentages. The encephalisation quotient was calculated using the formula of Martin [17] for the expected brain mass as shown below:

$$EQ = \frac{M_{\text{brain}}}{0.059 M_{\text{body}}^{0.76}} \text{ (Martin's formula for expected brain mass)}$$

Where

EQ = Encephalisation quotient

M<sub>brain</sub> = Absolute brain weight [g]

M<sub>body</sub> = Body weight [g]

### Statistical Analysis

Data obtained for each postnatal period was expressed as the mean ± SEM (Standard Error of the Mean) and presented in tables and graphs. The values were subjected to one-way analysis of variance (ANOVA), followed by Turkey's post-hoc test to determine the significance of the mean. The association between the values of the body weight with brain weight, and nose-rump length with brain length, were determined using Pearson's coefficient of correlation, at the 95 % confidence interval. The values of P < 0.05 were considered significant. GraphPad Prisms, version 4 for Windows 8 was used for the statistical analysis.

## RESULTS

The mean body weights of the African grasscutters on postnatal days 6, 72 and 450 were 160.11 ± 7.46 g, 273.39 ± 6.70 g and 2925.56 ± 141.96 g, respectively, while the mean nose-rump lengths were 182.00 ± 3.87 mm, 216.89 ± 5.18 mm and 470.33 ± 8.47 mm, respectively. The mean tail lengths were 70.67 ± 0.96 mm, 84.78 ± 1.58 mm and 173.32 ± 7.92 mm, respectively, while the mean ano-

genital distances were  $14.01 \pm 0.20$  mm,  $16.69 \pm 0.18$  mm and  $34.59 \pm 1.17$  mm, respectively.

The mean brain weight, length and volume of each of the postnatal periods are presented in Table 1. The morphometric indices of the whole brain adopted for brain size comparison at the different postnatal periods included the relative brain weight, relative brain length and encephalisation quotient. The decrease in relative brain weight across the different postnatal periods was consistent and statistically significant ( $P < 0.05$ ), such that, while the value on postnatal day 6 was  $3.32 \pm 0.19$  %, the value on postnatal day 450 was  $0.44 \pm 0.03$  % (Table 2). There was a consistent decrease in encephalisation quotient across the different postnatal periods; there was a significant ( $P < 0.05$ ) decrease in the encephalisation quotient from juvenile to adulthood in the African grasscutter. The relative brain length of the animals on postnatal day 450 was  $13.59 \pm 0.42$  % (Table 2). The value was significantly ( $P < 0.05$ ) higher than corresponding values obtained on postnatal days 6 and 72.

There was a very strong positive correlation ( $r = 0.85$ ;  $P < 0.01$ ) between nose-rump length and brain length on postnatal day 6. This implies that as at day 6 post-partum, the brain length of the African grasscutter increased at approximately the same rate with the nose-rump length. The positive correlation result was subjected to regression analysis, and a regression formula was deduced on a graph (Fig. 1) as follows:

$$y = 0.132x + 18.00$$

where

$$y = \text{brain length}; x = \text{known nose-rump length.}$$

Thus, for a 6-day-old African grasscutter whose nose-rump length is obtained (x), the approximate length of the brain (y) can be deduced from the above formula. This formula offers the advantage of obtaining the approximate brain length in a 6-day-old African grasscutter.

**Table 1. Brain morphometric parameters in the African grasscutter at different postnatal periods**

Parameter	Postnatal period	Minimum	Maximum	Mean ( $\pm$ SEM)
<b>Absolute brain weight</b> [g]	Day 6	4.73	5.62	$5.21 \pm 0.15$
	Day 72	6.65	7.00	$6.77 \pm 0.04$
	Day 450	11.35	13.00	$12.22 \pm 0.23$
<b>Absolute brain length</b> [mm]	Day 6	41.00	43.00	$41.91 \pm 0.26$
	Day 72	50.90	55.00	$53.18 \pm 0.52$
	Day 450	60.10	70.00	$63.74 \pm 1.47$
<b>Brain volume</b> [ml]	Day 6	5.32	6.91	$5.91 \pm 0.22$
	Day 72	8.91	9.92	$9.41 \pm 0.11$
	Day 450	10.05	11.81	$10.42 \pm 0.8$

**Table 2. Mean ( $\pm$  SEM) value of brain size indices of the African grasscutter at different postnatal periods  
abcd = means in rows with different superscripts are significantly ( $P < 0.05$ ) different**

Brain parameter	Postnatal period		
	Day 6	Day 72	Day 450
<b>Relative brain weight</b> [%]	$3.32 \pm 0.19^a$	$2.49 \pm 0.07^b$	$0.44 \pm 0.03^c$
<b>Encephalisation quotient</b>	$1.89 \pm 0.09^a$	$1.62 \pm 0.03^b$	$0.49 \pm 0.02^c$
<b>Relative brain length</b> [%]	$23.03 \pm 0.19^a$	$24.63 \pm 0.62^a$	$13.59 \pm 0.42^b$

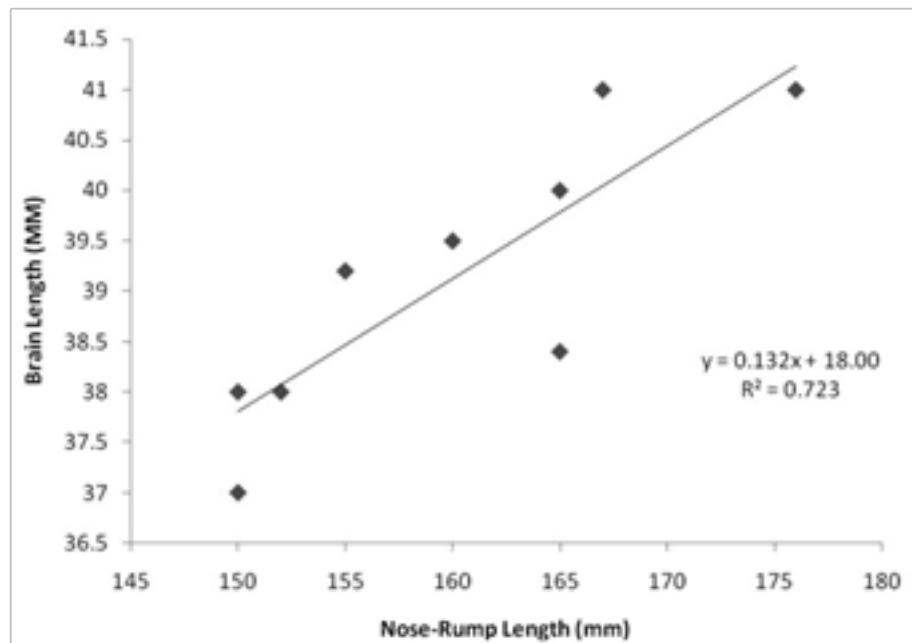


Fig. 1. Positive linear relationship between nose-rump length and brain length of the African grasscutter on postnatal day 6

## DISCUSSION

The neonatal period varies between species. In humans, it is generally accepted as the time elapsed between birth and 28 days of age. As the African grasscutter has a lower life expectancy than humans; in the present study, animals of 3- and 6-day old were classified as neonates. Similarly, as juvenile refers to an immature individual, the animals of 72 days' old were grouped as juveniles. This is in tandem with the grouping presented by Asibe y and Ado [3] in which African grasscutters with two sets of cheek teeth (1 set of premolar and 1 set of molar) were classified as juveniles. Adu and Yeboah [1] confirmed that the African grasscutter reaches sexual maturity at 7 months, when the female attains about 2kg body weight. Thus, animals that have attained sexual maturity and above 2kg body weight, aged 450 days and above, were classified and used as adults.

To determine the level of intelligence of the different postnatal age groups of the African grasscutter, the encephalisation quotient of each postnatal group was computed using the formula of Martin [17], an improvement on the formula of Jerison [12]. The result of the encephalisation quotient in the present study points to a higher memory and cognition in the neonate and juvenile African grasscutters, compared to the adults. Similarly, in their study of postnatal neurogenesis, Olude et al. [22] reported a high

level of plasticity in the juvenile African giant pouched rat, suggested the best learning abilities in the group; thus, proposed the juvenile rats as the most suited for experimental research. The fact that neurones are lost via apoptosis during neurogenesis as the animal advanced in age may be the reason for a lower encephalisation quotient in adult than juvenile or neonatal African grasscutters. Ageing has also been known to pose some detrimental effects on brain cells, gross morphology of the brain and cognition [26]. Most physiological studies of memory and cognition make use of adult rodents. Based on the result of the present study, neonates or at least juvenile rodents may be preferred to adults, for memory and cognition related studies. This does not underscore the assumption that larger rodents such as the adult African grasscutter or the adult African giant pouched rat may be better models for electrophysiological studies as they have absolutely larger neurones that can easily be used for intracellular electrode recordings than smaller-sized rodents like the Wistar rat.

The absence of a significant difference in the relative brain weight of the neonate and juvenile, but the presence of a significant difference in the encephalisation quotient further demonstrates that encephalisation quotient is a more sensitive marker than relative brain weight as it takes into account allometric effects. Moore [20] observed that expression of brain size among different species, based on

their encephalisation quotient, provided a ranking of animals that coincided better with observed complexity of behaviour than that provided due to brain size, based on the relative brain weight. The encephalisation quotient of the adult African grasscutter was lower than the 1.19 reported for the adult African crested porcupine (*Hystrix cristata*) by Papini [25]. Both animals (African grasscutter and African crested porcupine) are large rodents, belonging to the same sub-order Hystricomorpha. The marked difference in their encephalisation quotient further tests the hypothesis that cognitive ability in animals is not taxa-specific. The difference in encephalisation quotient of the two animals may be due to their varied habitats, and that high cognitive ability is required to solve challenging ecological problem of predator evasion posed to the African crested porcupine. Similarly, Krubitzer et al. [14] reported that the encephalisation quotient of tree squirrels was higher than that of ground squirrels, as higher cognition was needed in the tree climbing squirrels.

The encephalisation quotient of adult African grasscutter recorded in the present study is almost the same as the value of 0.40 reported for adult African grasscutter, but higher than 0.19 reported for adult African giant pouched rat by Byanet and Dzenda [5]. This finding may indicate higher cognitive abilities in the adult African grasscutter than in the adult African giant pouched rat, partly due to their varied habitats. The African giant pouched rat is adapted to solitary life in burrows [10], with less exposure to predation; the African grasscutter lives on grassland, and therefore relatively more exposed to predation than the African giant pouched rat.

The relative brain length of the adult African grasscutter from the present study was higher than the value of 10.76% reported for the adult African giant pouched rat [11], but less than the 15% reported for the adult squirrel [13]. The differences are due to species variations, and may be extrapolated to their varied cognitive abilities. The brain length of the adult African grasscutter from the present study is comparable to the cranial length of 7.89 cm obtained for the adult African grasscutter by Onwuama et al. [24]. The higher cranial length than brain length is expected owing to the space occupied by the cranial meninges. There is a need for further research to determine if a very strong correlation exists between head length and brain length, so as to obtain a formula that can be used to estimate brain length of the African grasscutter without

sacrificing the animal. The regression formula obtained from the very strong positive correlation between nose-rump length and brain length in 6-day-old neonates is important as it can be applied in estimating brain length of live African grasscutter neonates of 6 days' old, by measuring their nose-rump length.

## CONCLUSIONS

The present study has provided information on the brain size of the African grasscutter, and related the finding to the behaviour of the animal. It has explained the need to prefer the use of juveniles to adult rodents as models for physiological studies of memory and cognition. It has generated a regression formula that can be used to estimate the brain length of a live African grasscutter neonate of 6 days' old. The results of the present study, which has added to existing information on the neurobiology of the rodent, will serve as a lead for future cognitive studies involving the African grasscutter.

## REFERENCES

1. **Adu, E. K., Yeboah, S., 2000:** The efficacy of the vaginal plug formation after mating for pregnancy diagnosis and embryonic resorption in utero in the greater cane rat (*Thryonomys swinderianus*, Temminck). *J. Trop. Anim. Health Prod.*, 32, 1—10.
2. **Amori, G., Gippoliti, S., 2002:** Rodents and the bushmeat harvest in Central Africa. In **Mainka, S., Trivedi, M.:** *Links between Biodiversity Conservation, Livelihoods and Food Security. The Sustainable Use of Wild Species for Meat.* IUCN Species Survival Commission, 24, 95—100.
3. **Asibey, E. O. A., Addo, P. G., 2000:** The grasscutter, a promising animal for meat production. In **Turnham, D.:** *African Perspectives. Practices and Policies Supporting Sustainable Development.* Scandinavian Seminar College, Denmark, in association with Weaver Press, Harare, Zimbabwe, 120 pp.
4. **Bronner, G.N., Hoffmann, M., Taylor, P.J., Chimimba, C.T., Best, P., Matthee, C.A., Robinson, T.J., 2003:** A revised systematic checklist of the extant mammals of the southern African subregion. *Durban Mus. Novit.*, 28, 56—95.
5. **Byanet, O., Dzenda, T., 2014:** Quantitative biometry of body and brain in the Grasscutter (*Thryonomys swinderianus*) and



- African giant rat (*Cricetomys gambianus*): encephalization quotient implication. *Res. Neurosci.*, 3, 1—6.
6. **Deary, I. J., 2000:** *Looking Down on Human Intelligence: from Psychometrics to the Human brain*. Oxford: Oxford University Press, DOI:10.1093/acprof:oso/9780198524175.001.0001.
  7. **Gage, G. J., Kipke, D. R., Shan, W., 2012:** Whole animal perfusion fixation for rodents. *JVE*, 65, e3564.
  8. **Gläscher, J., Rudrauf, D., Colom, R., Paul, L. K., Tranel, D., Damasio, H., Adolphs, R., 2010:** Distributed neural system for general intelligence revealed by regional mapping. In *Proceedings of the National Academy of Sciences of the United States of America*, doi: 10.1073/pnas/10910397107.
  9. **Herculano-Houzel, S., 2007:** Encephalization, neuronal excess and neuronal index in rodents. *Anat. Rec.*, 290, 128—1287.
  10. **Ibe, C. S., Onyeausi, B. I., Hambolu, J. O., 2014:** Functional morphology of the brain of the African giant pouched rat (*Cricetomys gambianus*, Waterhouse, 1840). *Onderstepoort J. Vet. Res.*, 81, 7. <http://dx.doi.org/10.4102/ojvr.v81i1.644>.
  11. **Ibe, C. S., Onyeausi, B. I., Hambolu, J. O., Ayo, J. O., 2010:** Sexual dimorphism in the whole brain and brainstem morphology in the African giant pouched rat (*Cricetomys gambianus*, Waterhouse 1840). *Folia Morphol.*, 69, 69—74.
  12. **Jerison, H. J., 1977:** The theory of encephalisation. *Ann. N. Y. Acad. Sci.*, 299, 146—160.
  13. **Kinser, P. A., 2000:** *Chart of Approximate Brain and Body Sizes of Various Animals*. In <http://serendip.brynmawr.edu/bb/kinser/Sizechart.html>. Accessed: 07/09/2015. 17:44:23 GMT.
  14. **Krubitzer, L., Campi, K. L., Cooke, D. F., 2011:** All rodents are not the same: a modern synthesis of cortical organization. *Brain Behav. Evol.*, 78, 51—93.
  15. **Lefebvre, L., Reader, S. M., Sol, D., 2004:** Brains, innovations and evolution in birds and primates. *Brain Behav. Evol.*, 63, 233—246.
  16. **Marino, L., 2002:** Convergence of complex cognitive abilities in cetaceans and primates. *Brain Behav. Evol.*, 59, 21—32.
  17. **Martin, R. D., 1984:** Body size, brain size and feeding strategies. In **Chivers, D., Wood, B., Bilsborough, A.:** *Food Acquisition and Processing in Primates*. Plenum Press, New York, 73—103.
  18. **McDaniel, M. A., 2005:** Big-brained people are smarter: A meta-analysis of the relationship between *in vivo* brain volume and intelligence. *Intelligence*, 33, 337—346.
  19. **Mensah, G. A., Okeyo, A. M., 2005:** Continued harvest of the diverse African animal genetic resources from the wild through domestication as a strategy for sustainable use: A case of the larger grasscutter: *Thryonomys swinderianus*. In [http://agtr.ilri.cgiar.org/index.php?option=com\\_content&task=view&id=177&Itemid=199](http://agtr.ilri.cgiar.org/index.php?option=com_content&task=view&id=177&Itemid=199). Accessed: 27/10/2012, 23: 12: 34 GMT.
  20. **Moore, J., 1999:** *Allometry*. University of California, San Diego. In <http://pages.ucsd.edu/~jmoore/courses/allometry/allometry.html>. Accessed: 02/10/2017, 01: 45: 23 GMT.
  21. **Narr, K. L., Woods, R. P., Thompson, P. M., Szeszko, P., Robinson, D., Dimtcheva, T. et al., 2007:** Relationships between IQ and regional cortical gray matter thickness in healthy adults. *Cereb. Cortex*, 17, 2163—2171.
  22. **Olude, A. M., Olopade, J. O., Ihunwo, A. O., 2014:** Adult neurogenesis in the African giant rat (*Cricetomys gambianus*, Waterhouse). *Metabol. Brain Dis.*, 29, 857—866.
  23. **Onebunne, A., 2010:** *Grasscutter Farming — the Pathway to Wealth*. In <http://grasscutterfarmingbest.blogspot.com>. Accessed: 16:08:2014. 16:07:27 GMT.
  24. **Onwuama, K. T., Ojo, S. A., Hambolu, J. O., Salami, O. S., Dzenda, T., 2014:** Gross-anatomical and morphometric studies of the grasscutter (*Thryonomys swinderianus*), axial skeleton. *Stand. Sci. Res. Ess.*, 2, 406—417.
  25. **Papini, M. R., 2008:** Evolution of the vertebrate brain and behaviour. In *Comparative Psychology: Evolution and Development of Behaviour*. 2nd edn., Psychology press, 270 Madison Avenue, New York, 273—277.
  26. **Peters, R., 2006:** Ageing and the brain. *Postgrad. Med. J.*, 2006, 82, 84—88.
  27. **Rieke, G., 2011:** Lecture notes: Emergence of intelligence. *Natural Sciences*, 102, University of Arizona.
  28. **Roth, G., Dicke, U., 2005:** Evolution of the brain and intelligence. *Trends in Cognitive Sciences*, 9, 250—257.
  29. **Sahin, B., Aslan, H., Unal, B., Canan, S., Bilgig, S., Kaplan, S., Tumkaya, L., 2001:** Brain volumes of the lamb, rat and birds do not show hemispheric asymmetry: A stereological study. *Image Anal. Stereol.*, 20, 9—13.
  30. **Simonton, D. K., 2003:** An interview with Dr. Simonton. In **Plucker, J. A.:** *Human Intelligence: Historical Influences, Current Controversies, Teaching Resources*. Accessed online from [http://indiana.edu/\\_intell](http://indiana.edu/_intell). Accessed: 21/04/2014; 04:23:31 GMT.
  31. **Van der Merwe, M., 2007:** Discriminating between *Thryonomys swinderianus* and *Thryonomys gregorianus*. *African Zoology*, 42, 165—171.
  32. **Zilles, K., Palomero-Gallagher, N., Amunts, K., 2013:** Development of cortical folding during evolution and ontogeny. *Trends Neurosci.*, 36, 75—84.

Received July 14, 2017

Accepted August 23, 2017



## ANATOMICAL COMPARISON OF THE RENAL ARTERIES IN THE RABBIT AND EUROPEAN HARE

Flešárová, S., Maženský, D.

Department of Anatomy, Histology and Physiology,  
University of Veterinary Medicine and Pharmacy, Komenského 73, 041 81 Košice  
Slovakia

slavka.flesarova@uvlf.sk

### ABSTRACT

The aim of this paper was to compare the level of origin of the renal arteries in the rabbit and hare. The study was carried out on ten adult rabbits and ten adult European hares using the corrosion cast technique. After the euthanasia, the vascular network was perfused with saline. Batson's corrosion casting kit No. 17 was used as a casting medium. After polymerization of the medium, the maceration was carried out in KOH solution. We found variable levels of the origin of renal arteries in the rabbit, in the hare and between both species. In the rabbit, the right renal artery originated at the level of the second lumbar vertebra in 70 % of the cases and at the level of the first lumbar vertebra in 30 % of the cases, and the left-sided renal artery originated in 60 % of the cases at the level of the second lumbar vertebra and at the level of the third lumbar vertebra in 40 % of the cases. In the hare, the bilateral renal arteries originated at the level of the second lumbar vertebra. According to the results, it can be concluded that the origin level of the renal arteries from the abdominal aorta is more variable in the domesticated rabbit in comparison with the hare.

**Key words:** abdominal aorta; corrosion cast; European hare; rabbit; renal artery

### INTRODUCTION

Different species of mammals serve as experimental models for urologic procedures comprising the surgical and diagnostic techniques. The most frequently utilized species are the pig [7], dog [5] and rabbit [3, 18].

Knowledge of the variations of renal vascular anatomy play a significant role in exploration and treatment of renal transplantation, renal artery embolization, renal trauma, renovascular hypertension, angioplasty or vascular reconstruction for congenital and acquired lesions, conservative or radical renal surgery and surgery for abdominal aortic aneurysms.

The arterial arrangement of the kidneys has been the object of numerous anatomical studies in pigs [2, 12, 13, 19], dogs [4, 6, 14] and rabbits [17]. The urological literature still lacks significant knowledge concerning the renal arterial system of wild species.

The aim of this study was to describe the origin, localization and variations of the renal arteries in two related species: the domesticated rabbit and European hare.

## MATERIALS AND METHODS

This study was carried out on 10 adult European hares (*Lepus Europaeus*, L. 1758, age 140 days) and on 10 adult rabbits (*Oryctolagus cuniculus f. domestica*, L. 1758, age 140 days). We used hares (obtained from ISFA APRC, Nitra, Slovakia) of both sexes (female n = 5; male n = 5) with a weight range between 2.5–3.2 kg, and New Zealand White rabbits (obtained from HYLAPA s. r. o., Prešov, Slovakia) of both sexes (female n = 5; male n = 5), in an accredited experimental laboratory of the University of Veterinary Medicine and Pharmacy in Košice, Slovakia. The animals were kept in cages under standard conditions (temperature 15–20 °C, relative humidity 45 %, 12-hour light period), and fed with a granular feed mixture (O-10NORM TYP, Spišské krmne zmesi, Spišské Vlasy, Slovakia). The drinking water was available to all animals ad libitum. The animals were injected intravenously with heparin (50 000 IU.kg<sup>-1</sup>) 30 min

before they were sacrificed by intravenous injection of embutramide (T-61, 0.3 ml.kg<sup>-1</sup>). Immediately after euthanasia, the vascular network was perfused with a physiological solution. During manual injection through the ascending aorta, the right atrium of the heart was opened in order to lower the pressure in the vessels in order to ensure an optimal injection distribution. Batson's corrosion casting kit No. 17 using a volume of 50 ml (Dione, České Budějovice, Czechia) was used as the casting medium. The maceration was carried out in 2–4 % KOH solution for a period of 5 days at 60–70 °C. This study was carried under the authority decision No. 2647/07-221/5.

## RESULTS

The renal arteries arising from the lateral surfaces of the abdominal aorta supply the kidneys. According to the more lateral position of the left kidney, the left renal artery was longer than the right one. In all of the cases, the right renal artery originated cranially to the left renal artery. Each renal artery was directed towards the renal hilus of the corresponding kidney. After it reached the renal hilus, it was

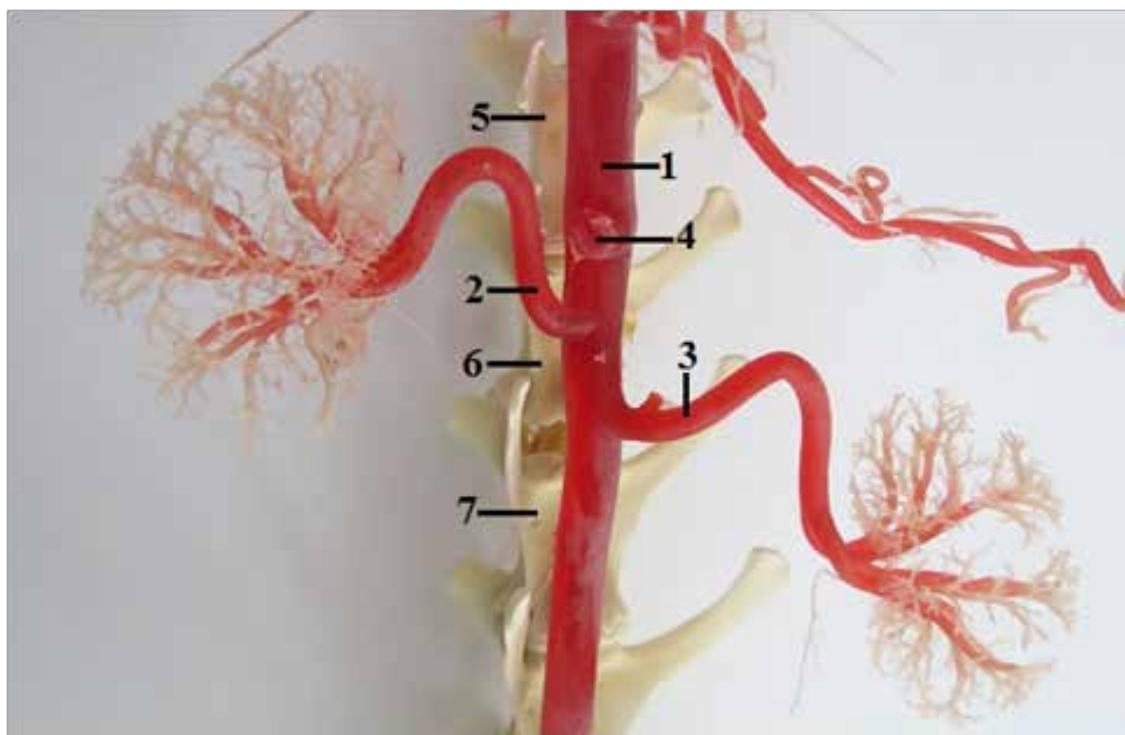


**Fig. 1. Origin of the right and left renal arteries at the level of the second lumbar vertebra in the rabbit**  
1 — abdominal aorta; 2 — right renal artery; 3 — left renal artery; 4 — cranial mesenteric artery; 5 — first lumbar vertebra;  
6 — second lumbar vertebra; 7 — third lumbar vertebra. Macroscopic image, ventral view

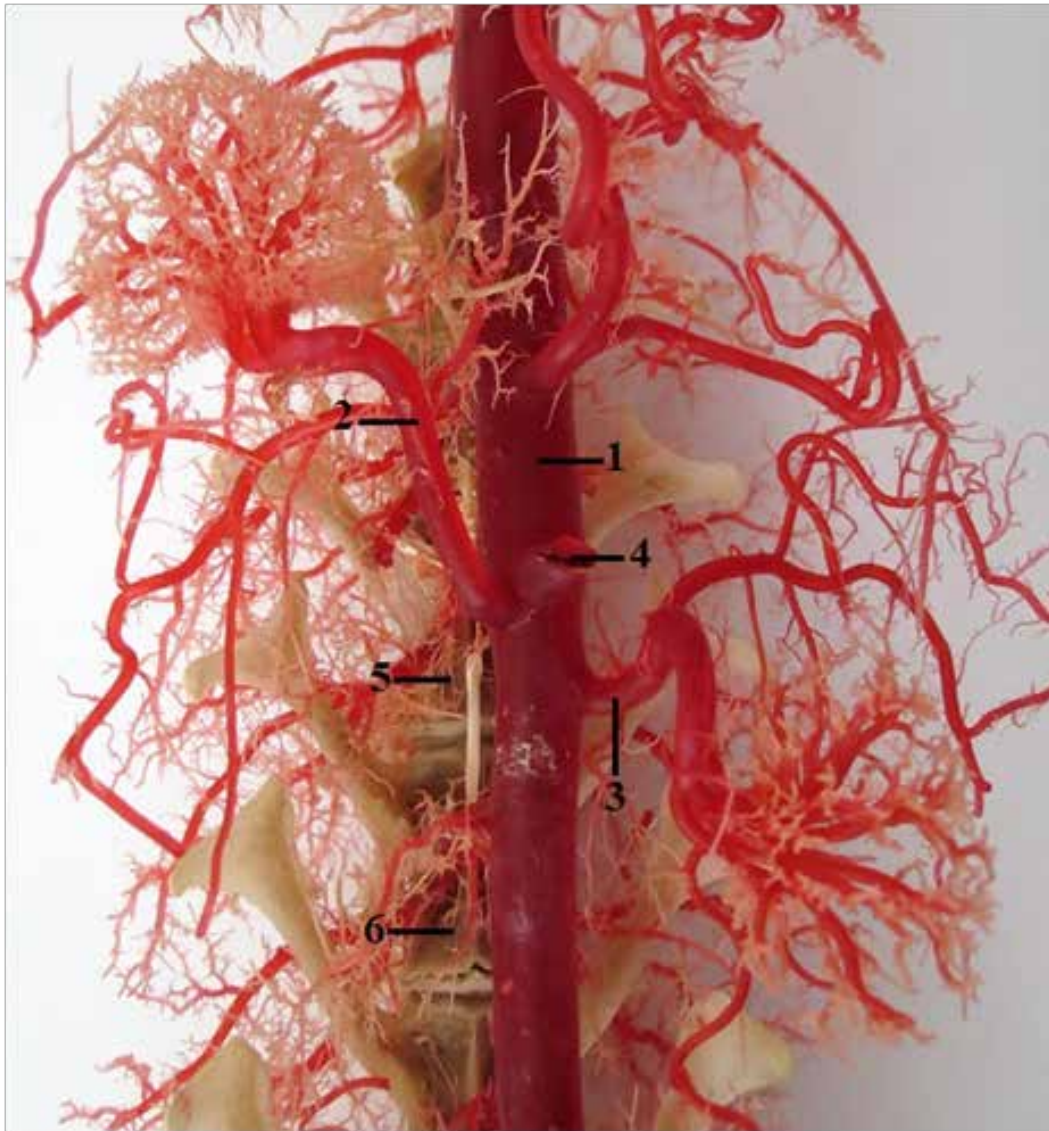


**Fig. 2. Origin of the right and left renal arteries at the level of the second lumbar vertebra in the hare**  
 1 — abdominal aorta; 2 — right renal artery; 3 — left renal artery;  
 4 — cranial mesenteric artery; 5 — first lumbar vertebra; 6 — second lumbar vertebra. Macroscopic image, ventral view

divided into two or more branches, which gave rise to the interlobar arteries, which penetrated into the kidney.

In domesticated rabbit, the right renal artery originated at the level of the second lumbar vertebra in 70% of the cases: in 40% of the cases at the middle of the vertebral body (Fig. 1), in 20% of the cases at its cranial end and in 10% of the cases at its caudal end. In the remaining 30% of the cases, the origin was located at the level of the caudal end of the second lumbar vertebra. The origin of the left renal artery was located at the level of the second lumbar vertebra in 60% of the cases as follows: at the caudal end of the vertebral body in 40% of the cases (Fig. 1), at the cranial end in 10% of the cases and at the middle of the vertebral

body in 10% of the cases. In 40% of the cases, the left renal artery arose at the level of the cranial end of the third lumbar vertebra.

In the European hare, the right renal artery arose at the level of the second lumbar vertebra: in 60% of the cases at the middle of the vertebral body (Fig. 2), in 30% of the cases at its cranial end and in 10% of the cases at the caudal end of the vertebral body. The left renal artery originated also at the level of the second lumbar vertebra. The origin was located at the level of the caudal end of the vertebral body in 70% of the cases (Fig. 2), in the middle of the vertebral body in 20% of the cases and at the cranial end in 10% of the cases.

## DISCUSSION

The general scheme of the arterial arrangement of rabbit kidneys is one independent single renal artery for each kidney. The renal arteries originate from the lateral surfaces of the abdominal aorta. The origin of the right renal artery is located cranially to the origin of the left renal artery [8, 10, 15]. We found the same arrangement on the corrosion casts in the rabbit and hare. Before entering the renal hilus, each of the renal arteries was divided into two or three interlobar arteries [9]. The cranial ureteral artery intended for the cranial part of the ureter was described as a branch arising from the corresponding renal artery [1]. The studies of aforementioned authors did not deal with the level of origin of the renal arteries from the abdominal aorta. The cranial ureteral artery was not present in our specimens.

Despite the frequent use of rabbits in experimental studies, the literature dealing with the vascular anatomy of the kidney in detail is still lacking. In the European rabbit, it has only been described as the presence of multiple renal arteries. The left renal artery has been described as double in 2.63% of the cases [11], while in our study we found a single left renal artery.

The anatomical variations of the renal arteries associated with several diseases are the purpose of different studies. The atypical anatomical arrangement of renal arteries is closely related to the obstructions of the urethra and blood pressure changes. The presence of variant renal arteries is of great significance in the renal vascular surgery. The presence of aberrant renal arteries limits the transplant [16].

## CONCLUSIONS

*The knowledge about the presence of anatomic variations of the renal arteries in experimental animals and related wild species is fundamental for academics-researchers and surgeons. This is the first work dealing with the description of renal arteries origin in the European hare of which we are aware.*

## REFERENCES

1. Douglas, C. G., Hossler, F. E., 1995: Vascular anatomy of the rabbit ureter. *Anat. Rec.*, 242, 47—56.
2. Evan, A. P., Connors, B. A., Lingeman, J. E., Blomgren, P., Willis, L. R., 1996: Branching patterns of the renal artery of the pig. *Anat. Rec.*, 246, 217—223.
3. Fernandez, F., Fernandez, G., Loske, A. M., 2009: Treatment time reduction using tandem shockwaves for lithotripsy: an *in vivo* study. *J. Endourol.*, 23, 1247—1253.
4. Fuller, P. M., Huelke, D. F., 1973: Kidney vascular supply in rat, cat and dog. *Acta Anat.*, 84, 516—522.
5. Groman, R. P., Bah, A., Berridge, B. R., Lees, G. E., 2004: Effects of serial ultrasound-guided renal biopsies on kidneys of healthy adolescent dogs. *Vet. Radiol. Ultrasound.*, 45, 62—69.
6. Jain, R. K., Dhingra, L. D., Kumar, S., Sharma, D. N., 1985: Vascularization of kidneys in dogs (*Canis familiaris*). *Indian J. Anim. Sci.*, 55, 406—409.
7. Kaouk, J. H., Gill, I. S., Desai, M. M., Banks, K. L., Raja, S. S., Skacel, M. et al., 2003: Laparoscopic anastrophic nephrolithotomy: feasibility study in a chronic porcine model. *J. Urol.*, 169, 691.
8. Krause, W., 1884: *The Anatomy of Rabbits. Processed in Topographical and Surgical Consideration* (In German). Verlag von Wilhelm Engelmann, Leipzig, 258—263.
9. Mierzwa, J., 1975: The arterial system of kidneys in the rabbit. *Folia Morphol.*, 34, 407—417.
10. Nejedlý, K., 1965: *Biology and Systematic anatomy of Laboratory Animals* (In Czech). SPN, Prague, 460—474.
11. Nowicki, W., Brudnicki, W., Iwanczyk, M., Jablonski, R., Skoczylas, B., 2010: *Variation in Branches of the Abdominal Aorta in European Rabbit*. *EJPAU*, 13, 10. <http://www.ejpau.media.pl/volume13/issue4/art-10.html> Accessed September 28, 2010.
12. Pereira-Sampaio, M. A., Favorito, L. A., Sampaio, F. J., 2004: Pig kidney: anatomical relationships between the intrarenal arteries and the kidney collecting system. Applied study for urological research and surgical training. *J. Urol.*, 172, 2077—2081.
13. Pereira-Sampaio, M. A., Favorito, L. A., Henry, R. W., Sampaio, F. J., 2007: Proportional analysis of the pig kidney arterial segments. *J. Endourol.*, 21, 784—788.
14. Pereira-Sampaio, M. A., Marques-Sampaio, B. P. S., Henry, R. W., Favorito, L. A., Sampaio, F. J. B., 2009: The dog kidney as experimental model in endourology: anatomic contribution. *J. Endourol.*, 23, 989—993.
15. Popesko, P., Rajtova, V., Horak, J., 1990: *Anatomic atlas of small laboratory animals I*, 1st edn., Priroda, Bratislava, 255 pp.
16. Ramesh Rao, T., 2011: Aberrant renal arteries and its clinical significance: a case report. *Int. J. Anat. Var.*, 4, 37—39.

17. Shalgum, A., Marques-Sampaio, B. P. S., Dafalla, A., Pereira-Sampaio, M. A., 2011: Anatomical relationship between the collecting system and the intrarenal arteries in the rabbit: contribution as an experimental model. *Anat. Histol. Embryol.*, 41, 130—138.
18. Styn, N. R., Wheat, J. C., Hall, T. L., Roberts, W. W., 2010: Histotripsy of VX-2 tumor implanted in a renal rabbit model. *J. Endourol.*, 24, 1145—1150.
19. Šulla, I. J., Lukáč, I., Šulla, I., Maršala, M., 2013: Experimental model of spinal cord compression injury in minipigs: A behavioral and MRI study. In *Proceedings of the Annual Meeting: Evolution of Neurosurgery*, San Francisco, USA, October 19—23, 80.

*Received July 7, 2017*

*Accepted August 25, 2017*





## CHANGES IN TEMPERATURE OF THE EQUINE SKIN SURFACE UNDER BOOTS AFTER EXERCISE

Solheim T. N., Tarabová L., Faixová Z.

Institute of pathological physiology, University of Veterinary Medicine and Pharmacy  
Komenského 73, 041 81 Košice  
Slovakia

lucia.tarabova@uvlf.sk

### ABSTRACT

Equine distal limbs have evolved to have long tendons coupled with strong, tendinous muscles positioned proximally on the leg, thus enabling the horse to achieve highly efficient locomotion. The tradeoff is, that the tendons are left unprotected and prone to injuries, therefore they are often protected by various boots and bandages, which may insulate the limbs and cause hyperthermia in the underlying tendons. The actual mechanism for the degeneration of tendons is currently unknown, but damaging temperature increases due to hysteresis in hard-working horses has been suggested as a possible cause. This study compared the skin temperature of the palmar/plantar metacarpal/metatarsal regions of the limbs after exercise with various types of boots and bandages — primarily tendon boots, leather boots and fleece bandages.

Several horses were measured before and after the completion of a standard exercise test. The boots or bandages were removed immediately after the exercise and the temperature was measured at 3 separate places with A Testo 850i infrared thermometer. The differences

in temperature increases between the various kinds of boots were compared. The results showed a significantly higher average temperature increase in horses wearing boots or bandages compared to the bare limb. The fleece bandages seemed to accumulate the highest amount of heat, followed by the tendon boots.

**Key words:** boot; equine limb; temperature; tendon

### INTRODUCTION

The horse has become one of the most successful animal athletes and is used at both the amateur and professional levels in numerous types of sporting events. Its athletic capabilities have developed through evolution, from the modern horse's ancestor; the small Eohippus. Since the first appearance of these animals some 50 million years ago, the horse has evolved into the high-speed, long-legged creatures of modern times [1].

Some of the morphological developments that have imparted advantages for high-speed locomotion include the

utilization of the collagenous components of the muscles to reduce energy requirements in posture and locomotion [1]. The proximally positioned muscles are coupled to the long, slender tendons to minimize the weight of the distal limb, thus contributing in enabling the horse to achieve efficient high-speed locomotion [13].

This evolutionary, comparative lack of muscles below the carpus is not entirely without risk. The tradeoff is that the tendons are left unprotected and prone to injuries. A study showed that of all limb injuries (82 % of all incidents) at UK racetracks between the years 1996 and 1998, 46 % were due to flexor tendon and/or suspensory ligament injuries, with a more recent study showing the superficial digital flexor tendon in the forelimb being the most prone to injury [7, 15]. Severe tendon injuries can end the career of a racehorse and even if they do return to racing, their performance may be affected [6, 12]. Seventy per cent of racehorses in Japan with tendon injuries failed to return to their previous level of performance in a single race [12].

Many horse owners choose to try to protect the tendons from injury by applying various kinds of boots and bandages to the limbs during exercise and competitions. These boots and bandages may insulate the limb, thus preventing effective heat loss during exercise, leading to elevated temperatures in the tendons [2, 8]. This elevated temperature might reach damaging levels in the centre of the flexor tendons in horses exercising at maximal effort. Repeated hyperthermic insults may decrease tendon cell viability or alter the tendon cell metabolism and communication – thus affecting the tendon extracellular matrix [3, 4, 9].

The mechanisms of tendon degeneration are generally poorly understood, but it has been hypothesized that the energy increase due to hysteresis may provide one mechanism, predisposing it to subsequent mechanical failure [16].

The aim of this study was to investigate the effect of different types of bandages and boots on the skin temperature of the palmar/plantar aspect of the metacarpus, as measured with an infrared thermometer, on the bare limb before exercise and the booted or bandaged limb after completion of a standard exercise test.

## **MATERIALS AND METHODS**

### **Animals**

Sixteen horses of varying age, sex, and breed were used

in this study. All horses were free of lameness and showed no signs of illness or injury, except for horse number 4, which was wearing air boots. We were informed that this horse had an allergic reaction on the left forelimb at the level of the pastern, but showed no signs of pain or lameness before, during or after the standard exercise test.

### **Instrumentation**

A Testo 805i smart probe infrared thermometer with a wireless probe and smartphone operation was used to measure the skin temperature. The thermometer had a measuring range of  $-30^{\circ}\text{C}$  to  $+250^{\circ}\text{C}$  and an accuracy of  $\pm 1.5^{\circ}\text{C}$  in the range of 0 to  $+250^{\circ}\text{C}$ . The resolution was  $0.1^{\circ}\text{C}$  and the operating temperature  $-10^{\circ}\text{C}$  to  $+50^{\circ}\text{C}$ . The temperature was measured as close to the leg as possible, due to recommendations of the retailer.

### **Procedure**

The skin temperature of each limb was measured at 3 different places: at the palmar/plantar aspect of the metacarpus/metatarsus — proximally, distally, and in the middle region. The temperature was measured before exercise and directly after completion of the standard exercise test. The boots/bandages on the other limbs were kept on while measurement of the first leg was completed. When the boots were removed, one by one, the temperature was immediately recorded.

Both hind limbs and forelimbs were used in this study. Some horses wore the same type of boots/bandages on both hind limbs and forelimbs, some were fitted with different types on each leg (with one leg bare), and some with boots only on forelimbs or hind limbs. The boots and bandages used in this study were supplied by the horse owners themselves, and might have varied slightly in composition and material. The results for the different boots were pooled into groups according to style and material: traditional tendon boots, fleece bandages, leather tendon boots, traditional boots made from sympatex, traditional boots made of neoprene and tendon “air boots”.

The standard exercise test consisted of:

- 10 minutes of walk,
- 5 minutes of trot,
- 2.5 minutes of canter,
- 5 minutes of walk.

The standard exercise test was conducted both outside and inside in a riding arena, with varying exercise surfaces.



The ambient temperatures varied from  $-6^{\circ}\text{C}$  to  $5^{\circ}\text{C}$ . The wind speed and humidity were not recorded. Slippery weather conditions (such as snow and ice) made it difficult for some horses exercising outdoors to complete the canter phase of the standard exercise test, and it were partly performed in the trot at a good pace.

### Data processing

The average increase in temperature for the different types of boots where calculated and presented in a table with the use of Microsoft Excel.

## RESULTS

The results of temperature measurements during the study are presented in Table 1.

**Table 1. average temperature increase for the different boots and bandages worn by the horses**

Type of boots	Average temperature increase [ $^{\circ}\text{C}$ ]
Fleece bandages	16.5
Tendon boots	14.3
Leather tendon boots	14.3
Air tendon boots	13.0
Sympatex traditional boots	12.3
Neoprene traditional boots	11.9
Nothing	3.0

These results indicated that the fleece bandages accumulated the most amount of heat during an exercise, followed by the tendon boots and leather tendon boots showing the same average temperature increase. The neoprene traditional boots show the lowest average increase in temperature, followed by the sympatex traditional boots and air tendon boots.

All the boots show a significantly higher average increase in temperature compared with the bare limb after exercise.

The highest measurement observed in this study occurred with the tendon boot, and were observed to be  $33.8^{\circ}\text{C}$ .

The highest heat measurements were seen at the proximal and distal regions of the limb in fleece bandages, ten-

don boots and the traditional neoprene boots. The leather tendon boots and the traditional sympatex boots showed a tendency of accumulating the highest amount of heat in the proximal and middle regions.

## DISCUSSION

Clothing, or in this case, boots and bandages, acts as a barrier to evaporative and convective cooling. The boots and bandages created a microenvironment between the skin and fabrics, which was generally hotter and more humid than the ambient environment. The temperature and humidity depends on several factors, including the condition of the macroenvironment, movement, permeability of the fabric, encapsulation, and the metabolic heat produced during exercise [5].

The fleece bandages showed the highest average increase in temperature. This correlated well with the results of the thermographic investigation in the study of Westerman et al. [14], where the limbs associated with a fleece bandage were significantly more proximal than that covered with a tendon boot.

The high temperature increase might be due to the insulating properties of the microfleece, causing heat to accumulate under the bandage, or to the fact that it is highly encapsulating compared to the open-fronted boots, covering the entire metacarpal/metatarsal regions of the limbs.

The traditional tendon boots are open-fronted, which possibly could facilitate some air circulation to occur under the tendon boots or allow for some evaporative and convective cooling to occur in the uncovered portions of the equine limb. If this was the case, the temperatures were expected to be lower for these kinds of boots compared to those covering the entire metacarpal or metatarsal regions. In our study, the average temperature increase was lower for the open-fronted tendon boots compared to the fleece bandages, but the traditional neoprene and sympatex boots encapsulating the entire metacarpal/metatarsal regions of the leg showed an even lower average temperature increase. The fact that 3 out of 4 horses wearing traditional neoprene boots did not complete the gallop phase of the standard exercise test, due to slippery exercise conditions, must be taken into consideration as this might have led to lower temperature recordings than may have been seen otherwise if the gallop phase were completed. In comparison, another

study found that the open-fronted tendon boots did not result in a relevant reduction in temperature compared to the traditionally fully enclosed boots, which might imply that the thermal properties of the materials used in these boots played just as important a role as the fact that some are open-fronted [8].

The traditional neoprene boots consist of a single layer of neoprene fabric, whilst the tendon boots used consist of either leather, leather with neoprene or a thermoplastic elastomer combined with neoprene. For heat dissipation to occur at the surface of the limb, conduction of heat through both materials for the tendon boots (or a thicker layer in the case of tendon boots consisting only of leather), but only a single layer for the traditional neoprene boots, needs to occur. The thermal conductivity for neoprene is much lower ( $0.054 \text{ W.m.K}^{-1}$ ) than that of the thermoplastic elastomers (for example PVC with a thermal conductivity of  $0.14\text{--}0.17 \text{ W.m.K}^{-1}$ ), and might be responsible for much of the heat retention in both the traditional neoprene boot and tendon boot, but the added thickness of the thermoplastic elastomer might cause the dissipation of heat to occur at a slower rate, and have significant effects on the accumulation of heat during exercise [17].

In comparing the two tendon boots of similar design apart from their differing material (leather and thermoplastic elastomers/neoprene), no significant difference in average increase of temperature were seen. But, in comparing the tendon boots perforated to allow heat dissipation to tendon boots without perforation, a lower average increase in temperature were observed for the perforated tendon boots. This also correlated well with the results in the study of Hopegood et al. [8] which also indicated that greater heat emissions, and thus heat dissipation, took place in these perforated boots compared to the traditional tendon boots.

Hopegood et al. [8] also found that there were significantly lower heat emissions from the middle of the boot compared to the top and bottom in perforated and traditional tendon boots. This was also true for the fleece bandages, tendon boots and the traditional neoprene boots. The leather tendon boots and the traditional sympatex boots showed a tendency of accumulating the highest amount of heat in the proximal and middle regions. It is unclear whether this was due to a greater insulating effect of the boots in this regions or due to a higher heat production underneath those areas relative to the middle region of the metacarpus/metatarsus.

All horses used in this study were of a sufficient fitness level to cope with the intensity of the standard exercise test, but it was not possible to determine and control the speed of the different horses exercising in this study. The workload is the main determinant of the rate of heat production, and might have varied slightly for each horse. Three of the horses wearing the traditional neoprene boots did not complete the gallop phase of the standard exercise test, and this might have had an impact of the results. In addition, it is not possible to control the natural day-to-day variabilites in the body temperature of the horses.

The temperature was measured with an infrared thermometer, which has been shown to produce accurate measures of skin temperatures [10]. However, the temperature was measured as quickly as possible after the removal of the boots and bandages, some heat might have been allowed to escape before the measurements were completed.

The horses were exercised in different weather conditions and with ambient temperatures ranging from  $-6$  to  $5 \text{ }^\circ\text{C}$ . The skin surface temperature varied in correlation with the ambient temperature, and it might therefore have had an impact on the results in this study [11]. Lastly, the boots and bandages were supplied by the owners of the horses, and might have varied slightly in material and design, which might have affected the results of the present study. These results need to be researched further in larger studies, and the effect of boot materials and design on heat insulation needs to be investigated further.

Westermann et al. [14] suggested that although skin surface temperature in the study paralleled that of deeper tissues, it may not be accurately indicating the temperature of the underlying tissues and structures. In this study, it was not possible to measure the temperature of the underlying tendons during or after the exercise with a booted or bandaged limb. Further research could focus on measuring these temperatures during or after exercise with different commercial available boots and bandages.

Furthermore, future research could focus on measuring temperatures during the actual exercise, by use of thermal probes with time-lapse recording equipment or motion thermal imaging camera. It could also be of interest to measure the heart-rate and speed of the horses at the same time. This would allow for the evaluation of temperature development throughout the entire exercise.

## CONCLUSIONS

It is clear from the resulting average increase in temperatures that both boots and bandages insulate the limbs during exercise, and could possibly result in detrimental effects on the tendon during high intensity exercise.

The fleece bandages showed the highest average increase, followed by the tendon boots. The perforated tendon boots seem to show a lower increase in temperature compared to the traditional tendon boots. The traditional neoprene boots show the lowest temperature increase, followed by the sympatex traditional boots.

In addition to this, it was found that most of the boots and bandages showed a higher increase in the temperature of the underlying skin in the proximal and distal regions, except for leather tendon boots and sympatex boots, whilst the latter is highly likely due to the low amount of data. These findings point at the importance of the designing of boots and bandages to minimise tendon exposure to high temperatures, but warrants further investigation.

## REFERENCES

1. **Back, W., Clayton, H. M., 2001:** *Equine Locomotion*. Harcourt Publishers Ltd., London, 384 pp.
2. **Baxter, K., 2013:** The effect of equine exercise bandages on distal forelimb temperatures during exercise. *South Downs Vet. Phys.*, 1—123.
3. **Birch, H. L., Wilson, A. M., Goodship, A. E., 1997:** The effect of exercise-induced localised hyperthermia on tendon cell survival. *J. Exp. Biol.*, 200, 1703—1708.
4. **Burrows, S., Patterson-Kane, J., Fleck, R., Becker, D., 2009:** Alterations in gap junction communication in tenocyte monolayers following an episode of hyperthermia. *The Bone and Joint Journal*, 91-B, Supp. 2, 348.
5. **Davis, J. K., Bishop, P. A., 2013:** Impact of clothing on exercise in the heat. *Sports Med.*, 43, 695—706.
6. **Ely, E. R., Avella, C. S., Price, J. S., Smith, R. K., Wood, J. L., Verheyen, K. L., 2009:** Descriptive epidemiology of fracture, tendon and suspensory ligament injuries in national hunt horses in training. *Equine Vet. J.*, 41, 372—378.
7. **Ely, E. R., Verheyen, L. P., Wood, J. L. N., 2004:** Fractures and tendon injuries in national hunt horses in training in the UK: A pilot study. *Equine Vet. J.*, 36, 365—367.
8. **Hopegood, L., Sander, L., Ellis, A. D., 2013:** The influence of boot design on exercise associated surface temperature of tendons in horses. *Comp. Ex. Phys.*, 9, 147—152.
9. **Hosaka, Y., Ozoe, S., Kirisawa, R., Ueda, H., Takehana, K., Yamauchi, M., 2006:** Effect of heat on synthesis of gelatinases and pro-inflammatory cytokines in equine tendinocytes. *Biomed. Res.*, 27, 233—241.
10. **Kelechi, T., Michel, Y., Wiserman, J., 2006:** Are infrared thermistor thermometers interchangeable for measuring localized skin temperature? *J. Nurs. Meas.*, 41, 19—30.
11. **Mogg, K. C., Pollitt, C. C., 1992:** Hoof and distal limb surface temperature in the normal pony under constant and changing ambient temperatures. *Equine Vet. J.*, 24, 134—139.
12. **Oikawa, M., Kasashima, Y., 2002:** The japanese experiment with tendonitis in racehorses. *Journal of Equine Science*, 13, 41—56.
13. **Smith, R. K. W., Goodship, A. E., 2008:** Tendon and ligament physiology: responses to exercise and training. In **Hinchcliff, K. W., Geor, R. J., Kanep A. J.:** *Equine Exercise Physiology, the Science of Exercise in the Athletic Horse*. Elsevier Ltd, London, 106—131.
14. **Westermann, S., Windsteig, V., Schramel, J. P., Peham, C., 2014:** Effect of a bandage or tendon boot on skin temperature of the metacarpus at rest and after exercise in horses. *Am. J. Vet. Res.*, 75, 375—379.
15. **Williams, R. B., Harkins, L. S., Hammond, J., Wood, J. L. N., 2001:** Racehorse injuries, clinical problems and fatalities recorded on British racecourses from flat racing and national hunt racing during 1996, 1997 and 1998. *Equine Vet. J.*, 33, 478—486.
16. **Wilson, A. M., Goodship, A. E., 1994:** Exercise-induced hyperthermia as a possible mechanism for tendon degeneration. *J. Biomechanics*, 27, 899—905.

Received August 22, 2017

Accepted September 19, 2017



## ANATOMICAL ARRANGEMENT OF THE SUBCLAVIAN ARTERY BRANCHES IN THE RABBIT AND EUROPEAN HARE

Maženský, D., Flešárová, S.

Department of Anatomy, Histology and Physiology  
University of Veterinary Medicine and Pharmacy, Komenského 73, 041 81 Košice  
Slovakia

david.mazensky@uvlf.sk

### ABSTRACT

The aim of this study was to compare the anatomical arrangements of the branches arising from the subclavian arteries in the domesticated rabbit and hare. The study was carried out on ten adult rabbits and ten adult European hares using the corrosion cast technique. After the euthanasia, the vascular network was perfused with saline. The arterial system of the entire body was injected by Batson's corrosion casting kit No. 17. After polymerization of the medium, the maceration was carried out in KOH solution. The arrangement of the origins of the branches of the bilateral subclavian arteries were more variable in the hare. The number of branches arising from the subclavian artery were more regular in the rabbit on the right side and in the hare on the left side. In the rabbit, we found in two cases, the origins of the branches of the left subclavian artery from the aortic arch. The anatomical differences found between the rabbit and the hare may possibly be associated with their different ways of life.

**Key words:** European hare; origin; rabbit; subclavian artery

### INTRODUCTION

The subclavian arteries of both sides of the body continue cranially to reach the cranial border of the first rib forming a convex curve. After their turn, they continue into the corresponding thoracic limb as the axillary arteries.

The branches arising from the subclavian artery are the vertebral artery, deep cervical artery, dorsal scapular artery and supreme intercostal artery. Some or all of these branches can be fused to form a common stem of origin known as the costocervical trunk. The subclavian artery gives off at the level of thoracic entrance the internal thoracic artery and superficial cervical artery [6, 8].

The vertebral artery emerges from the thoracic cavity through the thoracic entrance. It then passes through the transverse foramen of the sixth cervical vertebra into the transverse canal of the cervical vertebrae, in which it continues in the cranial direction. It supplies the cervical part of the spinal cord, brain, meninges, cervical vertebral bodies and neighboring musculature.

The deep cervical artery leaves the thoracic cavity through the first intercostal space and supplies the muscles of the neck from the withers to the nape. The dorsal scapular artery after leaving the thoracic cavity through

the first intercostal space supplies the muscles and skin of the withers [6, 8]. The supreme intercostal artery continues caudally on the ventral surface of the heads of the ribs and gives off the dorsal intercostal arteries supplying the first four intercostal spaces [6, 7]. The internal thoracic artery is directed ventrocaudally on the dorsal surface of the sternum. It participates by supplying blood to the ventral part of lateral thoracic wall, sternum, thoracic mammary complexes, mediastinum, pericardium, thymus, diaphragm, abdominal musculature and skin. The superficial cervical artery is directed to the lateral surface of the external jugular vein. This artery supplies the cervical lymph-nodes and neighboring musculature [6, 8].

The literature dealing with the arterial system in the rabbit and hare in detail is rather [6, 7]. The aim of this study was to describe the origin, localization and variations of the subclavian artery branches in two related species: the domesticated rabbit and European hare.

## MATERIALS AND METHODS

This study was carried out on 9 adult European hares (*Lepus Europaeus*, L. 1758, age 140 days) and on 9 adult domesticated rabbits (*Oryctolagus cuniculus f. domestica*, L. 1758, of the same age). We used hares (obtained from ISFA APRC, Nitra, Slovakia) of both sexes (female n=5; male n=5), with a weight range between 2.5–3.2 kg and New Zealand White rabbits (obtained from HYLAPA s. r. o., Prešov, Slovakia) of both sexes (female n=5; male n=5), in an accredited experimental laboratory of the University of Veterinary Medicine and Pharmacy in Košice, Slovakia. The animals were kept in cages under standard conditions (temperature 15–20°C, relative humidity 45%, 12-hour light period), and fed with a granular feed mixture (O-10 NORM TYP, Spišské krmne zmesi, Spišské Vlachy, Slovakia). The drinking water was available to all animals ad libitum. The animals were injected intravenously with heparin (50 000 IU.kg<sup>-1</sup>) 30 min before they were sacrificed by intravenous injection of embutramide (T-61, 0.3 ml.kg<sup>-1</sup>). Immediately after euthanasia, the vascular network was perfused with a physiological solution. During manual injection through the ascending aorta, the right atrium of the heart was opened in order to lower the pressure in the vessels which enabled an optimal injection distribution. 50 ml of Batson's corrosion casting kit No.17 (Dione, České Budějovice, Czechia)

was used as the casting medium. The maceration was carried out in 2–4% KOH solution for a period of 5 days at 60–70°C. The study was carried out under the authority decision No.2647/07-221/5.

## RESULTS

### Rabbit

In all specimens, the left subclavian artery arose from the aortic arch as the second branch after the origin of the brachiocephalic trunk. The left subclavian artery gave off, two branches in one case, three branches in two cases, four branches in two cases and five branches in four cases. In one case, a common trunk for the left supreme intercostal artery, left deep cervical artery, left dorsal scapular artery and left internal thoracic artery arose directly from the aortic arch caudally to the origin of the left subclavian artery. Also in one case, the left vertebral artery arose from the aortic arch as an independent branch cranially to the origin of the left subclavian artery.

In two cases, the first branch originating from the left subclavian artery was the left supreme intercostal artery (Fig. 1) and also in two cases a common trunk dividing into the left supreme intercostal artery, left deep cervical artery and left dorsal scapular artery. In one case, the first branch was the left vertebral artery, left superficial cervical artery, left internal thoracic artery, a common trunk for the left supreme intercostal artery, left deep cervical artery, left dorsal scapular artery and left internal thoracic artery, and a common trunk for the left supreme intercostal artery and left deep cervical artery. A common trunk consisting of the left deep cervical artery and left dorsal scapular artery was present as the second branch in three cases (Fig. 1). The left vertebral artery as the second branch was present also in three cases. In two cases, the second branch was the left internal thoracic artery and in one case the left superficial cervical artery. The third branch was formed as follows: the left vertebral artery in three cases (Fig. 1), the left internal thoracic artery in two cases, the left superficial cervical artery in two cases and the left supreme intercostal artery in one case. In two cases, the left superficial cervical artery was present as the fourth branch. In one case, were present as the fourth branch of the left vertebral artery, the left superficial cervical artery, a common trunk for the left deep cervical artery and left dorsal scapular artery, and a com-

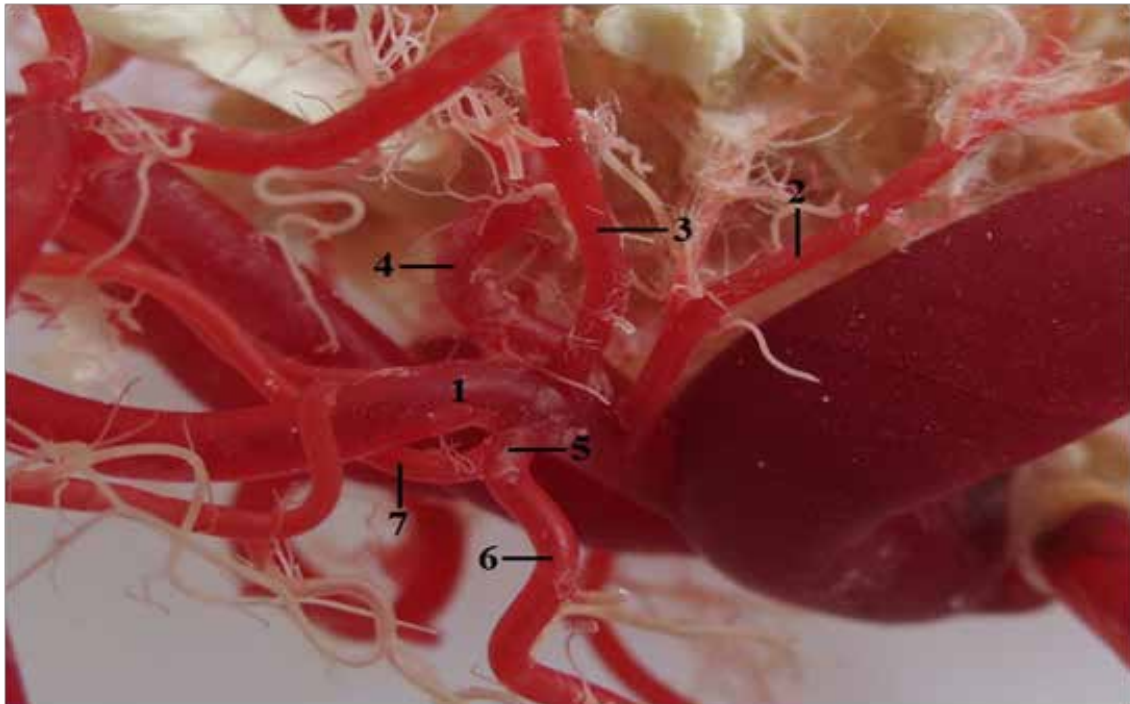


**Fig. 1. The branches of the left subclavian artery in the rabbit**

1 — left subclavian artery; 2 — left supreme intercostal artery; 3 — common trunk for the left dorsal scapular artery and left deep cervical artery; 4 — left vertebral artery; 5 — common trunk; 6 — left internal thoracic artery; 7 — left superficial cervical artery. Macroscopic image, dorsolateral view

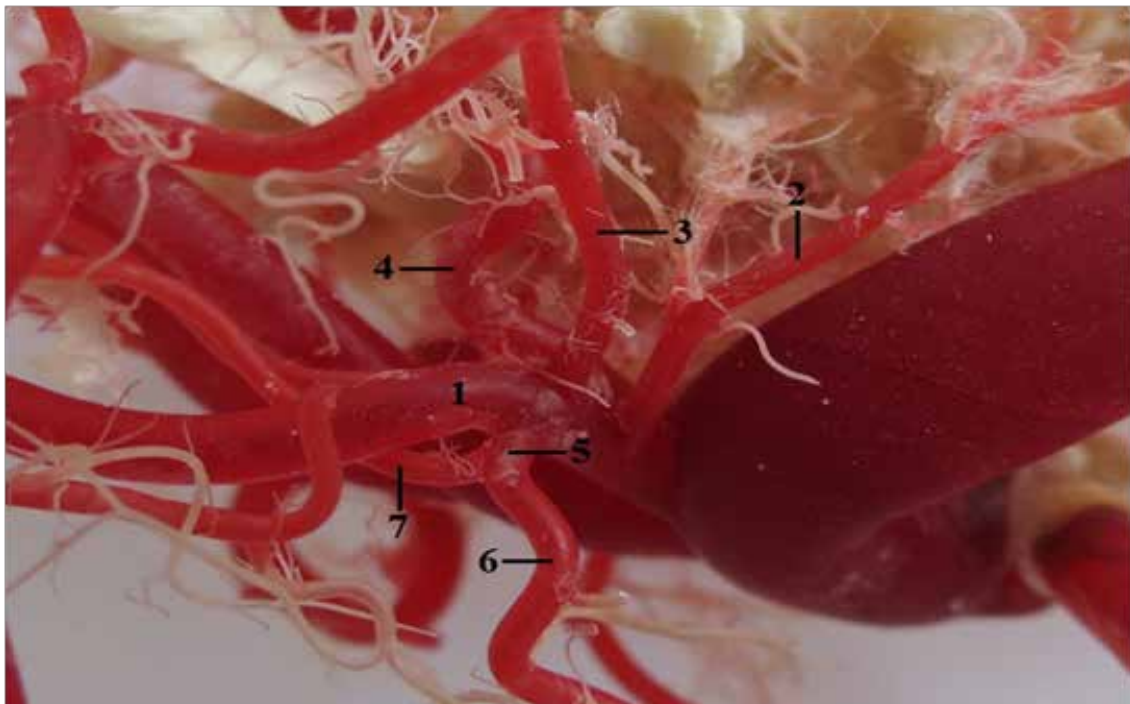


**Fig. 2. The branches of the right subclavian artery in the hare**

1 — right subclavian artery; 2 — common trunk; 3 — right supreme intercostal artery; 4 — common trunk for the right dorsal scapular artery and right deep cervical artery; 5 — right vertebral artery; 6 — right internal thoracic artery; 7 — right superficial cervical artery. Macroscopic image, craniolateral view

mon trunk formed by the left internal thoracic artery and left superficial cervical artery (Fig. 1). The left superficial cervical artery or the left internal thoracic artery constituted the fifth branch in two cases.

The right subclavian artery originated from the brachiocephalic trunk in all specimens. Three branches of the right subclavian artery were present in five cases and four branches in four cases.

As the first branch in three cases was present a common trunk for the right supreme intercostal artery, right deep cervical artery, right dorsal scapular artery and right internal thoracic artery or the right vertebral artery. In two cases, the first branch was represented by the right superficial cervical artery and in one case by the first right superficial cervical artery. The second branch showed the following arrangement: the right vertebral artery in four cases, the right internal thoracic artery in three cases and a common trunk for the right supreme intercostal artery, right deep cervical artery, right dorsal scapular artery and right internal thoracic artery in one case. The right superficial cervical artery as the third branch originated in four cases. In two cases, the right vertebral artery represented the third branch. In one case, as the third branch was present, the doubled right superficial cervical artery, a common trunk for the right supreme intercostal artery, right deep cervical artery, right dorsal scapular artery and right internal thoracic artery or a common trunk for the right supreme intercostal artery, right deep cervical artery and right dorsal scapular artery. A common trunk for the right supreme intercostal artery, right deep cervical artery and right dorsal scapular artery was present as a fourth branch in two cases. In one case, it was the right superficial cervical artery and the second was the right superficial cervical artery.

### European hare

The left subclavian artery originated from the aortic arch in all corrosion casts. It gave off five branches in eight cases and four branches in one case.

The left supreme intercostal artery was the first branch in all cases. The left internal thoracic artery was the second branch in seven cases, and a common trunk for the left deep cervical artery and left dorsal scapular artery in two cases. The third branch was, in six cases a common trunk for the left deep cervical artery and left dorsal scapular artery; in one case the left vertebral artery; in one case the left internal thoracic artery; and also in one case a com-

mon trunk for the left vertebral artery, left deep cervical artery and left dorsal scapular artery. The left vertebral artery was found as the fourth branch in seven cases and the left superficial cervical artery in two cases. The left superficial cervical artery represented the fifth branch in seven cases and the left internal thoracic artery in one case.

The right subclavian artery as a branch of the brachiocephalic trunk was present in all specimens, and it gave off three branches in five cases, five branches in three cases and six branches in one case.

The first branch showed the following arrangement: a common trunk for the right supreme intercostal artery, right deep cervical artery, right dorsal scapular artery and right internal thoracic artery in five cases (Fig. 2), the right internal thoracic artery in two cases, the right supreme intercostal artery in one case and the right superficial cervical artery also in one case. The second branch was formed in six cases by the right vertebral artery (Fig. 2), in two cases by the right supreme intercostal artery and in one case by the right internal thoracic artery. The right superficial cervical artery was found as the third branch in five cases (Fig. 2), a common trunk for the right deep cervical artery and right dorsal scapular artery in three cases and the right deep cervical artery in one case. The right vertebral artery represented the fourth branch in two cases, the right supreme intercostal artery in one case, and the right dorsal scapular artery also in one case. The right superficial cervical artery was the fifth branch in two cases, the right internal thoracic artery in one case and the right vertebral artery also in one case. In one case, was formed the sixth branch by the right superficial cervical artery.

### DISCUSSION

The origin, course and direction of the subclavian arteries in our corrosion casts of the rabbit arterial system were similar to the observations of Craigie [1] and Popesko et al. [7]. From the left subclavian artery originated three branches [7] or five branches [1], but in our specimens their number varied from two to five.

As the first branch arising from the left subclavian artery we found a common trunk for the left supreme intercostal artery, the left deep cervical artery and the left dorsal scapular artery [7]. The same arrangement was found only in two cases. Also, in two cases, the first branch was the left

supreme intercostal artery. The left vertebral artery, left superficial cervical artery, left internal thoracic artery, a common trunk for the left supreme intercostal artery, left deep cervical artery, left dorsal scapular artery and left internal thoracic artery, and a common trunk for the left supreme intercostal artery and left deep cervical artery were the first branch only in one case. The second branch in our specimens was a common trunk for the left deep cervical artery and left dorsal scapular artery in three cases, the left vertebral artery in two cases, the left internal thoracic artery in two cases and the left superficial cervical artery in one case. Popesko et al. [7] described the left internal thoracic artery as the second branch. The left vertebral artery is the third branch arising independently from the left subclavian artery (Popesko et al. [7]). In our specimens, the third branch was represented by: the left vertebral artery in three cases, the left internal thoracic artery in two cases, the left superficial cervical artery in two cases and the left supreme intercostal artery in one case.

The origin, course and direction of the right subclavian artery in our specimens have been covered previously by the descriptions of Craigie [1] and Popesko et al. [7]. The right subclavian artery gives off five [1] or three branches [7]. In our specimens, three branches were present in five cases and four branches in four cases.

The first branch found by Popesko et al. [7] was a common trunk for the right supreme intercostal artery, right deep cervical artery, right dorsal scapular artery and right vertebral artery. The same arrangement of the first branch was present in our specimens in three cases. In two cases, the right superficial cervical artery and in one case the first right superficial cervical artery represented the first branch. The second branch showed the following arrangement: the right vertebral artery in four cases, the right internal thoracic artery in three cases and a common trunk for the right supreme intercostal artery, right deep cervical artery, right dorsal scapular artery and right internal thoracic artery in one case. Popesko et al. [7] described the right internal thoracic artery as the second branch. In the literature, the third branch was designated as the right superficial cervical artery (Popesko et al. [7]). The same arrangement was present in our specimens in four cases. In the rest of the cases, the third branch was formed as follows: the doubled right superficial cervical artery in one case, a common trunk for the right supreme intercostal artery, right deep cervical artery, right dorsal scapular ar-

tery and right internal thoracic artery in one case, common trunk for the right supreme intercostal artery, right deep cervical artery and right dorsal scapular artery in one case.

The vertebral artery, superficial cervical artery, deep cervical artery, supreme intercostal artery and the internal thoracic artery as subclavian artery branches without order of their origins were listed by Craigie [1].

The arrangement of origins of the branches of the bilateral subclavian arteries were more variable in the hare. The number of branches arising from the subclavian artery was more regular in the rabbit on the right side and in the hare on the left side. In the rabbit, we found in two of the cases, the origins of the branches of the left subclavian artery from the aortic arch.

The detailed knowledge of the arrangement of the arterial system still represents an extensive gap in the literature. We believe that the anatomical knowledge contributes to a better understanding of behavioral differences between familiar species in domesticated as well as in experimental studies and the veterinary daily practice, too [2, 3, 4, 5].

## CONCLUSIONS

The results of our study indicated high variability in the arrangement of the branches arising from the bilateral subclavian arteries. The anatomical differences found between the rabbit and the hare are possibly associated with the different ways of life.

## REFERENCES

1. **Craigie, E. H., 1948:** *Bensley's Practical Anatomy of the Rabbit*. Blakiston Company, Philadelphia, 325—326.
2. **Dugat, D., Rochat, M., Ritchey, J., Payton, M., 2011:** Quantitative analysis of the intramedullary arterial supply of the feline tibia. *Vet. Comp. Orthop. Traumatol.*, 24, 313—319.
3. **Hossmann, K. A., 1998:** Experimental models for the investigation of brain ischemia. *Cardiovasc. Res.*, 39, 106—120.
4. **Iwama, H., Akama, Y., Tase, C., 2000:** Global brain ischemia produced by clamping left subclavian artery and bicarotid trunk in the rabbit. *Am. J. Emerg. Med.*, 18, 31—35.
5. **Mazensky, D., Danko, J., 2010:** The importance of the origin of vertebral arteries in cerebral ischemia in rabbit. *Anat. Sci. Int.*, 85, 102—104.



6. Nickel, R., Schummer, A., Seiferle, E., 1981: *The Anatomy of the Domestic Mammals. The Circulatory System, the Skin, and the Cutaneous Organs of the Domestic Mammals*. Verlag Paul Parey, Berlin, 72—77.
7. Popesko, P., Rajtova, V., Horak, J., 1990: *Anatomic Atlas of Small Laboratory Animals I*. 1st edn., Príroda, Bratislava, 67—78.
8. Popesko, P., Hajovska, B., Marvan, F., Komarek, V., Vrzgulo, M., 1992: *Anatomy of Farm Animals*. Príroda, Bratislava, 396—399.

Received September 1, 2017

Accepted September 25, 2017



## EVALUATION OF THE GENOTOXIC EFFECT OF THE COMMERCIAL FUNGICIDE TANGO® SUPER ON BOVINE LYMPHOCYTES

Grajciarová, M., Holečková, B.

Institute of Genetics  
University of Veterinary Medicine and Pharmacy, Komenského 73, 041 81, Košice  
Slovakia

[martinagrajciarova@gmail.com](mailto:martinagrajciarova@gmail.com)

### ABSTRACT

This study investigated the potential genotoxic effects of the fungicide Tango® Super using methods of conventional cytogenetic analysis, fluorescence *in situ* hybridization (FISH) and detection of DNA fragmentation in bovine lymphocytes. After exposure of two donor cell cultures to several concentrations of fungicide (0.5, 3.0 and 15.0 mg.ml<sup>-1</sup> for conventional cytogenetic analysis; 0.5 and 3.0 mg.ml<sup>-1</sup> for FISH) we detected the insignificant occurrence of chromosome and chromatid breakages. In both donors we observed a significant decrease in mitotic index (MI) percentage with increasing concentrations of fungicide ( $P < 0.01$ ;  $P < 0.001$ ), which indicated a cytotoxic effect of the preparation. Electrophoretic analysis of DNA fragmentation in lymphocytes exposed to increasing concentrations (0.5; 1.5; 3.0; 6.0 and 15.0 mg.ml<sup>-1</sup>) of this preparation showed its ability to induce formation of fragments, which is a characteristic manifestation of the last stage of apoptosis.

**Key words:** chromosomal analysis; DNA fragmenta-

tion; fluorescence *in situ* hybridization; lymphocyte culture; systemic fungicide

### INTRODUCTION

Pesticides intended for the protection of plants against pests form the largest group of toxic chemical substances introduced into the environment. In addition to the load on the environment, these substances can also raise risk to health of humans and other animals [4, 5, 6].

Tango® Super is a spray fungicide with two active ingredients, fenpropimorph and epoxiconazole, with systemic and contact effects. It is used in the form of an emulsion to control leaf and spikelet diseases of cereals. This commercial preparation is known for various undesirable effects on humans and other animals. However, the genotoxic effects of the fungicide Tango® Super and its influence on farm animal's genetic material have not been investigated sufficiently.

Fenpropimorph belongs to the group of morpholins and inhibits the biosynthesis of sterols, compounds essen-

tial to fungi [1]. It has been assumed that this compound is not carcinogenic to man but experiments have shown that it induces malformations in rats (cheilognathopalatoschisis) and rabbits (skeletal retardations) [8]. Epoxiconazole belongs to the group of triazoles and affects budding of spores, growth of infectious mycelium and its branching. Studies revealed its effect on laboratory rats resulting in a significant increase in cholesterol and high levels of its residues in the liver, kidneys and testes [8].

The objective of our study was to evaluate the potential genotoxic effects of the fungicide Tango® Super by means of conventional cytogenetic analysis, fluorescence *in situ* hybridization (FISH) and detection of DNA fragmentation in bovine lymphocytes.

## MATERIALS AND METHODS

Our study was conducted in order to test the commercial fungicide Tango® Super (BASF SE, Germany), containing two active ingredients, fenpropimorph (cis-2,6-dimethyl-4-{2-methyl-3-[4-(2-methyl-2-propanyl)phenyl]propyl}morpholine; 250 g.l<sup>-1</sup>) and epoxiconazole (2RS,3SR)-1-[3-(2-chlorophenyl)-2,3-epoxy-2-(4-fluorophenyl)-propyl]-1H-1,2,4-triazole; 84 g.l<sup>-1</sup>).

Heparinized blood collected from two young healthy bulls was cultivated in 5 ml of the cultivation medium RPMI 1640 (Sigma, St. Louis, MO, USA), enriched with 15 % bovine foetal serum (BOFES, Sigma, Chemical Co. St. Louis, MO, USA), growth factors, antibiotics and an antimycotic (penicillin 100 U.ml<sup>-1</sup> a streptomycin 100 µg.ml<sup>-1</sup>, amphotericin B 0.25 µg.ml<sup>-1</sup>), and phytohaemagglutinin (PHA, 180 µg.ml<sup>-1</sup>, Wellcome, Dartford, England). Twenty four hours before the termination of the cultivation we added the fungicide Tango® Super to the cell culture of lymphocytes in concentrations of 0.5, 3.0 and 15.0 mg.ml<sup>-1</sup>. Fifty minutes before the end of cultivation, we added the inhibitor colchicine at a dose of 5 µg.ml<sup>-1</sup> (Merck, Darmstadt, Germany). Ethyl methane sulphonate (EMS, Sigma, St. Louis, MO, USA) in the concentration of 250 µg.ml<sup>-1</sup> was used as a positive control and dimethyl sulfoxide (DMSO, Sigma, St. Louis, MO, USA) in concentration of 0.1 % as a negative one.

The preparations intended for conventional cytogenetic analysis were stained with a 3 % solution of Giemsa stain diluted with phosphate buffer pH 7. A light microscope (Nikon, ECLIPSE E200) was used to evaluate the chro-

mosome and chromatid breakages in 100 well-distributed chromosomes in metaphase cells. We evaluated also the mitotic index (MI), a ratio between the cells in metaphase and 1 000 cells that did not undergo division.

The statistical evaluation of the MI reduction and induction of chromosomal aberrations by the pesticide was carried out by c2 method.

For the fluorescence *in situ* hybridization, 15 min before the termination of pre-hybridization, the preparation was placed into a denaturation solution (70 % formamide/2xSSC), dehydrated in alcohol sequence (70 %, 80 %, 96 % ethanol) and then a hybridization mixture prepared by mixing hybridization buffer MM with salmon DNA, DNA isolated from calf thymus and whole chromosome probes (BTA5 a BTA1) was pipetted onto the preparation. The preparation was then stained with 10 µ DAPI (4',6'-diamidino-2-fenolindol) and stable chromosomal aberrations of the type of reciprocal and non-reciprocal translocations were evaluated under a fluorescence microscope (NIKON LABOPHOT 1A/2, fluorescence filter FITC/TRITC).

For electrophoresis, DNA was isolated by means of the Apoptotic DNA Ladder kit (Roche Diagnostics GmbH, Mannheim, Germany). The DNA was analysed by electrophoresis in 1 % agarose solution (90 min., 75 V, buffer 1x TAE; TRIS-acetate-EDTA), stained with Gel Red™ (Biotium) and the results were documented by means of the Gel documentation system D1-HD (Major Science).

## RESULTS

After 24 h exposure of lymphocyte cultures to various concentrations of fungicide Tango® Super (0.5, 3.0 and 15.0 mg.ml<sup>-1</sup>), the conventional cytogenetic analysis showed the presence of unstable aberrations involving chromatid and chromosome breakages. The increased frequency of chromatid breakages was observed in both donors but the increase in chromosome breakages was detected only in one donor. Separately we investigated formation of chromatid and chromosomal gaps the frequency of which increased in both donors starting from the 3.0 mg.ml<sup>-1</sup> concentration of fungicide. Although the increase in frequency of breakages was insignificant, evaluation of the mitotic index (MI) showed a significant decrease in mitotic index percentage with increasing concentration of the fungicide in both

**Table 1. Unstable chromosome aberrations and gaps in cultivated bovine peripheral lymphocytes after 24h exposure to fungicide Tango® Super. Results were obtained by conventional cytogenetic analysis.**

Dose	Number of metaphases	Gaps		Breakages		Exchanges		% B (± SD)	% G + B (± SD)	% MI
		G I.	G II.	CB	IB	CE	IE			
<b>DONOR 1</b>										
Negative control (DMSO)	100	1	0	1	2	0	0	2.0 ± 0.14	4.0 ± 0.2	3.5
<b>Tango® Super concentration</b>										
0.5 µg.ml <sup>-1</sup>	100	1	1	3	1	0	0	4.0 ± 0.20a	6.0 ± 0.24a	2.9
3.0 µg.ml <sup>-1</sup>	100	4	3	2	1	0	0	3.0 ± 0.17a	10.0 ± 0.30a	1.5**
15.0 µg.ml <sup>-1</sup>	100	3	5	4	1	0	0	5.0 ± 0.22 a	13.0 ± 0.34*	1.1***
Positive control (EMS 250 µg.ml <sup>-1</sup> )	100	6	2	15	4	1	0	21 ± 0.40***	29 ± 0.45***	1.2***
<b>DONOR 2</b>										
Negative control (DMSO)	100	3	0	1	0	0	0	1.0 ± 0.1	4.0 ± 0.2	3.3
<b>Tango® Super concentration</b>										
0.5 µg.ml <sup>-1</sup>	100	2	1	1	2	0	0	3.0 ± 0.17a	6.0 ± 0.24a	2.6
3.0 µg.ml <sup>-1</sup>	100	5	1	1	2	0	0	3.0 ± 0.17a	9.0 ± 0.29a	1.6*
15.0 µg.ml <sup>-1</sup>	100	4	4	2	1	0	0	3.0 ± 0.17a	11.0 ± 0.31a	1.2**
Positive control (EMS 250 µg.ml <sup>-1</sup> )	100	5	2	14	5	0	0	19.0 ± 0.39***	26.0 ± 0.43***	1.3***

a — insignificant; \*, \*\*, \*\*\* — significant at the levels  $P < 0.05$ ,  $P < 0.01$ ,  $P < 0.001$ , respectively; G1, G2 — chromatid and chromosome gaps; CB, IB — chromatid and chromosome breakage; CE, IE — chromatid and chromosome exchange; MI — mitotic index

**Table 2. Frequency of aberrations in cultivated bovine peripheral lymphocytes after 24 h exposure to the fungicide Tango® Super. Results were obtained by fluorescence *in situ* hybridization**

	Number of metaphases	Fragmentation BTA5	Fragmentation BTA1	Separation in centromere BTA5	Separation in centromere BTA1	Monosomy BTA5	Monosomy BTA1
<b>DONOR 1</b>							
Control (DMSO)	250	0	0	0	0	0	0
<b>Tango® Super concentration</b>							
0.5 µg.ml <sup>-1</sup>	250	1	1	0	0	0	0
3.0 µg.ml <sup>-1</sup>	250	1	0	0	0	0	1
<b>DONOR 2</b>							
Control (DMSO)	250	0	0	0	0	0	0
<b>Tango® Super concentration</b>							
0.5 µg.ml <sup>-1</sup>	250	1	0	0	0	0	0
3.0 µg.ml <sup>-1</sup>	250	0	0	2	0	0	0

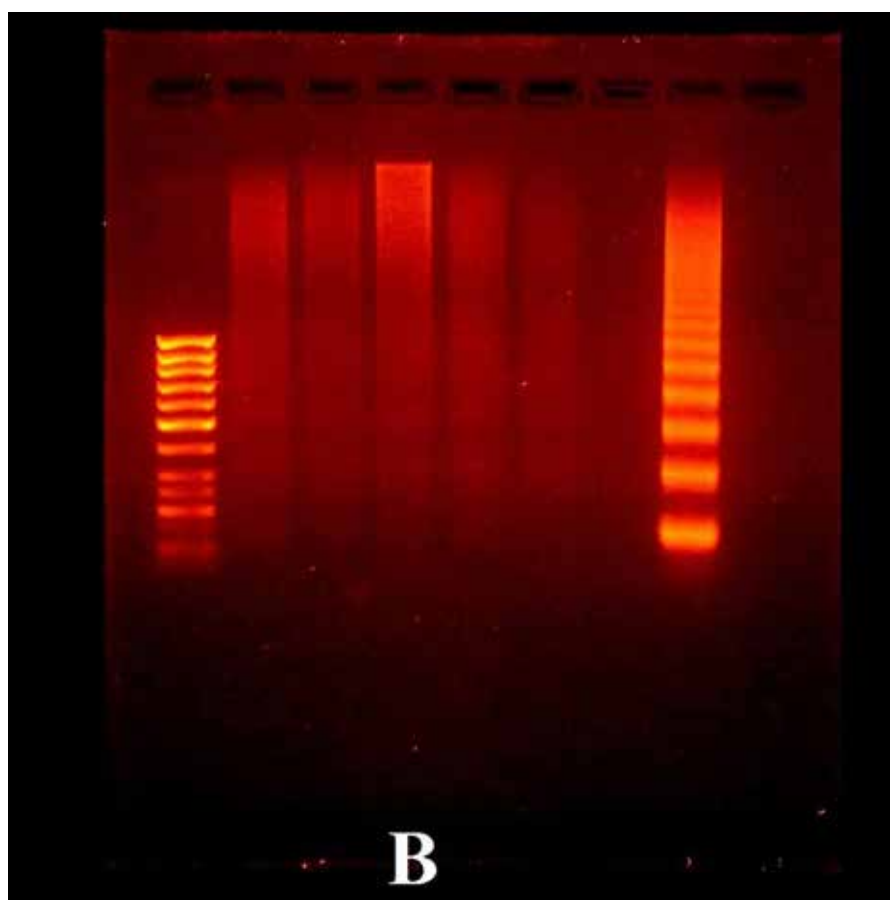
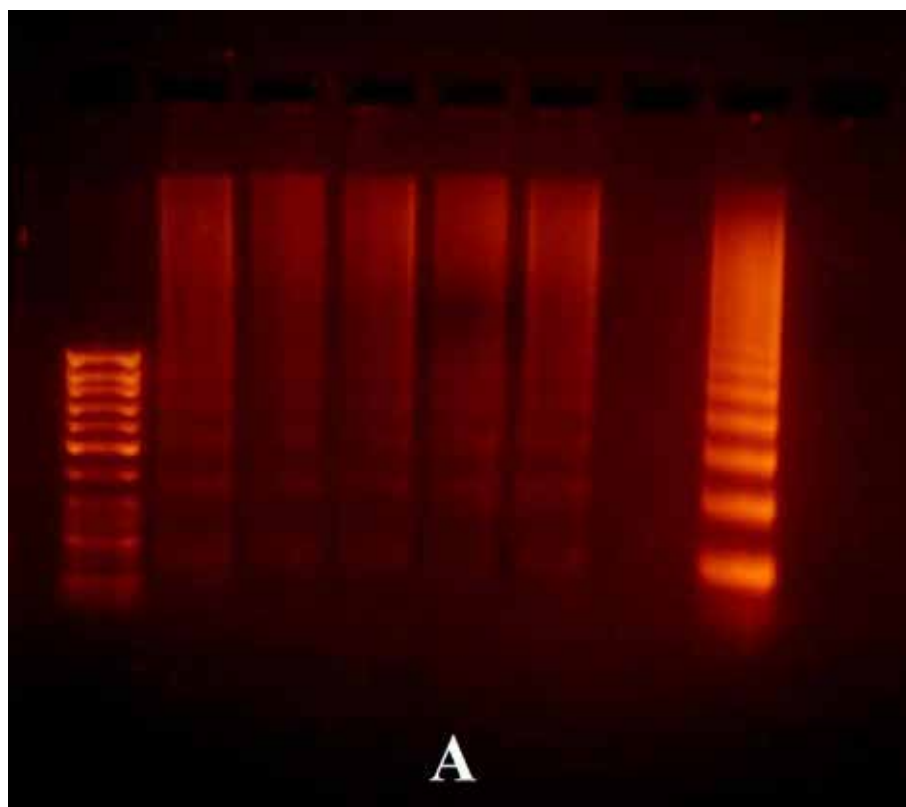


**Fig. 1. Fragmentation of DNA in cultivated bovine lymphocytes exposed to the tested fungicide**  
 Pathways from the left: standard of molecular weight 100 bp, Tango® Super 0.5; 1.5; 3.0; 6.0; 15.0 mg.ml<sup>-1</sup>; negative control DMSO;  
 positive control — U937 cells treated by camptothecin 4 mg.ml<sup>-1</sup>; negative control — water; A — donor 1, B — donor 2

donors ( $P < 0.01$ ;  $P < 0.001$ ). The changes observed in the mitotic index can be considered a manifestation of cytotoxic properties of the preparation. The frequency of chromosomal aberrations and % MI in cultivated lymphocytes following the 24 h exposure to fungicide Tango® Super are presented in Table 1.

In the second part of our study, we investigated the effect of Tango® Super (0.5 a 15.0 mg.ml<sup>-1</sup>) by means of fluorescence *in situ* hybridization, using whole-chromosome probes BTA1 (green fluorescence stain) and BTA5 (red fluorescence stain) for the detection. In the lymphocytes from the first bull, both concentrations of the fungicide caused the production of fragments which formed separate groups. Their development was considered proof that the preparation causes breakages. BTA1 monosomy was observed after exposure to the concentration of 3.0 mg.ml<sup>-1</sup>. In lymphocytes from the second bull, the concentration of 0.5 mg.ml<sup>-1</sup> produced one fragment and 3.0 mg.ml<sup>-1</sup> induced two separations in the centromere which were categorised again as a specific aberration. The frequency of aberrations after 24 h exposure to the fungicide Tango® Super is presented in Table 2.

In the third part of our study we used electrophoretic analysis of DNA fragmentation in agarose gel and found out that all tested concentrations of the fungicide (0.5; 1.5; 3.0; 6.0; 15.0 mg.ml<sup>-1</sup>) were able to induce fragments (Fig. 1).

## DISCUSSION

The genotoxic effects of the fungicide Tango® Super on the health of humans and other animals have not yet been studied sufficiently. Conventional cytogenetic analysis used in our study failed to confirm the genotoxic effect of the tested fungicide as no significant dose-dependent increase in chromosomal aberrations was observed in comparison with the negative control (DMSO). Our results are supported by the findings of Galdíková et al. [3] who failed to observe a significant clastogenic effect of this preparation on bovine lymphocytes. Schwarzbacherová et al. [9] conducted experiments with Tango® Super and reported that it induced apoptosis already at a concentration of 1.5 mg.ml<sup>-1</sup>, with the highest proportion of apoptotic cells occurring between concentrations 3.0 and 6.0 mg.ml<sup>-1</sup>. Similar to the above study, our results obtained by electrophoretic separation of characteristic DNA fragments allowed us to as-

sume that the fungicidal preparation is capable of inducing apoptosis. The formation of fragments (DNA laddering) is a typical feature of degradation of DNA by DNases that are activated by caspases in the key phase of apoptosis [2]. The test of DNA fragmentation is considered a simple and rapid method of evaluation of cell apoptosis [7].

## CONCLUSIONS

When evaluating the potential genotoxic effect of various types of fungicides, it is important to investigate their lowest concentrations as their long-term use may result in development of tumour diseases. The conventional cytogenetic method used in our study indicated a significant dose-dependent decrease in the percentage of the mitotic index and the presence of unstable aberrations. By means of the FISH method, we evaluated the formation of DNA fragments, separation in the centromere, and monosomy. Electrophoretic analysis allowed us to detect DNA fragmentation induced by all concentrations, probably due to apoptosis.

## ACKNOWLEDGEMENT

*The study was supported by grants VEGA 1/0043/15 and VEGA 1/0176/16.*

## REFERENCES

1. Bjornlund, L., Ekelund, F., Christensen, S., Jacobsen, C. S., Kroh, P. H., Johnsen, K., 2000: Interaction between saprotrophic fungi, bacteria and protozoa on decomposing wheat roots in soil influenced by the fungicide fenpropimorph (Corbelâ): a field study. *Soil Biol. Biochem.*, 32, 967–975.
2. Elmore, S., 2007: Apoptosis: A review of programmed cell death. *Toxicol. Pathol.*, 35, 495–516.
3. Galdíková, M. et al., 2014: Chromosomal aberrations induced by fungicide Tango® Super in bovine peripheral lymphocytes. *Priemyselná toxikológia (Industrial Toxicology)* (In Slovak). Slovak Technical University, Bratislava, 33–37.
4. Garaj-Vrhovac, V., Zeljezic, D., 2002: Assessment of genome damage in a population of Croatian workers employed in pesticide production by chromosomal aberration analysis,

- Micronucleus assay and Comet assay. *J. Appl. Toxicol.*, 22, 249—255.
5. **Matušova, M., Ďurčanská, J., 2010:** Evaluation of official control of pesticide residues in foodstuffs in 2009 (In Slovak). *Slovenský veterinársky časopis* (Slovak Veterinary Journal), 35, 186—191.
  6. **Pistl, J., Kovalkovičová, N., Legáth, J., Mikula, I., Holovská, V., 2004:** *Immunotoxicology in Veterinary Medicine* (In Slovak). 1st edn., University of Veterinary Medicine, Košice, 154 pp.
  7. **Saadat, Y. R., Saeidi, N., Zununi Vahed, S., Barzegari, A., Barar, J., 2015:** An update to DNA ladder assay for apoptosis detection. *Bioimpacts*, 5, 25—28.
  8. **Schmidt, F., Marx-Stoelting, P., Haider, W., Heise, T., Kneuer, C., Ladwig, M. et al., 2016:** Combination effects of azole fungicides in male rats in a broad dose range. *Toxicology*, 355—356, 54—63.
  9. **Schwarzbacherova, V., Wnuk, M., Lewinska, A., Potocki, L., Zebrowski, J., Koziorowski, M., 2017:** Evaluation of cytotoxic and genotoxic activity of fungicide formulation Tango® Super in bovine lymphocytes. *Environ. Pollut.*, 220, 255—263.

Received July 1, 2017

Accepted September 27, 2017



## DETECTION OF MUTATIONS IN SELECTED PROTO-ONCOGENES OF CANINE LYMPHOMA

**Bóna, G., Šiviková, K.**

Department of Biology and Genetics, Institute of Genetics  
University of Veterinary Medicine and Pharmacy, Košice  
Slovakia

katarina.sivikova@uvlf.sk

### ABSTRACT

Lymphomas belong among the most frequently diagnosed tumours of the haematopoietic system in dogs. The clinical manifestations and genetic and molecular basis of canine lymphoma resembles those of human non-Hodgkin lymphoma and therefore it can serve as a suitable model for the study of this disease. Neoplastic diseases are the consequence of a number of genetic and epigenetic changes in somatic cells. One of such changes are gene mutations that can subsequently cause changes in the activity of proto-oncogenes and tumour suppressor genes. The aim of our study was to detect potential mutations in selected exons of proto-oncogenes in DNA isolated from samples of lymphoma obtained from two donors — a Bernese Mountain Dog and a female mongrel. On the basis of literary data descriptions of human and canine haematopoietic neoplastic diseases, our investigations of potential changes in DNA focused on proto-oncogenes C-KIT — exons 8, 17; NRAS — exons 1, 2;

FLT3 — exons 14, 15 and 20. The investigated samples were amplified by polymerase chain reaction (PCR) and subjected to sequencing. The DNA sequences were compared with reference sequences in the database Ensembl. The comparison of sequences of the C-KIT gene revealed an A/G transition at the 35th nucleotide of exon 8 in the mongrel. It involved a synonymous exchange of the nucleotide in the codon that did not cause a change in the amino acid. In the same sample we recorded several point mutations in the intron regions surrounding the exons 14 and 20 of the FLT3 gene. Changes in the intron regions can affect the expression of genes and thus can play an important role in the origin and development of tumours. No genetic mutations were detected in any gene regions of the Bernese Mountain Dog. In the case of the NRAS gene, no changes were observed in any sample collected from the donors.

**Key words:** canine lymphoma; carcinogenesis; C-KIT; FLT3; NRAS; proto-oncogene



## INTRODUCTION

Tumour diseases are currently one of the most frequently occurring diseases resulting in high mortality rates [11]. Tumours are considered genetic diseases as their origin and development is associated essentially with changes at the genetic or epigenetic levels in proto-oncogenes and tumour-suppressor genes [15].

Lymphomas are a heterogeneous group of tumour diseases of the immune system blood cells of the lymphoid line. On the basis of pathological findings, lymphomas are divided to two basic categories: non-Hodgkin lymphoma (NHL) and Hodgkin lymphoma (HL). In humans, lymphomas account for 3–4% of all tumour diseases [9]. However, in dogs they belong among the most frequent types of tumours [14]. The frequency of disease occurrence and similar carcinogenic load on humans and dogs (*Canis lupus familiaris*) in their common environment are advantageous with respect to investigation of individual types of tumours [5].

The most frequent changes described in relation to lymphomas in humans are translocations in genes MYC, BCL2, BCL6, short mutations/deletions in genes TNFAIP3, PRDM1, EZH2, or amplification of gene JAK2 [1]. Mutations in proto-oncogenes C-KIT, FLT3 and NRAS have been described in association with a number of haematological malignancies including lymphomas. The frequency of these mutations in canine lymphomas has not been specified [13].

The aim of our study was to detect potential genetic changes in selected sections of DNA (exons and/or introns) of the three above mentioned proto-oncogenes.

## MATERIALS AND METHODS

### DNA isolation

Samples of genomic DNA were isolated from dog lymphomas by a column-based method employing QIAGEN DNeasy® Blood and Tissue Kit (Qiagen, Venlo, the Netherlands). Sample 1 was isolated from the lymph node tissue of a 10 years old female mongrel. Sample 2 was obtained from the spleen of a 12 years old Bernese Mountain Dog. The reference DNA sample was isolated from the blood of a healthy Jack Russell Terrier. was used as a positive control.

### Selection of primers, PCR and electrophoresis

Primers were selected by means of software Primer3Plus on the basis of the reference DNA sequences obtained from the database Ensembl. Table 1 shows sequences of the proposed oligonucleotides, access codes of genes and length of the proposed products.

The total volume of the reaction mixture used for PCR was 25 µl, which consisted of: 21.1 master-mix (FirePOL®); 1.2 µl forward primer; 1.2 µl reverse primer; 0.5 µl DNA polymerase (FirePOL®); 1.0 µl sample. The PCR programme consisted of five steps: initial denaturation of DNA at 95 °C for 5 min; denaturation of DNA at 95 °C for 30 s; annealing of primers at 54–56 °C for 45 s; amplification of the product at 72 °C for 45 s; final extension at 72 °C for 45 s. Steps 2–4 were repeated in 30–35 cycles. The PCR products were analysed by electrophoresis in agarose gel, stained by intercalation stain GelRed (Biotinum, Hayward, CA, USA) and visualised under UV light (GenoView Smart M-VWR GenoView, Radnor, PA, USA).

**Table 1. Primers selected for PCR**

Gene (database access code)	Investigated region	Forward primer (5'→3')	Reverse primer (5'→3')	Product length (bp)
<b>C-KIT</b> (ENSCAFG0000002065.4)	exon 8	TTCACTACTGGTCCGATGC	CCTATCTGAAGTTCAACTACC	340 bp
	exon 17	GTGACATAGCAGCATTCTCG	GCATGGTATCTCAAAGGTAGG	333 bp
<b>FLT3</b> (ENSCAFG00000006716)	exons 14, 15	GGCCCTTCCCTTTCATCCAA	CCATGCCTCCCATTTTGTGC	572 bp
	exon 20	GGTGGTGGCCAGTAAAGAT	GAAGCTTTTGGATGCTGCCA	388 bp
<b>NRAS</b> (ENSCAFG00000009532)	exon 1	TTCACGTGTATGCAGCCGAT	TACTCCTGAATGCAGACCC	379 bp
	exon 2	TGGAAAGAAGCTCAGCTAGGAGC	TCCCTAATGCGGTATCCTCA	387 bp

## DNA sequencing

The DNA sequencing was done by an ABI PRISM 3100-Avant Genetic Analyser (Applied Bio-systems, Waltham, MA, USA) in the Laboratory of Biomedical Microbiology and Immunology of the University of Veterinary Medicine and Pharmacy (UVMP) in Košice. The sequences obtained from samples were compared with reference sequences using algorithms BLAST (“Basic Local Alignment Search Tool”): BLASTN and BLASTX, at web interface Ensembl.

## RESULTS

From the C-KIT gene we obtained sufficient amounts of amplified sections of exons 8 and 17 from both samples (Fig. 1a). In sample 1 (mongrel) we detected a nucleotide exchange — transition G/A (Fig. 1b) in exon 8 at the 67290

nucleotide of C-KIT gene (ENSCAFG00000002065.4) (Fig. 1c). In the database Ensembl this mutation is described as single-nucleotide polymorphism (SNP) (under identification number rs22299980). No mutation in exon 17 was observed in the mongrel. In the Bernese Mountain Dog (sample 2) no mutations were detected in either of two exons.

From the FLT3 gene we obtained from both samples sufficient amount of amplified sections that included exons 14—15 and 20 and the surrounding intron regions (Fig. 2a). In sample 1 (mongrel) we detected several changes in intron regions close to exons 14 and 15 (Fig. 2d); in 34 nt position in front of exon 14 — transversion A/C (Fig. 2b), and in 263 nt position, between exons 14 and 15 — transition G/A (Fig. 2c).

When comparing sample 1 with the reference sequence (Fig. 3a), we detected a transition C/T (Fig. 3b) in the intron region behind exon 20, in 242 nt position. In the sec-

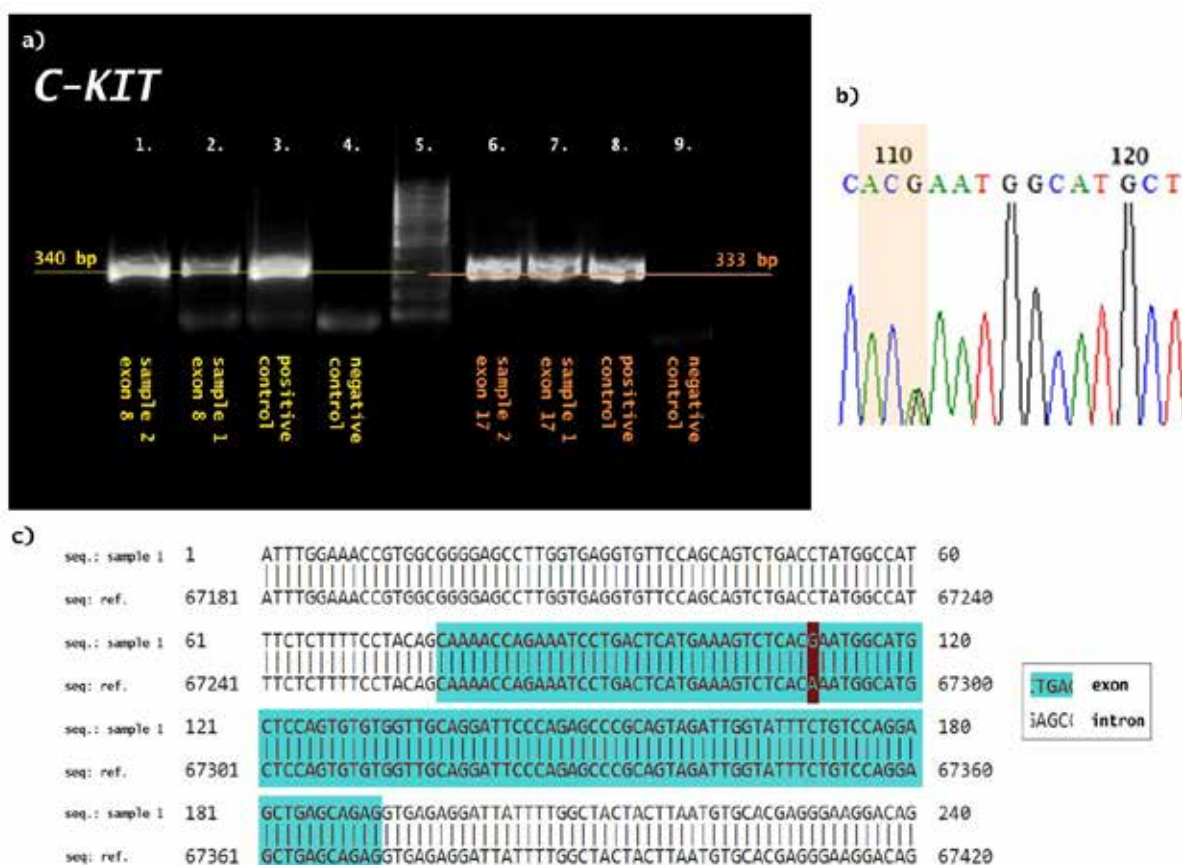


Fig. 1. Electrophoretic evaluation of the amplification of C-KIT gene sections — exons 8 and 17 — the 100 bp DNA ladder is located in the central (5th) column. Numbers of bp shown on the sides of the picture give the exact number of base pairs in the proposed section. DNA sequence with highlighted nucleotide exchange — G/A transition in exon 8 at the 67290 nucleotide of C-KIT gene. Comparison of DNA sequence of sample 1 (mongrel) with reference sequence; nucleotide exchange is located at the 33rd nucleotide of exon 8

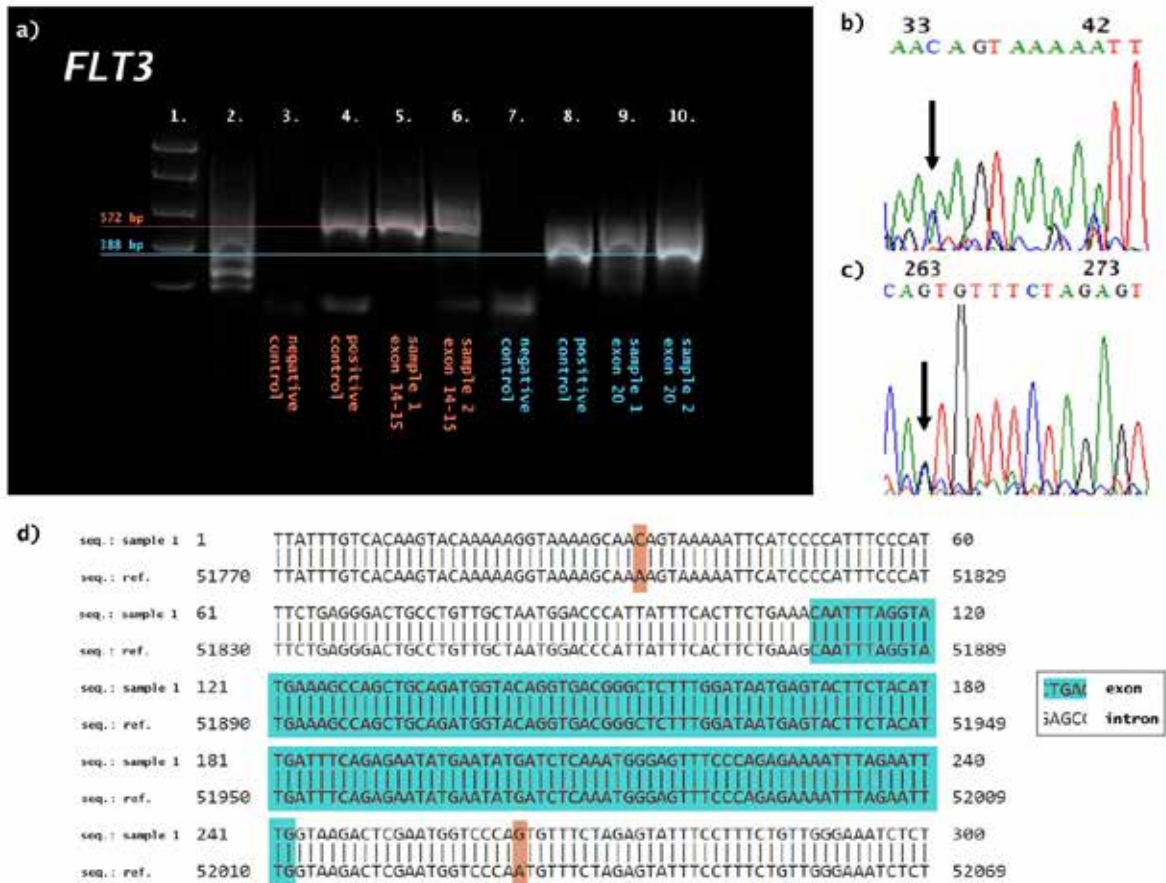


Fig. 2. a) Electrophoretic determination of amplification of gene FLT3 sections — exons 14, 15 and 20. The first column shows DNA ladder with divisions 100 bp, 400 bp, 800 bp, 2000 bp and 5000 bp. The 100 bp DNA ladder is in the second column. Coloured numbers of base pairs on the left of this figure correspond to the exact number of bp of the proposed product; b) DNA sequence with highlighted nucleotide exchange — C/A transversion in FLT3 gene, position 34; c) SDNA sequence with highlighted nucleotide exchange — G/A transition in FLT3 gene, position 263; d) Comparison of DNA sequence of sample 1 (mongrel) with reference sequence — gene FLT3, exon 14

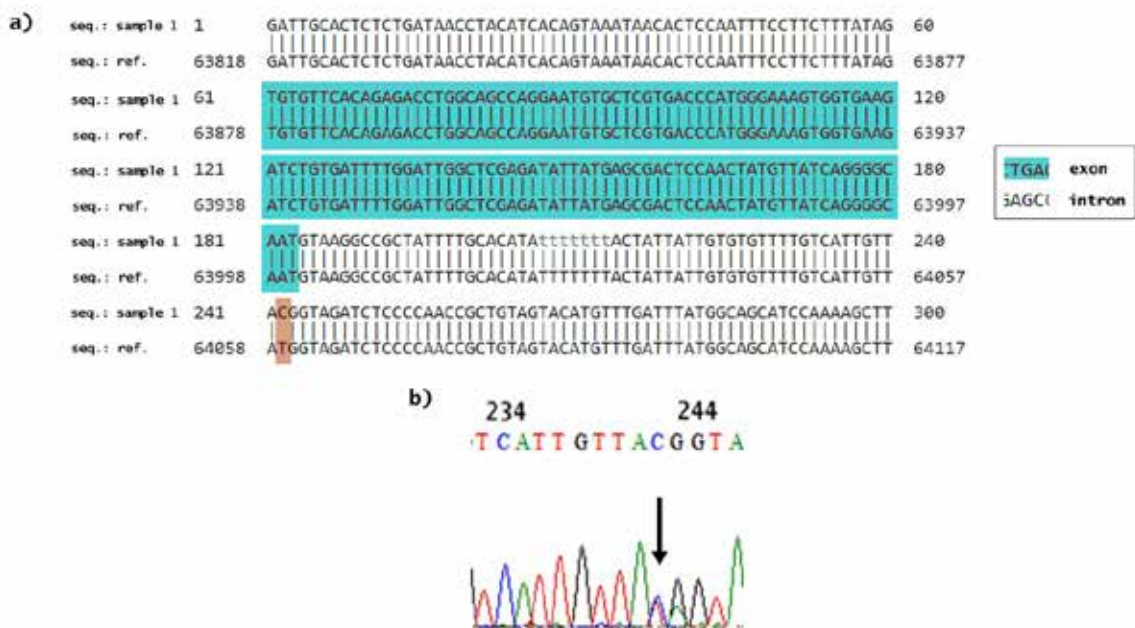


Fig. 3. Comparison of DNA sequence of sample 1 (mongrel) with the reference sequence — FLT3 gene, exon 20  
DNA sequence with arrow indicating nucleotide exchange — C/A transversion, FLT3 gene, position 242

ond sample no exchange in DNA sequence was observed either in exons 14, 15 and 20, or their surroundings.

From the NRAS gene we obtained from both samples sufficient amounts of amplified sections that included exons 1 and 2. No changes in the selected sections were observed in any of the two samples.

## DISCUSSION

Lymphomas belong among the most frequent tumour diseases in dogs. The selection of proto-oncogenes in our samples from the mongrel and Bernese Mountain Dog was based on the data from the literature describing mutations in proto-oncogenes C-KIT, FLT3 and NRAS.

Proto-oncogene C-KIT encodes a tyrosine kinase receptor that is essential for normal haematopoiesis, pigmentation, fertility and other functions. The canine KIT protein is composed of 975 amino acids. Our study showed no mutations in selected exons (8 and 17) of the C-KIT gene resulting in the exchange of amino acids in this protein. Synonymous exchange, A/G transition, was recorded in 425th codon, nucleotide 67290, encoding the amino acid threonine. This involves a synonymous variant, i.e. a change that has already been observed in dogs [13] and does not affect the significance of the codon. Our results agree with those of Giantin et al. [3] according to which the occurrence of mutations in canine lymphoma C-KIT gene is rare.

In relation to the damage in the C-KIT gene, cases have been described of acute myeloid leukaemia [13] and adipose cell tumours [6]. London et al. [6] reported the occurrence of intragene tandem duplications in exons 11 and 12 associated with tumour diseases of mastocytes. In dogs with acute myeloid leukaemia diagnosis, Usher et al. [13] found silent mutations in exon 8, codon 425, and a number of point mutations resulting in changes in AMK sequence in the exon 17. In the aggressive canine T-cell lymphomas, Giantin et al. [3] observed increased expression of C-KIT oncogene in comparison with less aggressive forms of the disease, while in B-cell lymphomas expression of this protein was reduced.

FLT3 is a tyrosine-kinase receptor included in the same family of receptors as KIT. It plays an important role in normal development and proliferation of stem and progenitor cells of the haemopoietic system [10]. In the sample obtained from the Bernese Mountain Dog in our study

we did not record any exchange in the investigated exons. Several point mutations were detected in FLT3 gene in the sample from the mongrel, namely three exchanges in the intron regions in the surroundings of exons 14–15 and exon 20. Transversion A/C in 51803 nt position has not yet been described in the database Ensembl. Transition G/A in position 52033 nt and transition C/T in position 64059 nt of the gene have been described in the database Ensembl as intron variants, i.e. single nucleotide polymorphisms. Intron sequences have been considered in the past as useless DNA, however, the recent results of molecular genetics indicate that intron SNP may affect initiation, elongation and termination of transcription, polyadenylation, export of mRNA from cell nucleus and the stability of the relevant mRNA [4].

Usher et al. [13], described intragene tandem duplications in exons 14 and 15 of gene FLT3 in 3 out of 57 cases of canine acute myeloid leukaemia. In this study, the authors identified also point mutation changing importance of a codon in exon 20. Other authors [12] reported the occurrence of intragene tandem duplications and increased values of mRNA of the gene in 2 out of 7 cases.

The family of RAS genes includes genes NRAS, HRAS and KRAS, that encode small intracellular proteins (189 amino acids) bound to cellular membrane. The primary structure of protein RAS is conserved in a large number of mammals. These genes exhibit GTPase activity, partaking in a number of signalling pathways. They mediate signals affecting proliferation, differentiation and apoptosis of cells [8]. Mutations in the proto-oncogenes of RAS family have been frequently described in relation to various neoplasms in rodents and man. Activating point mutations have been observed particularly in exons 1 and 2 of NRAS gene, namely in codons 12, 13 and 61 [2].

In our study we observed no change in genetic code in comparison with reference sequence, which is in agreement with observations of Mayr et al. [7] who reported that activation of proto-oncogene NRAS in canine lymphoma is rare.

## CONCLUSIONS

The results of our study allowed us to conclude that proto-oncogenes C-KIT and NRAS probably did not play an important role in the process of lymphomagenesis in dogs.

We identified a silent mutation caused by nucleotide exchange in exon 8 of gene C-KIT and SNP in intron regions in the surroundings of exons 14, 15 and 20 of gene FLT3. SNP can be found in various regions of genomic DNA and occur relatively frequently in dogs. SNP in introns may cause their erroneous expression, either due to aberrant splicing or error in the regulation region of the gene and thus affect the process of carcinogenesis.

More information may be obtained by the study of the changes in gene expression or epigenetic changes, particularly in the Bernese Mountain Dog, since our study dog was in an advanced stage of the disease.

## ACKNOWLEDGEMENT

*This study was supported by the projects VEGA 1/0043/15 and VEGA 1/0176 MŠ SR.*

## REFERENCES

1. Devita, V. T., Lawrence, T. S., Rosenberg, S. A., 2015: *Cancer: Principles and Practice of Oncology*, 10th edn., Lippincott Williams and Wilkins, 2234 pp.
2. Edwards, M. D., Pazzi, K. A., Gumerlock, P. H., 1993: cN-ras is activated infrequently in canine malignant lymphoma. *Toxicol. Pathol.*, 21, 288—291.
3. Giantin, M., Aresu, L., Aricò, A., Gelain, M. E., Riondato, F., Comazzi, S. et al., 2013: Evaluation of tyrosine-kinase receptor c-kit mutations, mRNA and protein expression in canine lymphoma: Might c-kit represent a therapeutic target? *Vet. Immunol. Immunopathol.*, 154, 153—159.
4. Chorev, M., Carmel, L., 2012: The function of introns. *Frontiers in genetics*, 3, 1—15.
5. Ito, D., Frantz, A. M., Modiano, J. F., 2014: Canine lymphoma as a comparative model for human non-Hodgkin lymphoma: recent progress and applications. *Vet. Immunol. Immunopathol.*, 159, 192—201.
6. London, C. A., Galli, S. J., Yuuki, T., Hu, Z. Q., Helfand, S. C., Geissler, E. N., 1999: Spontaneous canine mast cell tumors express tandem duplications in the proto-oncogene c-kit. *Exp. Hematol.*, 27, 689—697.
7. Mayr, B., Winkler, G., Schaffner, G., Reifinger, M., Brem, G., 2002: N-ras mutation in a feline lymphoma. Low frequency of N-ras mutations in a series of feline, canine and bovine lymphomas. *Vet. J.*, 163, 326—328.
8. Richter, A., Escobar, H. M., Gunther, K., Soller, J. T., Winkler, S., Nolte, I. et al., 2005: RAS gene hot-spot mutations in canine neoplasias. *J. Hered.*, 96, 764—765.
9. Roman, E., Smith, A. G., 2011: Epidemiology of lymphomas. *Histopathology*, 58, 4—14.
10. Small, D., 2006: FLT3 mutations: biology and treatment. *ASH Education Program Book*, 2006, 178—184.
11. Stewart, B. W., Wild, C. P., 2014: *World Cancer Report 2014*. Lyon, International Agency for Research on Cancer, 630 pp.
12. Suter, S. E., Small, G. W., Seiser, E. L., Thomas, R., Breen, M., Richards, K. L., 2011: FLT3 mutations in canine acute lymphocytic leukemia. *BMC cancer*, 11, 38.
13. Usher, S. G., Radford, A. D., Villiers, E. J., Blackwood, L., 2009: RAS, FLT3, and C-KIT mutations in immunophenotyped canine leukemias. *Exp. Hematol.*, 37, 65—77.
14. Valli, E. V., San Myint, M., Barthel, A., Bienzle, D., Caswell, J., Colbatzky, F. et al., 2011: Classification of canine malignant lymphomas according to the World Health Organization criteria. *Vet. Pathol.*, 48, 198—211.
15. Weinberg, R., 2013: *The Biology of Cancer*. Garland Science, 876 pp.

*Received June 5, 2017*

*Accepted September 28, 2017*



## OPPORTUNISTIC PROTOZOAN INFECTIONS OF CARNIVORES

Mravcová, K., Ferko, M., Štrkolcová, G., Goldová, M.

Institute of Parasitology  
University of Veterinary Medicine and Pharmacy, Komenského 73, 041 81 Košice  
Slovakia

maria.goldova@uvlf.sk

### ABSTRACT

Giardiasis and cryptosporidiosis are protozoan infections of the digestive tract and one of the most frequent causes of enteritis in dogs and cats, associated with acute and chronic diarrhoea. Generally, the risk of infection is higher for younger individuals in which the overall clinical picture and the course of disease are more serious. In this study we investigated the prevalence of giardiasis and cryptosporidiosis in dogs in Košice district of eastern Slovakia. From September 2015 until November 2016, we examined samples of faeces from 100 dogs from two shelters. *Giardia duodenalis* was diagnosed by the flotation method according to Faust, and by the molecular biologic method (Nested PCR). For the diagnosis of cryptosporidium oocysts, we used a staining method according to Kinyoun, and for detection of the presence of *Cryptosporidium* spp. a sandwich ELISA method. The total prevalence of these protozoan infections were 22% (22/100), and of that, 19% of the samples (19/100) were positive for *Giardia duodenalis* and 3% (3/100) for the *Cryptosporidium* spp. In the shelter in Haniska, the giardia cysts were present in 9/54 samples (16.6%) and cryp-

tosporidia oocysts in 1/54 (1.85%) samples of the faeces. In the Malá Farma shelter, 10/46 (21.73%) samples were positive for *G. duodenalis* and 2/46 (4.34%) showed positivity for *Cryptosporidium* spp.

**Key words:** cryptosporidiosis; dog shelters; giardiasis

### INTRODUCTION

In September 2004, the World Health Organization (WHO) included cryptosporidiosis and giardiasis in the “Neglected Diseases Initiative” [19]. These protozoan infections belong among opportunistic waterborne and foodborne diseases [23]. They can cause serious infections with pronounced clinical signs, particularly in immunosuppressed individuals [13].

Giardiasis is a protozoan parasitic disease affecting the gastrointestinal tract. *Giardia duodenalis* is located in the distal duodenum and proximal and central jejunum, blocking the absorption of nutrients. It is one of the most wide spread intestinal infections in both the temperate and tropical zones. Giardiasis can present with a broad range of clini-



cal manifestation from asymptomatic through moderate up to serious, and the outcome may also be fatal. The clinical signs usually include diarrhoea frequently alternating with constipation, abdominal pain, excess fat in the faeces (steatorrhea) and flatulence [14]. Young and immunodeficient individuals are afflicted most frequently. In addition to its classical intestinal presentation, giardiasis may cause ocular complications, arthritis, skin allergies or myopathy. Moreover, giardiasis is now a well-established cause of failure to thrive, stunting and growth retardation in human and other animals, diminished cognitive functions, and chronic fatigue. Finally, *Giardia* may lead to post-infectious functional gastrointestinal disorders such as irritable bowel syndrome and functional dyspepsia. A few cases of *Giardia trophozoites* associated with tumoral masses have also been reported, but a definite cause and effect relationship between giardiasis and cancer have yet to be established [12].

*Giardia duodenalis* is divided into eight genetically distinct genotypes (assemblages) A-H; the A and B assemblages exhibit the greatest zoonotic potential. Assemblages C and D were detected in dogs and other canines [3].

Cryptosporidia are single celled parasites included in the phylum Apicomplexa. They are cosmopolitan parasites with an affinity for the digestive tract, but affecting also the respiratory tract. Clinical manifestations are common in the young, while in older animals the infections may be asymptomatic. The disease in carnivores is caused by oocysts of *Cryptosporidium canis*, *C. felis*, *C. parvum*, *C. muris* and *C. meleagridis* [16]. In humans the disease is caused mainly by *Cryptosporidium hominis*, particularly in immunodeficient patients and may raise serious risk with fatal consequences to HIV-positive individuals. Children infected with *C. hominis* shed higher levels of oocysts because they have an underdeveloped immune system and oocysts can proliferate easier, possibly contributing to the increased prevalence and spread of *C. hominis* within these communities [22]. Because humans are infected mostly with *Cryptosporidium hominis* and *C. parvum*, the role of companion animals in the transmission of human cryptosporidiosis may be limited. Even though a small number of humans are infected with *C. canis* and *C. felis*, recent findings of concurrent *C. hominis* infection in *C. canis*-infected persons suggest that many of the *C. canis* infections in humans may be due to anthroponotic rather than zoonotic transmission [4].

Giardiasis and cryptosporidiosis are transmitted directly by the faecal-oral route and by the consumption of

food or water contaminated with cysts and oocysts [7]. The transmission of both diseases can occur from man to man, from animal to animal, and by zoonotic transmission (from animal to man and vice versa). Another potential way of transmission is indirect, through a contaminated environment [17]. Waterborne contamination is a growing concern causing widespread disease outbreaks. Factors that have contributed to the emergence of cryptosporidiosis in animals include increased environmental contamination and trends in livestock production [18].

The aim of this study was to determine the prevalence of giardiasis and cryptosporidiosis in dog shelters located in the Košice district of eastern Slovakia, and to suggest potential ways to decrease these opportunistic infections.

## MATERIALS AND METHODS

From September 2015 until November 2016, we examined the faeces of dogs from two shelters: Union for mutual help between humans and animals (UVP) in Haniska vilage (54 samples) about 34 km away from Košice and Malá Farma (private shelter) at the periphery of Košice (46 samples) in eastern Slovakia.

The faeces were collected from dogs of different age categories and breeds including mongrels. The faecal samples were examined by flotation method according to Faust et al. [6] using zinc sulphate solution (specific gravity 1.18 g.cm<sup>-3</sup>), with microscopic observation of *Giardia* cysts [8]. The molecular diagnosis of *Giardia duodenalis* was performed by the nested PCR as described by Sulaiman et al. [20], based on the amplification of the triosephosphate isomerase (*tpi*) gene. *Cryptosporidium* oocysts were diagnosed using the staining method of Kinyoun [8]. The presence of *Cryptosporidium* spp. was confirmed by the commercial kit sandwich ELISA (Diagnostic automation, Inc., CA, USA, 91302).

## RESULTS

In the UVP shelter, the dogs lived in rather crowded sheds and the hygiene level in this shelter was low. Also, veterinary care of the animals was limited. The total prevalence of *Giardia duodenalis* in this shelter reached 16.6% (9/54). In faecal smears stained with the Kinyoun stain,

we detected *Cryptosporidium* spp. in 1 out of 54 examined dog (1.85%). This sample was positive also by the ELISA method.

In the private shelter in Malá Farma, *G. duodenalis* cysts were present in 21.73% of the samples (10/46). The examination of faecal smears stained according to Kinyoun, showed the presence of *Cryptosporidium* spp. oocysts in 2.17% (1/46) of the samples and the ELISA test confirmed the presence of *Cryptosporidium* antigen in 4.34% of the samples (2/46).

Eight of the microscopically positive samples were subjected to genotyping of *G. duodenalis* by the nested PCR. After BLAST analysis and subsequent comparison of the sequences of our positive samples with sequences existing in GenBank, we detected 99% to 100% similarity with assemblage C in four samples which corresponded to access number JN587492, obtained from dog from Croatia, and AY228641, obtained from a dog from the USA.

## DISCUSSION

The examination of dogs kept under poor hygiene conditions in dog shelters in Košice district showed a high prevalence of giardiasis. Of the total of 100 samples, cysts of *G. duodenalis* were found in 19 samples (19%). In the stained faecal smears we found *Cryptosporidium* spp. only in 2% of the samples (2/100) and cryptosporidium antigen was detected in 3 samples. The sensitivity of the detection of *Cryptosporidium* spp. by ELISA test is higher.

In 2011, the prevalence of giardiasis in the dog shelters in Košice reached 69.1% in younger dogs and 39.9% in older ones [10]. This prevalence was higher in comparison with that determined in the study by Adamová et al. [1], conducted in 2014, which showed that the prevalence of *G. duodenalis* reached 33%. In the study conducted in Poland by Bajer et al. [2], the authors detected 31.9% prevalence of giardiasis. The prevalence of this parasitosis detected in Czechia was much lower in comparison with Poland and reached only 2.2% [5]. The zoonotic potential of *Giardia duodenalis* is related mainly to assemblages A and B, but the latest research indicated that the zoonotic risk is associated also with other assemblages. By means of molecular biologic methods, Štrkolcová et al. [21] confirmed for the first time in Europe, the occurrence of canine assemblage C of *Giardia duodenalis* in a patient in

Košice, which indicated the potential role of dogs in zoonotic transmission of this pathogen. In this study, the molecular PCR method confirmed the presence of assemblage C in 4 samples.

In 2011, 125 dogs were examined in Košice for the presence of *Cryptosporidium* spp. and the prevalence reached 7.2% in younger dogs and 1.4% in older ones [10]. Adamová et al. [1] observed that the prevalence of *Cryptosporidium* spp. reached 9.09% in the Košice district. The examination of samples of dog faeces in Spain showed the presence of *Cryptosporidium* spp. in 4.1% of the cases (8/194) [9]. In Poland, oocysts of *Cryptosporidium* spp. were found in 1.2–12.5% of the dogs [2, 15] but detection of the copro-antigen indicated a higher prevalence of this protozoan than that obtained by microscopical examinations [11].

Insufficient hygiene and welfare, stress and other factors may contribute to worsen the health of some animals. The dog shelters were inadequate with regard to their capacity and hygiene level. All of the above factors support transmission of these opportunistic protozoans with zoonotic potential. It is essential to prevent contact of sick individuals with humans and other animals. The presence of individuals infected with zoonotic species/assemblages/genotypes of cryptosporidia and giardia possess a threat to public health.

## CONCLUSIONS

Dogs, cats and domestic ruminants are typical hosts of cryptosporidia and giardia. These animals are in close contact with humans and thus present considerable risk of spreading these infections, particularly of the species with zoonotic potential. The examination of dogs in the two shelters confirmed that these infections are still present in the Košice region. Effective therapy is unknown up to the present. To decrease the prevalence of these protozoans one should start with measures that can improve the immunity of dogs and other animal species. It is also important to improve the conditions to which the animals are exposed, improve their hygiene and nutrition, and ensure regular sanitation of the premises. Other very important preventive measures include provision of adequate veterinary care and regular monitoring of the prevalence of these opportunistic infections.



## ACKNOWLEDGEMENTS

The study was supported by the grant of the State Agency VEGA No. 1/0455/15; Internal Grant Agency IGA UVLF 01/2016; Medical University Park in Košice (MediPark, Košice) ITMS:26220220185 supported by Operational Programme Research and Development (OP VaV-2012/2.2/08-RO) (Contract No. OPVaV/12/2013).

## REFERENCES

1. Adamová, V., Štrkolcová, G., Goldová, M., 2014: Giardiasis and cryptosporidiosis in dogs in Košice. *Folia Veterinaria*, 58, 2, 69–71.
2. Bajer, A., Bednarska, M., Rodo, A., 2011: Risk factors and control of intestinal parasite infections in sled dogs in Poland. *Vet. Parasitol.*, 175, 343–350.
3. Cacció, S. M., Ryan, U., 2008: Molecular epidemiology of giardiasis. *Mol. Biochem. Parasitol.*, 160, 75–80.
4. Cama, V., Gilman, R. H., Vivar, A., Ticona, E., Ortega, Y., Bern, C., Xiao, L., 2006: Mixed *Cryptosporidium* infections and HIV. *Emerg. Infect. Dis.*, 12, 1025–1028.
5. Dubná, S., Langrová, I., Nápravník, J., Jankovská, I., Vadlejch, J., Pekár, S., Frchtner, J., 2007: The prevalence of intestinal parasites in dogs from Prague, rural areas, and shelters of the Czech Republic. *Vet. Parasitol.*, 145, 120–128.
6. Faust, E. C., D'Antonio, J. S., Odom, V., Miller, M. J., Peres, C., Sawitz, W. et al., 1938: A critical study of clinical laboratory techniques for the diagnosis of protozoan cysts and helminth eggs in faeces. *Am. J. Trop. Med. Hyg.*, 18, 169–183.
7. Feng, Y., Xiao, L., 2011: Zoonotic potential and molecular epidemiology of *Giardia* species and Giardiasis. *Clin. Microbiol. Rev.*, 24, 110–140.
8. Garcia, L. S., Bruckner, D. A., 1977: Collection, preservation, and shipment of faecal specimens. Garcia, L. S., Bruckner, D. A. (Eds.): *Diagnostic Medical Parasitology*, 3rd edn., ASM Press, Washington D. C., 593–607.
9. Gil, H., 2017: Detection and molecular diversity of *Giardia duodenalis* and *Cryptosporidium* spp. in sheltered dogs and cats in northern Spain. *Infect. Genet. Evol.*, 50, 66–68.
10. Goldová, M., Valenčáková, A., Mojžišová, J., Halánová, M., Letková, V., Ravaszová, P., 2011: Occurrence of *Giardia* and *Cryptosporidium* in dogs. In *Proceedings of SEVC – 46th Southern European Veterinary Conference*, Sept. 29–Oct. 2, Barcelona.
11. Gundlach, J. L., Sadzikowski, A. B., Studzińska, M. B., Tomczuk, K., 2004: Invasion of *Giardia* spp. and *Cryptosporidium* spp. in dogs and cats. *Medycyna Weterynaryjna*, 60, 1202–1203.
12. Halliez, M. C. M., Buret, A. G., 2013: Extra-intestinal and long-term consequences of *Giardia duodenalis* infections. *World J. Gastroenterol.*, 19, 8974–8985.
13. Hunter, P. R., Hadfield, S. J., Wilkinson, D., Lake, I. R., Harrison, F. C. D. et al., 2007: Subtypes of *Cryptosporidium parvum* in humans and disease risk. *Emerg. Infect. Dis.*, 13, 82–88.
14. Jíra, J., 2009: *Medical Protozoology. Protozoan Diseases* (In Czech). Galén, 567 pp.
15. Majewska, A. C., Werner, A., Słodkiewicz, A., Dąbrowski, P., Luty, T., 2001: Prevalence of intestinal protozoan parasites in dogs and cats in the Poznań area. *Annals of Parasitology*, 47, 30.
16. Nichols, G. L., Chalmers, R. M., Hadfield, S. J., 2014: Molecular epidemiology of human cryptosporidiosis. *Cryptosporidium: Parasite and Disease*. Springer, 81–147.
17. Plutzer, J., Ongerth, J., Karanis, P., 2010: *Giardia* taxonomy, phylogeny and epidemiology: Facts and open questions. *International Journal of Hygiene and Environmental Health*, 213, 321–333.
18. Putigniani, L., Menichella, D., 2010: Global distribution, public health and clinical impact of the protozoan pathogen *Cryptosporidium*. *Interdiscip. Perspect. Infect. Dis.*, Epub, <https://www.ncbi.nlm.nih.gov/pubmed/207006669>.
19. Savioli, L., Smith, H., Thompson, R. C. A., 2006: *Giardia* and *Cryptosporidium* join the “Neglected Diseases Initiative”. *Trends Parasitol.*, 22, 203–208.
20. Sulaiman, I. M., Fayer, R., Bern, C., Gilman, R. H., Trout, J. M., Schantz, P. M. et al., 2003: Triosephosphate isomerase gene characterization and potential zoonotic transmission of *Giardia duodenalis*. *Emerg. Infect. Diseases*, 9, 1444–1452.
21. Štrkolcová, G., Mađar, M., Hinney, B., Goldová, M., Mojžišová, J., Halánová, M., 2015: Dog's genotype of *Giardia duodenalis* in human: first evidence in Europe. *Acta Parasitologica*, 60, 796–799.
22. Xiao, L., Bern, C., Limor, J., Sulaiman, I., Roberts, J., Checkley, W. et al., 2001: Identification of 5 types of *Cryptosporidium* parasites in children in Lima, Peru. *J. Infect. Dis.*, 183, 492–497.
23. Xiao, L., 2010: Molecular epidemiology of cryptosporidiosis: an update. *Exp. Parasitol.*, 124, 80–89.

Received July 10, 2017

Accepted October 2, 2017



## ULTRASONOGRAPHIC EXAMINATION OF SOME VESSELS IN DOGS AND THE CHARACTERISTICS OF BLOOD FLOW IN THESE VESSELS

Figurová, M., Kulinová, V.

Small Animal Clinic  
University of Veterinary Medicine and Pharmacy, Komenského 73, 041 81 Košice  
Slovakia

maria.figurova@uvlf.sk

### ABSTRACT

The examination by Doppler ultrasonography provides haemodynamic information about blood flow velocity in a respective vessel. It specifies high- and low-resistance flow patterns. The aim of our study was to record the flow in *a. carotis communis*, *a. femoralis* and *aa. renales* in 16 adult clinically healthy dogs of small and medium size; characterize the types of vessels and also determine the pulsatility index (PI) and the resistive index (RI) of these vessels. The *a. femoralis* is a high-resistance vessel with a pronounced three-peak waveform. The *aa. renales* gives a typical picture of a low-resistance flow pattern. The characteristics of *a. carotis communis* involves different images of its branches *a. carotis interna* and *a. carotis externa*. In the investigated groups we observed a medium degree of pulsatility (atypical high-resistance flow pattern with an absence of reverse flow). The mean measured values of indices for *a. carotis communis* were: left side PI 1.824 and RI 0.742; right side PI 1.891 and RI 0.746, and for *aa. renales*: PI  $1.366 \pm 0.04$  and RI  $0.684 \pm 0.05$ .

**Key words:** Duplex ultrasonography; pulsatility index PI; resistive index RI

### INTRODUCTION

Doppler ultrasonography is a precise non-invasive method used for the examination of blood flow, its direction, velocity and character in a blood vessel. It involves the physical interaction between ultrasound and the flowing blood (Fig. 1). The Doppler effect is a result of an apparent shift in frequency of the sound reflected from the moving target particles, i.e. the blood cells. The frequency of the reflected sound differs from the original frequency, a phenomenon referred to as a Doppler shift. We recognise four ways of Doppler imaging based on various physical principles of image production: pulsed wave (PW), continuous wave (CW), colour Doppler and power Doppler.

Doppler imaging helps to distinguish vessels from non-vascular structures, such as dilated biliary duct or renal diverticulum. Its practical use involves pathological imaging of vascular lumen, e.g. in case of a suspected thrombus

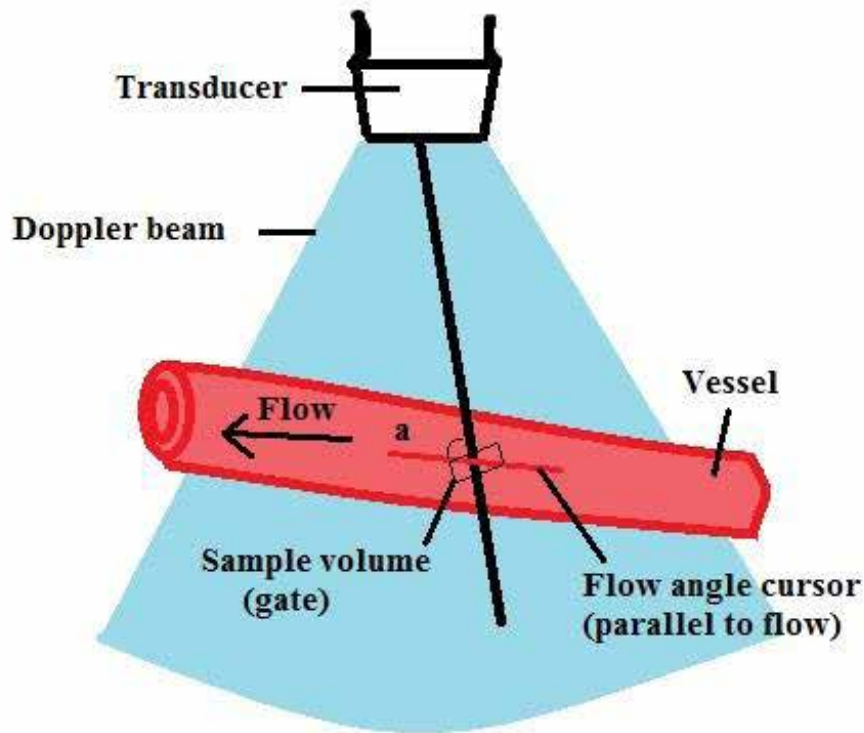


Fig. 1. Doppler principle  
Source: Mattoon and Nyland [8]

obturation, during localisation of pathological interconnection of vessels (porto system shunt) or examination of blood flow in the splanchnic region or detection of arteriovenous (AV) abnormalities and tumours. It is irreplaceable in cardiology for the examination of insufficiencies of valves, stenosis or septal defects [8].

#### Sonographic imaging of vessels in Real-time B-mode

Abdominal vessels have tubular structure in the longitudinal plane with well-defined walls. The walls are parallel, hyperechogenic, appearing as thin smooth lines. In the cross-section, the non-compressed vessels appear as circular or oval. The lumen is anechogenic due to the presence of blood, which does not produce an echo by itself (Fig. 2) [12]. At low velocity of flow and sufficient vessel diameter, the aggregated red blood cells can be observed as moving echoes. The two-dimensional real-time image is suitable for the detection of abnormally localised vessels (shunts), measurement of diameter (dilatation) of vessels and thickness of their walls. This image can allow one to identify abnormal intraluminal and perivascular structures (thrombus or tumour). However, a fresh thrombus may not give reflection as well as blood itself [6].



Fig. 2. Sonographic image of a vessel in B-mode.  
Measurement of wall thickness

Source: Small animal clinic of the UVMP in Košice

## HAEMODYNAMICS

### Flow velocity profiles of arteries

The pulsatile flow in the arteries reaches a maximum velocity during systole and a minimum during diastole. With the systolic ejection of blood into the aorta result-

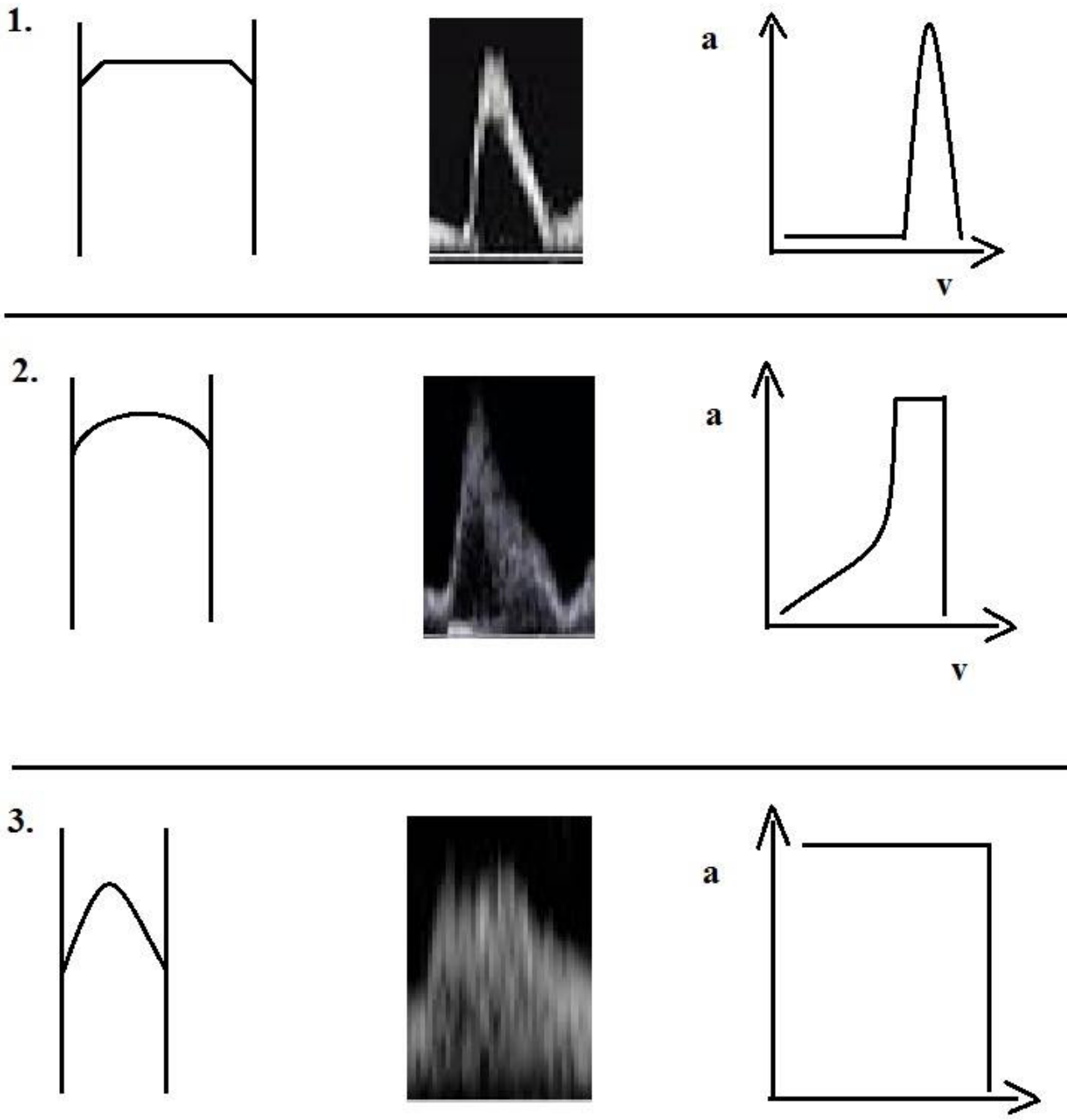


**Fig. 3. Flow velocity profiles**  
 1. Cylindrical flow. 2. Blunted parabolic flow. 3. Parabolic flow  
 Source: Szatmari et al. [14]

ing in pulsatile character of flow, its continuous flow in the periphery is maintained by the elasticity of the walls of the aorta and large vessels (representing blood reservoirs) and resistance of peripheral vessels [3]. The blood flow in most blood vessels is laminar, with the blood moving in thin concentric layers or lamellae. The central layers flow

the fastest, whereas frictional forces cause energy loss and slowing of the layers near the vessel walls [6].

The following blood velocity profiles have been described:

1. **Cylindrical:** In larger vessels, e.g. aorta and its large paired branches, the velocity of the blood is nearly

the same in the centre of the vessel and near the vessel wall where it is slowed down only moderately (narrow range of frequencies/velocities). As a result, the spectrum is characterised by a thin line in systole that outlines a clear space called a spectral window (empty space between the inner margin of the flow curve and the basal line) [19].

2. **Blunted parabolic:** This type of flow is basically a combination of the first two types. It occurs in middle-sized arteries (e.g. celiac trunk), the flow is similar to the cylindrical type in the centre of the vessel, however, the flow is more similar to the parabolic type in the peripheral parts of the vessel lumen. (Fig. 3).
3. **Parabolic:** In smaller arteries (e.g. renal artery) the centrally moving blood has higher velocity compared to the blood close to the vessel wall (wide range of frequencies/velocities),
4. **Turbulent:** The fourth type of flow velocity profile described in the literature is turbulent. It is observed as bifurcations, curves, stenosis or branches. It is characterised by a wide range of velocities from zero to both the negative and positive maximum velocities [14].

The width of the systolic peak is independent of the flow velocity profile.

1. **Cylindrical profile:** the overwhelming majority of red blood cells moves with uniform velocity. The spectrum is characterised by a thin line in systole that outlines a space called a spectral window.
2. **Blunted parabolic profile:** the flow resembles the cylindrical one in the centre of the vessel (red blood cells move with uniform velocity), however, in the peripheral parts of the vessel lumen the flow is more similar to the parabolic flow.
3. **Parabolic profile:** the centrally moving blood cells have higher velocity in comparison with cells close to the vessel wall, so the distribution of the velocity in the vessel is wide and no spectral window is observed [14].

### Doppler waveforms of blood vessels

The pulsatility of the waveform is related to the vascular impedance downstream to the point of measurement. Each cardiac contraction causes forward blood flow and

distension of the vessel. The subsequent diastolic reverse flow is due to blood rebounding up the aorta as the velocity wave is reflected from the high impedance of the peripheral vascular bed of the hind limbs [15]. As the vessel diameter returns to normal, the rebound energy provides the necessary energy to promote continuous flow in diastole [6, 14]. These types may occur in the body with both low and high flow velocity. Depending upon the organ, tissue or bodily parts, physiological or pathological waveforms may be obtained [3].

The following flow patterns have been described:

1. **High resistance flow pattern:** High pulsatility and high resistance to flow are indicated by sharp systolic peaks and flow reversal in early diastole (aorta) [14]. It has a three-phase character with high forward flow velocity, low reverse flow at the end of systole and slow forward flow in diastole (the so-called three-peak waveform). It is characterised by a short acceleration time (i.e. time from the onset of flow acceleration in systole up to reaching the maximum velocity) [3]. The high resistance flow pattern is typical of the aorta, limb arteries and external carotids (vessels supplying muscles and skin). It is pathological in the case of increased peripheral resistance in parenchymatous organs (e.g. rejection of renal graft) in places in front of stenosis and vessel occlusions [3].
2. **Low resistance flow pattern:** Low pulsatility and low resistance to flow are indicated by broad systolic peaks and continuous, high velocity flow in diastole and subsequent permanent flow with gradually decreasing velocity. Acceleration of the flow is slower so a longer time is needed for acceleration and there is no reverse flow at the end of systole. The low resistance flow pattern is characteristic of internal carotids and their branches and arteries supplying the parenchymatous organs with constant need of high flow per minute. It indicates pathology in regions in front of arteriovenous fistulae, in sites with collateral circulation and serious stenosis [3].
3. **Intermediate resistance flow pattern:** Intermediate pulsatility and intermediate resistance to flow are indicated by sharp systolic peaks (broader than in arteries of high resistance flow pattern) and a forward flow in diastole without reverse flow (e.g. in

the celiac trunk). The diastolic peak velocity is lower in comparison with the peak systolic velocity than in the low resistance flow pattern [14].

4. **Venous flow:** Most veins have low grade plasticity and periodicity. The shape of venous flow waveforms depends not only on the velocity of the blood flow, but also on the heart action and respiratory movements. Usually, the flow in the veins is laminar, affected by intrathoracic and intraabdominal pressure conditions (during inspiration and expiration) responsible for phasic changes. Close to the heart, the waveform acquires a three-phase character, with accelerated flow at ventricular systole and at the opening of atrioventricular valves. A short reverse flow appears at atrium systole. For example, *v. hepatica* and the cranial part of the ventriculo-coronary connection (VCC) have Doppler patterns with strong periodicity because of the effect of the right atrial pressure changes during the cardiac cycle. In the more distant parts of the body (limbs) the venous blood flow is affected mostly by respiration and the work of limb muscles and considerably less by heart action. Inspiration results in acceleration of flow in veins above the diaphragm but in deceleration of flow below the diaphragm. The evaluation of waveforms of veins is mostly based on the description of flow velocity profiles (laminar — turbulent, low — high, three-phase — flat, present — absent). When evaluating venous flow in the limbs of the above mentioned measurements and indices, only measurement of the maximum velocity (Vmax) and flow direction changes (including the length of duration) during various manoeuvres are used [3].

The aim of this study was to determine by Doppler ultrasonography the spectral waveform of vessels of the *a. carotis communis*, *a. femoralis* and *aa. renales*, and to determine their flow velocity profile, resistance flow pattern and values of the RI and PI indices and compare these parameters with previous studies and confirm and extend the database of relevant results.

## MATERIALS AND METHODS

Doppler ultrasonographic examinations of the vessels *aa. renales* and *a. femoralis* were carried out in a group of

10 clinically healthy dogs weighing 7—26 kg (3 West Highland Terriers of age 5—9 years, weighing 7—8 kg, and 7 medium size mongrels of age 3—9 years, weighing 15—26 kg). The same parameters of the *a. carotis communis* were measured in 6 Miniature Schnauzers of age 2—6 years, weighing 6—8 kg.

After arrival at the clinic, the prospective dogs were allowed to acclimatize and get used to the new environment for 5—10 minutes. Those that reacted wildly to stress factors (manipulation of the animals, unknown environment, length of the examination) were excluded from the study.

The selected dogs were examined without sedation after fasting for 12 hours, using an ultrasonographic apparatus Aloka Profound Alpha 6, equipped with linear (5—16 MHz) and microconvex (5—10 MHz) probes.

## RESULTS

The Doppler ultrasonographic examinations of the *a. femoralis* revealed a high resistance flow pattern and a cylindrical flow velocity profile with a spectral window. The systolic peak was followed by a retrograde flow in early diastole and then again by forward flow and lower reverse flow and ended by a forward flow (Fig. 4). The spectral pattern of the *a. femoralis* showed a waveform corresponding to the respiratory movements, heart action or transfer of pulsatility from the adjacent artery (Fig. 5).

The Doppler spectral pattern of the *aa. renales* was characteristic of a low resistance flow pattern and parabolic flow velocity profile. An early systolic peak (ESP), typical of this artery, can be seen in Fig. 6. The impedance indices in the medium size breeds were as follows: RI =  $0.632 \pm 0.05$ ; PI =  $1.153 \pm 0.02$ . In the medium size mongrels these indices reached: RI =  $0.688 \pm 0.08$ ; PI =  $1.341 \pm 0.08$ . In the West Highland Terriers, the RI index was  $0.734 \pm 0.03$  and PI  $1.605 \pm 0.03$ . The mean values of indices for all size categories were the following: RI =  $0.684 \pm 0.05$ ; PI =  $1.366 \pm 0.04$ .

The spectral pattern of *a. carotis communis* was specific. The systolic peak was broader with small, not very evident spectral window (blunted parabolic flow velocity profile). The systolic peak was not followed by a retrograde wave in early diastole (intermediate resistance flow pattern) but by continuous forward flow. This involved the so-called intermediate resistance waveform (combination of two arteries, *a. carotis interna* and *arteria carotis externa*) (Fig. 7).

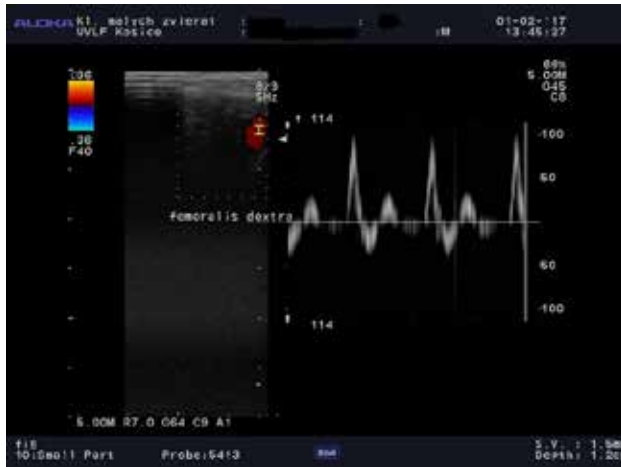


Fig. 4. Spectral Doppler pattern of *a. femoralis dextra*  
Source: Small animal clinic of the UVMP in Košice



Fig. 5. Spectral Doppler pattern of *v. femoralis*  
Source: Small animal clinic of the UVMP in Košice



Fig. 6. Spectral Doppler pattern of *aa. renales*  
Source: Small animal clinic of the UVMP in Košice



Fig. 7. Spectral Doppler pattern of *a. carotis communis*  
Source: Small animal clinic of the UVMP in Košice

The mean values of indices in the Miniature Schnauzers of *a. carotis communis sinistra* were: RI=0.742 and PI=1.824, and those of *a. carotis communis dextra* reached: RI=0.746 and PI=1.891. The impedance indices measured in the West Highland Terriers were higher: RI=0.715 and PI=1.617 in the left carotid and RI=0.788 and PI=1.911 in the right carotid.

## DISCUSSION

In veterinary practice, vessels are examined mostly by colour and power Doppler mapping. In cardiology, the spectral Doppler examination is used most commonly. Few

studies have been published dealing with the physiological values of the RI and the PI of individual vessels. In our study we investigated small and medium size dogs.

The *a. femoralis* is a vessel with a high resistance flow pattern and cylindrical flow velocity profile. Access to this vessel and its examination are not simple. There was observed a sharp systolic peak with a clear spectral window. Its flow velocity distribution was narrow and the systolic peak was followed by reverse flow in early diastole and then again by forward flow. The mean peak systolic velocity (PSV) in this artery in the study by Lee et al. [7] was  $110 \pm 17 \text{ cm.s}^{-1}$ . The mean early diastolic velocity (EDV) was  $11 \pm 5 \text{ cm.s}^{-1}$  and end diastolic velocity (EnDV) reached  $22 \pm 7 \text{ cm.s}^{-1}$  [7]. The differences in the results of the left and

right *a. femoralis* were insignificant. The examination of the *a. femoralis* was indicated because of the manifestation of weakness of hind limbs or a weak femoral pulse. Its typical three-phase waveform was subject to rapid changes in pathologies such as stenosis, thrombus obstruction, tumour, arteriovenous malformation (AVM) and other abnormalities. Similar pathological signs were described in systemic arterial dirofilariasis [17].

The *aa. renales* is a vessel with a low resistance flow pattern and parabolic flow velocity profile. The mean values of the impedance indices in this vessel reached  $0.684 \pm 0.05$  for the RI and  $1.366 \pm 0.04$  for the PI without significant difference between right and left limbs. In the medium breeds, the RI reached  $0.632 \pm 0.05$  and the PI  $1.153 \pm 0.02$  and in the medium size mongrels, the RI was equal to  $0.688 \pm 0.08$  and the PI  $1.341 \pm 0.08$ . In the West Highland Terriers, we measured  $0.734 \pm 0.03$  for the RI and  $1.605 \pm 0.03$  for the PI.

A urinary obstruction or vasoconstriction can increase the resistance of the renal vessels. In the case of the increased vascular resistance, the diastolic flow of blood is decreased more than the systolic one. The relatively higher decrease in the end diastolic velocity compared to the systolic velocity results in increased values of the RI and the PI. Thus, it is necessary to determine the upper limits for the RI and the PI in order to identify abnormally increased vascular resistance [9].

According to Mattson and Nyland [8], every value of the RI higher than 0.7 is considered abnormal. Such findings are non-specific and occur in a number of disorders such as acute renal disease, acute tubular necrosis and renal obstruction [8]. The authors conducted a study on 27 dogs without sedation and the upper limits were 0.72 for the RI and 1.52 for the PI. They examined the vessels by the power Doppler technique. The differences in the measured values between the right and left kidneys were insignificant [9]. In the study by Ochoa et al. [10], the limit for the RI was higher and the results had to exceed 0.75–0.8 to be considered abnormal.

The examination of the RI is important in case of acute obstructions. An increased RI was recorded 24 hours following the acute unilateral obstruction in dogs, however, due to the high number of false positive and false negative cases the reliability of the RI examination was limited [16]. Despite that, an increased RI and difference in the RI between both kidneys higher than 0.1 can support a detection of an acute unilateral obstruction in dogs [8].

Bude et al. [4] presented in their study the values of renal RI, which remained unchanged in kidneys without obstruction and increased in kidneys with obstruction following administration of furosemide. They described the effect of furosemide in combination with saline F1/1 on the renal RI. The authors evaluated the renal RI in children and juveniles aged 6 to 18 years before and after i.v. administration of furosemide, in combination with saline (F1/1). The RI index was increased in the obstructed kidney.

The administration of an infusion of F1/1 solution in combination with furosemide (diuretics) to dogs resulted in an increased RI in the kidney with experimentally induced obstruction and a decrease in the RI in the non-obstructed kidney [5, 11, 18]. The difference was primarily ascribed to the decrease in the RI index in the kidney free of obstruction. This “furosemide challenge” test technique is helpful in the detection of post-transplacental obstruction in dogs [8]. Our study presented physiological values in clinically healthy individuals of medium size dogs. The only exception was one dog; a West Highland Terrier with a RI value reaching  $0.734 \pm 0.03$ .

The study on dogs with leishmaniasis and various stages of renal damage showed that the RI index can serve as a reliable indicator of progressivity of the problem with high sensitivity but small specificity. All investigated animals exhibited an increased RI value, which suggested real advanced damage and proteinuria [1, 2].

The characteristics of *a. carotis communis* reflect differences in its branches, *a. carotis interna* and *a. carotis externa*. In the group of dogs observed in our study, the examinations showed medium pulsatility (atypical high resistance waveform with absence of reverse flow) and a blunted cylindrical flow velocity profile. Its waveform differs also in individual size categories of dogs. The mean values of *a. carotis communis* measured in the Miniature Schnauzers were as follows: left side PI = 1.824 and RI = 0.742; right side PI = 1.891 and RI = 0.746. In comparison, the RI and the PI in the left carotid of West Highland Terriers reached 0.715 and 1.677, respectively. In the right carotid of this breed, the RI and the PI were 0.788 and PI 1.912 respectively. In the Miniature Schnauzers the mean PSV was  $71.7 \text{ cm.s}^{-1}$  and EDV  $17.8 \text{ cm.s}^{-1}$ .

A pioneer evaluation of *a. carotis communis* was presented by Svicero et al. [13] who described their ultrasonography results in a Labrador breed. The aim of their study was to determine the physiological values of PSV,



EDV and RI. These authors did not observe significant differences between the right and the left vessels, the PSV reached  $75.8 \pm 16 \text{ cm}\cdot\text{s}^{-1}$ , EDV  $12.2 \pm 4 \text{ cm}\cdot\text{s}^{-1}$ , diameter of *a. carotis communis* was  $0.54 \pm 0.063 \text{ cm}$  and the RI was  $0.83 \pm 0.07$ . Lee et al. [7] described in their study the physiological parameters of blood flow velocity in *a. carotis communis* and the PI values of *a. basilaris*. The mean PSV of *a. basilaris* and *a. carotis communis* were  $72 \pm 19$  and  $115 \pm 17$ , respectively. The *a. carotis communis* were  $25 \pm 11$  and  $39 \pm 7$ , respectively. The PI of the basillary artery was  $1.37 \pm 0.13$ . The mean systolic and diastolic blood pressures were  $137 \pm 13$  and  $78 \pm 15 \text{ mmHg}$ , respectively.

The mean values of the RI and the PI indices of *a. carotis communis* and *aa. renales* obtained in our study agreed with the values reported by the above authors. Our results extend the database of the physiological values of these vessels.

## CONCLUSIONS

The Doppler ultrasonographic examination of the *a. femoralis* is unquestionably a simple, excellent and non-invasive method of examination of this vessel that should be used as one of the examination methods when various pathological states of hind limbs are suspected.

The mean values of the RI and PI indices of *aa. renales* were: RI  $0.684 \pm 0.05$ ; and PI  $1.366 \pm 0.04$ . These results are comparable with those obtained by other researchers. The RI results obtained in our study were below 0.7. We consider this a physiological limit. The exception was the West Highland terrier breed with a PI equal to 0.734. However, we examined only a very small sample of this breed.

The use of the RI as a marker of renal damage still seems controversial and obtaining the waveforms of good quality appears time and technique demanding.

The mean values of the indices of *a. carotis communis* for the Miniature Schnauzers were: left side PI = 1.824 and RI = 0.742; right side PI = 1.891 and RI = 0.746. The mean value of PSV was  $71.7 \text{ cm}\cdot\text{s}^{-1}$  and of EDV  $17.8 \text{ cm}\cdot\text{s}^{-1}$ . Our results corresponded to those reported by other researchers. These physiological values of the Miniature Schnauzer breed can serve for comparison in the study of pathological changes that correlate with the pathology of neurological disorders with an ischemic basis, or at thromboembolic states, atherosclerosis, arterial stenosis or tumours in the cervical region.

Our results obtained for the *a. carotis communis* in the Miniature Schnauzer can become a breed standard of characteristics of flow in this vessel.

## ACKNOWLEDGEMENT

*The study was supported by the project VEGA No. 1/0225/15.*

## REFERENCES

1. Baltazar, P. I., Da Silva Moura, L. S., Pessoa, G. T., Rodrigues, R. P. S., Sanches, M. P., Diniz, A. N. et al., 2016: Comparative B-mode and Doppler renal ultrasonography with histopathological findings in dogs positive for canine visceral leishmaniasis. *Microsc. Res. Tech.*, 79, 637–645.
2. Braga, J. F. V., Alves, F. R., 2016: Comparative B-mode and Doppler renal ultrasonography with histopathological findings in dogs positive for canine visceral leishmaniasis. *Microsc. Res. Tech.*, 79, 637–645.
3. Beňačka, J., Tvrdík, E., 2013: Doppler basis (In Slovak). In *Proceedings of the 9th Congress of Slovak Sonography*, Slovakia, Piešťany, 5.
4. Bude, R. O., DiPietro, M. A., Platt, J. F., Rubin, J. M., 1994: Effect of furosemide and intravenous normal saline fluid load upon the renal resistive index in nonobstructed kidneys in children. *J. Urol.*, 151, 438–41.
5. Choi, H., Won, S., Chung, W., Lee, K., Chang, D., Lee, H. et al., 2003: Effect of intravenous mannitol upon the resistive index in complete unilateral renal obstruction in dogs. *J. Vet. Intern. Med.*, 17, 158–62.
6. Finn-Bodner, S., Hudson, J. A., 1988: Abdominal vascular sonography. In Penninck, G. (Ed.): *The Veterinary Clinics of North America. Small Animal Practice. Ultrasonography*. Philadelphia, W. B. Saunders, 28, 887–942.
7. Lee, K., Choi, M., Yoon, J., Jung, J., 2004: Spectral waveform analysis of major arteries in conscious dogs by Doppler ultrasonography. *Veterinary Radiology and Ultrasound*, 45, 166–171.
8. Mattoon, J. S., Nyland, T. G., 2015: *Small Animal Diagnostic Ultrasound*, 3th edn., Missouri, Elsevier, 32–47, 125–127, 431–435, 581–584.
9. Novellas, R., Espada Y., de Gopegui, R. R., 2007: Doppler ultrasonographic estimation of renal and ocular resistive and

- pulsatility indices in normal dogs and cats. *Vet. Radiol. Ultrasound*, 48, 69—73.
10. **Ochoa, P.G., Lacasta, D., Sosa I., Gascon, M., Ramos, J.J., Ferrer, L.M., 2011:** *Fundamentals and Applications of Abdominal Doppler. Ultrasound Imaging — Medical Applications.* Chapter 14, **Minin, I. V., Minin, O. V.** (Eds.), published by InTech under CC BY-NC-SA 3.0 license, 342 pp.
  11. **Shokeir, A.A., Nijman, R.J., el Azab, M., Proovost A.P., 1997:** Partial ureteral obstruction: Effect of intravenous normal saline and furosemide upon the renal resistive index. *J. Urol.*, 157, 1074—7.
  12. **Spaulding, K. A., 1997:** A review of sonographic identification of abdominal blood vessels and juxtavascular organs. *Vet. Radiol. Ultrasound*, 38, 4—23.
  13. **Svicero, D. J., Doiche, D. P., Mamprim, M. J., Heckler, M. C., Amorim, R. M., 2013:** Ultrasound evaluation of common carotid artery blood flow in the Labrador retriever, *BMC Veterinary Research*, 9,195. <http://www.biomedcentral.com/1746-61/9/195>.
  14. **Szatmari, V., Sotonyi, P., Voros, K., 2001:** Normal duplex Doppler waveforms of major abdominal blood vessels in dogs: A review. *Vet. Radiol. Ultrasound*, 42, 93—107.
  15. **Taylor, K. J., Burns, P.N., Woodcock, J.P., Wells, P.N., 1985:** Blood flow in deep abdominal and pelvic vessels: ultrasonic pulsed-Doppler analysis. *Radiology*, 154, 487—493.
  16. **Ulrich, J. C., York, J. P., Koff, S. A., 1995:** The renal vascular response to acutely elevated intrapelvic pressure: resistive index measurements in experimental urinary obstruction. *J. Urol.*, 154, 1202—1204.
  17. **Upchurch, D.A., Ogden, D.M., Baker, D.G., 2015:** Bilateral femoral arterial dirofilariasis caused by *Dirofilaria immitis* in a dog. *Veterinary Record Case Reports*, 3: e000184. doi: 10.1136/vetreccr-2015-000184.
  18. **Yokoyama, H., Tsuji, Y., 2002:** Diuretic Doppler ultrasonography in chronic unilateral partial ureteric obstruction in dogs. *BJU Int.*, 90, 100—104.
  19. **Zwiebel, W.J., Fruechte, D., 1992:** Basics of abdominal and pelvic duplex, instrumentation, anatomy and vascular Doppler signatures. *Semin. Ultrasound CT MR*, 13, 3—21.

Received August 24, 2017

Accepted October 6, 2017



## DETERMINATION OF ANTIOXIDANT PARAMETERS OF PLEUROTUS MUSHROOMS GROWING ON DIFFERENT WOOD SUBSTRATES

Strapáč, I.<sup>1</sup>, Kuruc, M.<sup>1</sup>, Baranová, M.<sup>2</sup>

<sup>1</sup>Department of Chemistry, Biochemistry and Biophysics, Institute of pharmaceutical chemistry,

<sup>2</sup>Department of Food Hygiene and Technology, Institute of milk hygiene and technology  
University of Veterinary Medicine and Pharmacy, Komenského 73, 041 81 Košice  
Slovakia

imrich.strapac@uvlf.sk

### ABSTRACT

Extracts of the fruiting bodies of the Oyster mushroom (*Pleurotus ostreatus*) grown on wood substrates (beech, oak, linden, walnut, poplar) and extracts of the fruiting bodies of the Oyster mushroom (*Pleurotus pulmonarius*) grown in nature on aspen wood were used to determine the total phenols, total flavonoids, lycopene and  $\beta$ -carotene. The content of individual antioxidants varies considerably depending, not only on the substrate, but also on the extracting agents. The highest content of total phenols and total flavonoids was found in methanol and water extracts of the fruiting bodies of the Oyster mushrooms grown on oak and linden substrates. The maximum content of lycopene and  $\beta$ -carotene was determined in acetone and n-hexane (ratio 4:6) extracts of the fruiting bodies of the Oyster mushroom grown on an oak block. The results obtained in this study demonstrated that the quantitative and also probably the qualitative composition of the antioxidants in the fruiting bodies of Oyster mushrooms depended considerably on the substrate composition.

**Key words:** antioxidant activity;  $\beta$ -carotene; flavonoids; lycopene; *Pleurotus ostreatus*; *Pleurotus pulmonarius*; polyphenols; wood substrates

### INTRODUCTION

Today's world is full of opposites. Hunger and poverty on the one hand and incredible wealth on the other; bad way of living, large energy intake and its low use create conditions for the development of diseases of civilization. It has been assumed that daily stress and increased free radicals in the diet are the starters for these diseases, the occurrence of which is increasing. Currently researchers are looking for natural sources of substances, which have the ability to capture free radicals, to stimulate the immune system and bring many other health benefits [6]. Oyster mushrooms (*Pleurotus ostreatus*) contain a large spectrum of medicinal substances [1, 8, 15], chemical elements, vitamins [10, 17] and nutrients [4, 5]. Because of the presence of numerous nutritional components and various biologically active substances, the Oyster mushrooms have found a wide

potential medicinal usage as a part of treatment and prevention of diseases induced as a result of modern lifestyle or malnutrition [3, 9]. Many studies have drawn attention to the extreme variability of the composition of the fruit mushrooms of the Oyster (*Pleurotus ostreatus*), starting with the content of chemical elements up to the polysaccharides [12, 14]. The Oyster mushrooms growing on substrates consisting of residues of cereal crops (e.g. corn, rice bran and others) are most often examined. Only a few studies have been published about Oyster mushrooms growing on their natural substrate — wood [10].

The aim of this study was to compare the antioxidant properties of the fruiting bodies of the Oyster mushrooms grown on various wood substrates originating from one specific location. This way we tried, as much as possible, to eliminate differences in soil composition and the effects of climate conditions on the mycelium and the wooden substrate used. We presumed that by this approach we could obtain more reliable results and more precisely identify differences caused by growing Oyster mushrooms on different substrates. The Oyster mushrooms were cultivated on blocks of trees typical for the Slovak territory (beech, oak, linden, walnut, poplar and aspen).

## MATERIALS AND METHODS

### Chemicals

All chemicals and water — Folin-Ciocalteu reagent (Sigma-Aldrich Co., USA), gallic acid (Fisher Scientific, UK), n-hexane (Centralchem, s.r.o., Slovakia), aluminum chloride hexahydrate (LACHEMA BRNO, Czechia), distilled water (Reg Pur, s.r.o., Košice, Slovakia) and other (MIKROCHEM s.r.o., Slovakia) were of an analytical grade and p.a. purity.

### Materials

For our analysis we used fruiting bodies of the Oyster mushrooms (*Pleurotus ostreatus*) cultivated on various wood substrates (beech, oak, linden, walnut, poplar) on a private plot in Lemešany (Slovakia) and fruiting bodies of the Oyster mushrooms (*Pleurotus pulmonarius*) growing on their natural substrate – aspen wood. All Oyster mushrooms were cultivated by the same method (Fig. 1), which ensures the most natural conditions for the growth of mycelium and the development of fruiting bodies. The inoculated wood and growing fruiting bodies have to be protected against birds, snails and insects that can destroy the whole crop of Oyster mushrooms. Sufficiently large fruiting bodies (4 cm on average) were picked from blocks, weighed and dried at 40 °C in a dryer (Thermo scientific, Thermo electron led

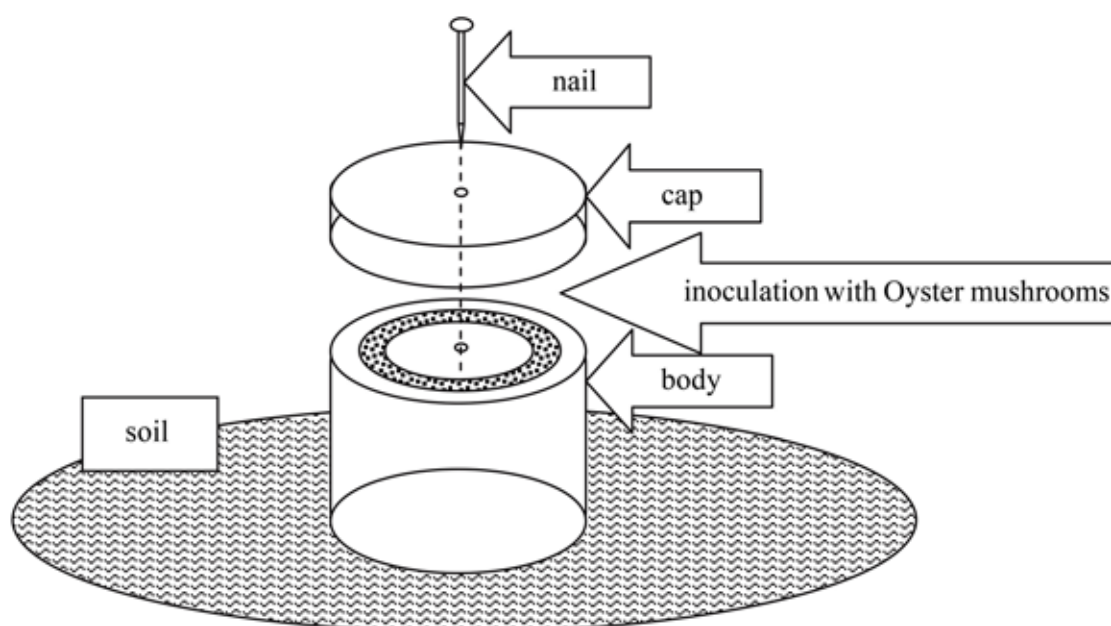


Fig. 1. Wooden block imbedded in soil and inoculated with Oyster mushrooms under garden conditions

Source: Self-made picture

GmbH, Germany) to a constant weight and homogenized with a homogenizer Straume (Ukraine). The obtained homogeneous powder was used for extraction.

### Preparation of extracts

Extracts were obtained by extracting 100 mg of dried and homogenized fruiting bodies of the Oyster mushrooms in 2 cm<sup>3</sup> of water or methanol, or a mixture of acetone and n-hexane (4:6), with vigorous stirring for 30 minutes. The extraction mixtures were then filtered through a filter paper (Whatman No. 4) and the filtrates were used to determine the content of total phenols, total flavonoids, lycopene and  $\beta$ -carotene.

### Determination of total phenols, total flavonoids, lycopene and $\beta$ -carotene

The total phenolic compounds were determined by a micro-method, using Folin-Ciocalteu reagent (Sigma, USA) according to the method described by Waterhouse [16]. Freshly prepared methanol and water extracts (20  $\mu$ l) of dried fruiting bodies of the Oyster mushrooms were used in the process.

The determination of the total flavonoids was carried out according to the method published by Konczak et al. [7] in freshly prepared methanolic and water extracts of dried fruiting bodies of Oyster mushrooms.

The content of the total phenolic substances and total flavonoids were expressed in gallic acid equivalents (GAE) that were read from the respective calibration curve.

The content of lycopene and  $\beta$ -carotene was determined by a spectrophotometric method of Nagata and Yamashita [11] and Dasgupta et al. [2]. Filtered extracts of dried fruiting bodies of Oyster mushrooms prepared in a mixture of acetone and n-hexane (4:6) were tested by UV-VIS spectrometry at wavelengths of 663 nm, 505 nm and 453 nm. The content of lycopene and  $\beta$ -carotene was calculated by means of the following [11]:

$$\begin{aligned} \text{lycopene (mg.100 cm}^{-3}\text{)} &= \\ &= -0.0458 * A_{663} + 0.372 * A_{505} - 0.0806 * A_{453} \end{aligned}$$

$$\begin{aligned} \beta\text{-carotene (mg.100 cm}^{-3}\text{)} &= \\ &= 0.216 * A_{663} - 0.304 * A_{505} + 0.452 * A_{453} \end{aligned}$$

Spectrophotometric measurements were carried out using a UV VIS spectrophotometer (Biochrom Libra S12, England). The wavelengths used for measurements are stated in the cited methods. The results are reported as means of three measurements with corresponding standard deviation (SD).

All samples for determination of the total phenolic compounds, the total flavonoids and the content of lycopene and  $\beta$  carotene were examined in triplicate.

## RESULTS AND DISCUSSION

The mean contents  $\pm$ SD of the total phenols (TP), total flavonoids (TF) in methanol and water extracts of dried fruiting bodies of Oyster mushrooms cultivated on various wood substrates (beech, oak, linden, walnut, poplar and aspen) are presented in Table 1.

The mean contents  $\pm$ SD of lycopene and  $\beta$ -carotene in the mixture of acetone and n-hexane (4:6) extracts of the dried fruiting bodies of the Oyster mushrooms cultivated on various wood substrates (beech, oak, linden, walnut, poplar and aspen) are presented in Table 2.

The ratios of evaluated substances in dried fruiting bodies of Oyster mushrooms cultivated on various wood substrates (beech, oak, linden, walnut, poplar and aspen) are summarised in Tables 2 and 3.

All samples of Oyster mushrooms contained biologically active phenolic compounds. It is evident, that the total content of phenolic substances depended on both wood substrates used to cultivate Oyster mushrooms (*Pleurotus ostreatus*) and the extracting agent. We observed that water extracts of fruiting bodies of Oyster mushroom had higher total phenolic content in comparison with the total phenolic content in the methanolic extracts (Table 1.). The highest levels of phenolic substances were detected in Oyster mushrooms cultivated on linden (10.014 mg GAE.g<sup>-1</sup> DW) and oak (9.306 mg GAE.g<sup>-1</sup> DW) in water extracts of dried fruiting bodies and also in their methanolic extracts (linden 2.057 mg GAE.g<sup>-1</sup> DW; oak 2.115 mg GAE.g<sup>-1</sup> DW). High levels of phenolic substances were detected also in water extracts of dried fruiting bodies of Oyster mushrooms cultivated on walnut (9.477 mg GAE.g<sup>-1</sup> DW). The lowest content of these substances was recorded in both types of extracts of dried fruiting bodies of Oyster mushrooms cultivated on poplar blocks (water: 8.667 mg GAE.g<sup>-1</sup> DW; methanol: 1.293 mg GAE.g<sup>-1</sup> DW).

Methanol extracts of dried fruiting bodies of *Pleurotus pulmonarius* growing on their natural substrate, aspen wood, exhibited extremely low levels of phenolic substances (0.937 mg GAE.g<sup>-1</sup> DW).

The comparison of the content of phenolic substances in

**Table 1. The mean content  $\pm$  SD of total phenols (TP) and total flavonoids (TF) in methanolic and water extracts of dried fruiting bodies of Oyster mushrooms cultivated on various wood substrates (beech, oak, linden, walnut, poplar and aspen)**

Substrate	Total phenolic substances				Total flavonoids			
	Methanolic extract		Water extract		Methanolic extract		Water extract	
	mg GAE.g <sup>-1</sup> DW	SD	mg GAE.g <sup>-1</sup> DW	SD	mg GAE.g <sup>-1</sup> DW	SD	mg GAE.g <sup>-1</sup> DW	SD
<b>beech</b>	1.503	0.005	8.827	0.007	2.418	0.007	3.002	0.012
<b>oak</b>	2.115	0.003	9.306	0.005	2.955	0.009	6.368	0.015
<b>linden</b>	2.057	0.003	10.014	0.005	2.659	0.013	5.820	0.013
<b>walnut</b>	1.294	0.005	9.477	0.005	2.608	0.011	3.176	0.012
<b>poplar</b>	1.293	0.007	8.667	0.009	2.154	0.013	2.632	0.013
<b>aspen</b>	0.937	0.005	8.838	0.007	1.833	0.011	4.016	0.014

SD — standard deviation; GAE — gallic acid equivalent; DW — dry weight

**Table 2. The mean content  $\pm$  SD of  $\beta$ -carotene and lycopene in the mixture of acetone and n-hexane (4:6) extracts of dried fruiting bodies of Oyster mushrooms cultivated on various wood substrates (beech, oak, linden, walnut, poplar and aspen) and the ratios of  $\beta$ -carotene : lycopene**

Substrate	$\beta$ -carotene		Lycopene		Ratio of
	mg.g <sup>-1</sup> DW	SD	mg.g <sup>-1</sup> DW	SD	$\beta$ -carotene : lycopene
<b>beech</b>	0.188	0.003	0.171	0.001	1.099
<b>oak</b>	0.231	0.002	0.153	0.002	1.510
<b>linden</b>	0.107	0.002	0.061	0.003	1.754
<b>walnut</b>	0.487	0.001	0.336	0.002	1.449
<b>poplar</b>	0.253	0.003	0.149	0.002	1.698
<b>aspen</b>	0.349	0.003	0.230	0.003	1.517

SD – standard deviation; DW – dry weight

**Table 3. The ratios of the content of total phenolic compounds and total flavonoids in water and methanolic extracts of dried fruiting bodies of Oyster mushrooms cultivated on various wood substrates (beech, oak, linden, walnut, poplar and aspen)**

Substrate	Ratios of the content of the evaluated substances (H <sub>2</sub> O : CH <sub>3</sub> OH extracts)	
	Total phenolic compounds	Total flavonoids
<b>beech</b>	5.873	1.242
<b>oak</b>	4.400	2.156
<b>linden</b>	4.868	2.189
<b>walnut</b>	7.324	1.218
<b>poplar</b>	6.703	1.222
<b>aspen</b>	9.443	2.191

water and methanolic extracts of our experimental samples of dried fruiting bodies of Oyster mushrooms showed interesting information. The ratio of the content of phenolic substances in water and methanolic extracts varied depending on the wood substrate (Table 3). The greatest difference in the content of phenolic substances in water and methanol extracts was in samples of dried fruiting bodies of *Pleurotus pulmonarius* growing on their natural substrate – aspen wood. Water extract contained 9.443-fold higher content of phenolic substances than the methanolic extract. High ratios of phenolic substances in water and methanolic extracts were found in dried fruiting bodies of Oyster mushrooms cultivated on walnut (7.324) and poplar (6.703) while low ratios were detected in dried fruiting bodies of Oyster mushrooms cultivated on linden (4.868) and oak (4.400).

The fruiting bodies of Oyster mushrooms contain remarkable quantities of different phenolic acids such as gallic acid, homogentisic acid, ferulic acid, p-coumaric acid, p-hydroxybenzoic acid, protocatechuic acid and chlorogenic acids, respectively [1, 13]. The ratio of the content of phenolic substances in water and methanolic extracts can demonstrate also the different qualitative and quantitative composition of fruiting bodies of Oyster mushrooms depending upon the wooden substrate used for their cultivation. It is evident, that the total content of phenolic substances depended on the wood substrates used for cultivation of the Oyster mushrooms (*Pleurotus ostreatus*) and on the extracting agents (Table 1). To draw a final conclusion about the dependence of the content of individual phenolic substances on the composition of the wood substrate, more extensive and detailed investigations are needed.

Water extracts of the fruiting bodies of the Oyster mushroom contained higher levels of total flavonoids in comparison with levels in methanolic extracts (Table 1). The highest levels of flavonoids were determined in Oyster mushrooms cultivated on oak blocks (in methanolic extract 2.955 mg GAE.g<sup>-1</sup> DW and in water extract 6.368 mg GAE.g<sup>-1</sup> DW) and linden block (2.659 mg GAE.g<sup>-1</sup> DW in methanolic extract and 5.820 mg GAE.g<sup>-1</sup> DW in water extract). The lowest content of these substances was detected in extracts of dried fruiting bodies of Oyster mushrooms cultivated on poplar blocks (2.154 mg GAE.g<sup>-1</sup> DW in methanolic extract and 2.632 mg GAE.g<sup>-1</sup> DW in water extract) and in methanolic extract (1.833 mg GAE.g<sup>-1</sup> DW) of Oyster mushrooms (*Pleurotus pulmonarius*) grown on their natural substrate – aspen wood.

The water extracts of the fruiting bodies of the Oyster mushroom grown on oak, linden and aspen contained more than a 2-fold higher level of flavonoids (2.156 to 2.191 times) than the methanolic extracts (Table 3). The water extracts of fruiting bodies of Oyster mushrooms grown on beech, walnut and poplar blocks showed only 1.218 to 1.242-fold higher levels of flavonoids than the methanolic extracts. The Oyster mushrooms contain several kinds of flavonoids, especially rutin and chrysin but also catechin and myricetin [1, 13]. The different ratio of the content of flavonoids in water and methanolic extracts can also be caused by different qualitative and quantitative composition of fruiting bodies of the Oyster mushrooms cultivated on different wood substrates. Additional detailed examinations are needed to explain this relationship and significance of differences between the types of wood used to cultivate Oyster mushrooms.

Table 2 presents biologically active  $\beta$ -carotene and lycopene in the mixture of acetone and n-hexane (4:6) extract of dried fruiting bodies of the Oyster mushrooms cultivated on various wood substrates (beech, oak, linden, walnut, poplar and aspen). These compounds are well known for their antioxidant properties. However, cultivation on different wood substrates resulted in different amounts of these substances in acetone – n-hexane extracts. The highest content of lycopene was found in an Oyster mushroom sample grown on a walnut block (0.336 mg.g<sup>-1</sup> DW) and the lowest in a sample grown on a linden block (0.061 mg.g<sup>-1</sup> DW). Low levels of lycopene were also found in extracts of the dried fruiting bodies of the Oyster mushrooms cultivated on beech and poplar blocks (0.153 mg.g<sup>-1</sup> DW and 0.149 mg.g<sup>-1</sup> DW, respectively).

All extracts of the dried fruiting bodies of the Oyster mushrooms contained higher amounts of  $\beta$ -carotene than lycopene (Table 2). Similar to lycopene, different levels of  $\beta$ -carotene were detected in the samples of the Oyster mushrooms grown on different wood substrates. The highest content of  $\beta$ -carotene was found in a sample of the Oyster mushrooms grown on a walnut block (0.487 mg.g<sup>-1</sup> DW). Low levels of  $\beta$ -carotene were found in extracts of the dried fruiting bodies of the Oyster mushrooms cultivated on linden and beech blocks (0.107 mg.g<sup>-1</sup> DW and 0.181 mg.g<sup>-1</sup> DW, respectively). Table 2 presents also the ratio of the content of  $\beta$ -carotene to lycopene. The content of  $\beta$ -carotene in extracts of fruiting bodies of Oyster mushrooms was 1.099 to 1.754-fold higher than the content of lycopene.

## CONCLUSIONS

Oyster mushrooms contain large amounts of substances with antioxidant properties. Our experiments showed that the content of phenolic compounds, flavonoids,  $\beta$ -carotene and lycopene in the fruiting bodies of the Oyster mushrooms can be influenced by different wood substrates used to cultivate these mushrooms. The ratio of the content of the flavonoids and phenolic substances in water and methanolic extracts demonstrated the different qualitative and quantitative composition of the fruiting bodies of the Oyster mushrooms dependent on wooden substrate used for their cultivation. Such a variable composition of the fruiting bodies of the Oyster mushrooms with their different antioxidant potential may distort clinical studies based on diets containing dried mushrooms. In our study the oak and linden blocks appeared to be the most suitable wood substrates for the cultivation of Oyster mushrooms. We also hope that this study may stimulate interest in the mycological field of research in Central Europe, which was for many centuries known for rich tradition in picking and consumption of mushrooms.

## REFERENCES

1. **Alves, M.J., Ferreira, I.C.F.R., Froufe, H.J.C., Abreu, R.M.V., Martins, A., Pintado, M., 2013:** Antimicrobial activity of phenolic compounds identified in wild mushrooms, SAR analysis and docking studies. *J. Appl. Microbiol.*, 115, 346—357.
2. **Dasgupta, A., Manjula, R., Krishnendu, A., 2013:** Chemical composition and antioxidant activity of a wild edible mushroom *Pleurotus flabellatus*. *Int. J. Pharm. Tech. Res.*, 4, 1655—1663.
3. **Deepalakshni, K., Mirunalini, S., 2014:** *Pleurotus ostreatus*: an Oyster mushroom with nutritional and medical properties. *Journal of Biochemical Technology*, 2, 718—726.
4. **Ergönül, P.G., Akata, I., Kalyoncu, F., Ergönül, B., 2013:** Fatty acid compositions of six wild edible mushroom species: Research report. *The Scientific World Journal*. Hindawi Publishing Corporation, 2013, 1—4. <http://dx.doi.org/10.1155/2013/1639.4>
5. **Chirinang, P., Intarapichet, K.O., 2009:** Amino acids and antioxidant properties of the Oyster mushroom, *Pleurotus ostreatus* and *Pleurotus sajor-caju*. *ScienceAsia*. 35, 326—331.
6. **Chovancová, A., Šturdík, E., 2005:** The influence of beta-glucans on the immune system of man (In Slovak). *Nova Biotechnologica*, 1, 105—121.
7. **Konczak, I., Sakulnarmrat, K., Bull, M., 2012:** Potential physiological activities of selected Australian herbs and fruits. In *Rural Industries Research and Development Corporation*, Project No. PRJ-004171, Pub. No. 11/097.
8. **Lakshman, D., Radha, K.V., 2012:** An effective quantitative estimation of lovastatin from *Pleurotus ostreatus* using UV and HPLC. *International Journal of Pharmacy and Pharmaceutical Sciences*, 4, 462—464.
9. **Lepšová, A., 2005:** *Mushrooms as an Elixir of Life* (In Czech), 2nd edn., Líbeznice: Vikend, CR, 88 pp.
10. **Mattila, P., Könkö, K., Euroola, M., Pihlava, J.M., Astola, J., Vahteristo, L. et al., 2001:** Contents of vitamins, mineral elements, and some phenolic compounds in cultivated mushrooms. *J. Agricult. Food Chem.*, 49, 2343—2348.
11. **Nagata, M., Yamashita, I., 1992:** Simple method for simultaneous determination of chlorophyll and carotenoids in tomato fruit. *Nippon Shokuhin Kogyo Gakkaishi*, 10, 925—928.
12. **Synytasya, A., Mícková, K., Jablonský, I., Sluková, M., Čopíková, J., 2008:** Mushrooms of genus *Pleurotus* as a source of dietary fibres and glucans for food supplements. *Czech Journal of Food Science*, 6, 441—446.
13. **Vamanu, E., 2014:** Antioxidant properties of mushroom mycelia obtained by batch cultivation and tocopherol content affected by extraction procedures: Research report. *BioMed Research International*, 2014, 1—8.
14. **Vetter, J., Hajdú, C.S., Györfi, J., Maszlavér, P., 2005:** Mineral composition of the cultivated mushrooms *Agaricus bisporus*, *Pleurotus ostreatus* and *Lentinula edodes*. *Acta Alimentaria*, 4, 441—451.
15. **Vetter, J., 2007:** Chitin content of cultivated mushrooms *Agaricus bisporus*, *Pleurotus ostreatus* and *Lentinula edodes*. *Food Chemistry*, 102, 6—9.
16. **Waterhouse, A. L., 2002:** Determination of total phenolics. In **Wrolstad R. E. (Ed.):** *Current Protocols in Food Analytical Chemistry*. New York, John Wiley and Sons Inc, pp. I1.1.1—8.
17. **Wittig, M., Krings, U., Berger, R.G., 2013:** Single-run of vitamin D photoproducts in Oyster mushroom (*Pleurotus ostreatus*) after UV-B treatment. *J. Food Comp. Anal.*, 31, 266—274.

Received September 4, 2017

Accepted October 12, 2017





## OCCURENCE OF MASTITIS IN DAIRY COWS SITUATED IN MARGINAL PARTS OF SLOVAKIA

Zigo, F.<sup>1</sup>, Vasil', M.<sup>1</sup>, Elečko, J.<sup>1</sup>, Farkašová, Z.<sup>1</sup>, Zigová, M.<sup>1,2</sup>

<sup>1</sup>Department of Animal Husbandry  
University of Veterinary Medicine and Pharmacy, Komenského 73, 041 81 Košice,  
<sup>2</sup>Department of Pharmacology  
Faculty of Medicine, Pavol Jozef Šafarik University, 040 11 Košice  
Slovakia

frantisek.zigo@uvlf.sk

### ABSTRACT

A relatively large part of the Slovak territory consists of the “marginal regions”, which in terms of the economy of ruminants keeping can efficiently produce animal commodities only occasionally. The geographic, social and economic stability of these regions is strongly influenced by the rearing of ruminants and the associated market milk production. The aim of this study was to evaluate the prevalence and aetiological agents of mastitis in two herds of dairy cows situated in the marginal parts of Slovakia. In total, 530 of the Slovak spotted breed and Holstein cows were involved in the study. The diagnosis of mastitis was performed on the basis of the clinical examination of the udder, macroscopic evaluation of the milk, determination of somatic cell count (SCC), and the bacteriological examination of the milk. The prevalence of mastitis in the two herds of dairy cows ranged from 34.7 % to 18.8 %, respectively. From the total of 2120 quarter milk samples, 36.3 % were positive to the California mastitis test (CMT). Also, pathogenic microorganisms causing intramammary infection (IMI) were

isolated from 25.6 % of the samples, which accounted for most subclinical mastitis forms (23.3 %), with the SCC under 400 000, mainly caused by coagulase-negative staphylococci (CoNS) and coliform bacteria *E. coli* and *Enterobacter aerogenes*. The clinical forms of mastitis accounted for 13.0 % of all infected cows and were caused mainly by the bacteria: *Streptococcus uberis*, *Streptococcus agalactiae*, *Staphylococcus aureus* and coagulase-negative staphylococci.

**Key words:** dairy cows; mastitis; milk production; prevalence; *Staphylococcus* spp.

### INTRODUCTION

Marginal regions cover relatively a large part of the Slovakia territory where the rearing of ruminants can efficiently produce animal commodities only occasionally. The geographic, social and economic stability of these regions are strongly influenced by the keeping of ruminants, particularly for marking milk production. The products from

ruminants are unique, especially with regard to providing high quality nutrition to consumers. Many of the milk products and specialties can be included among the most important functional foods [16].

Mastitis is considered to be the most frequent and most costly production disease in dairy herds. Mastitis is characterized by an inflammation in one or more quarters of the udder and can be either clinical or subclinical. The decrease in milk production per cow due to the clinical and subclinical prevalence of mastitis is usually recognised as the main cause of economic losses due to the disease [4, 5, 6].

The factors influencing the susceptibility of the mammary gland to infections are: the presence of bacteria at the teat end, level of efficacy of the protective characteristics of the teat canal, and defence mechanisms in the udder (Fig. 1) [11].

Contagious mastitis is caused by organisms transmitted from cow to cow; the primary reservoir of which is the cow itself. The predominant contagious pathogens involved in bovine mastitis are *Staphylococcus* spp. (*S. aureus* and *S. epidermidis*) [9, 12], *Streptococcus* spp. (*Str. agalactiae*, *Str. dysgalactiae*, *Str. uberis* and *Str. bovis*), coliforms (mainly *E. coli* and *Klebsiella pneumoniae*), and *Enterobacter aerogenes* [14, 15].

Clinical cases give rise to visible symptoms such as swelling, heat, pain in the affected quarters or clots and discolouration in the secretions. Losses caused by clinical mastitis include: reduced milk yield and quality, costs of veterinary care, discarded milk and shortening of productive life [2, 5]. Cows with subclinical mastitis do not show a visible udder inflammation and can be diagnosed by somatic cell count (SCC) and by detection of the presence

of the pathogens. The economic losses are more associated with sub-clinical mastitis which is 40% more prevalent than clinical mastitis. However, the cost of treatment of sub-clinical mastitis is much lower compared to that of clinical mastitis, accounting for 10–20 times higher [5].

The aim of this study was to evaluate, during early lactation, the prevalence and aetiological agents in two herds of dairy cows situated in the marginal parts of Slovakia.

## MATERIALS AND METHODS

### Animals and milking

The study was conducted in accordance with good veterinary practice. The practical part of the study was carried out on two farms situated in marginal parts of Slovakia (Orava and Zemplín). On the first farm (A) we investigated 150 Slovak spotted breed cows and on the second (B) 380 dairy cows of the Holstein breed, between second and fourth lactations. The dairy cows on both farms were kept in a free housing system with individual boxes with bedding and ad libitum access to water and a separate calving barn. The keeping of cows corresponded to standard animal hygiene rules. Both herds were fed a total mixed rations based on grass silage, maize silage and concentrates.

The cows from both herds were milked twice daily, herd A in a tandem parlour DeLaval 2x5 (Tumba, Sweden) and herd B in a parallel parlour Boumatic 2x12 Xpressway (Wisconsin, USA). The average milk yield was 6800 l and 7400 l per year in herds A and B, respectively. Blanket dry cow therapy (treatment of all quarters of all cows) was implemented in both herds.

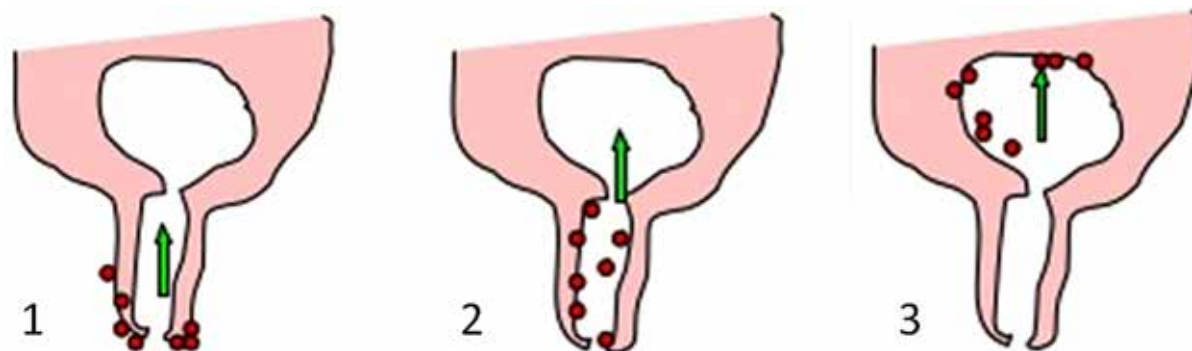


**Fig. 1. Process of udder infection**

1 — Organisms invade the udder through teat canal; 2 — Migrate up the teat canal and colonize the secretory cells; 3 — Colonized organisms produce toxic substances harmful to the milk producing cells. Source: Jackson and Cockcroft [3]

**Table 1. CMT scores related to average somatic cell counts 2120 (11 rejected) quarters**

CMT Score	SCC	% of quarters	Interpretation*
N (Negative)	0—200 × 10 <sup>3</sup>	63.2	Healthy quarter
T (Trace)	200—400 × 10 <sup>3</sup>	23.3	Subclinical mastitis
1	400—1000 × 10 <sup>3</sup>	6.5	Subclinical mastitis
2	1 000—3000 × 10 <sup>3</sup>	4.6	Serious mastitis Infection
3	Over 3000 × 10 <sup>3</sup>	2.0	Serious mastitis infection

\* — Jackson and Cockcroft [3]

**Table 2. Prevalence of mastitis in the quarters of the herds**

Herd	No. of examined cows	No. of examined quarters	Healthy quarters		Rejected quarters	Positive quarters		Infected quarters	
			n	%		n	%	n	%
A	226	904	484	60.7	4	416	46.2	312	34.7a
B	304	1216	862	66.2	7	354	29.3	227	18.8b
<b>Total</b>	<b>530</b>	<b>2120</b>	<b>1346</b>	<b>63.5</b>	<b>11</b>	<b>770</b>	<b>36.3</b>	<b>539</b>	<b>25.6</b>

a, b, c— values within the same column with different superscript letters differ significantly at P &lt; 0.05

**Table 3. Microorganisms isolated from mastitis in the herds**

Isolated microorganisms	n	Subclinical		Subacute		Acute	
		A %	B %	A %	B %	A %	B %
<i>Staph. aureus</i>	41	9.8	4.9	31.7	17.1	22.0	14.6
<i>Str. uberis</i>	17	11.8	-	47.1	-	41.2	-
<i>Str. agalactiae</i>	62	14.5	6.5	38.7	11.3	22.6	6.5
<i>Streptococcus</i> spp.*	55	14.5	12.7	38.2	11.0	-	7.3
CONS*	141	35.5	23.4	19.9	12.1	5.0	4.3
CPS*	24	37.5	16.7	33.3	20.8	-	-
<i>E. coli</i>	36	44.4	25	19.4	11.1	-	-
<i>Enterococcus</i> spp.	75	62.7	37.3	12	20	-	-
<i>Bacillus</i> spp.	48	43.8	20.8	25	2.1	-	8.3
<i>Enterobacter aerogenes</i>	17	64.7	35.3	47.1	-	-	11.8
Other*	23	56.5	34.7	8.6	-	-	-
<b>Total</b>	<b>539</b>	<b>35.3</b>	<b>20.6</b>	<b>26.3</b>	<b>11.5</b>	<b>6.9</b>	<b>4.1</b>

n — number of isolated bacteria; Other\* — *Proteus* spp., *Aerococcus* spp.; CPS\* — *S. aureus*, *S. hyicus*; *Streptococcus* spp. \* — *Str. faecalis*, *Str. dysgalactiae*, *Str. Suis*; CONS\* — *S. haemolyticus*, *S. chromogenes*, *S. xylosum*, *S. epidermidis*, *S. warneri*

### Collection of samples and laboratory analyses

Double milk samples were collected aseptically from 2120 quarters (530 cows) during the first month of lactation. Eleven quarters were atrophic. The teats were cleaned and the first few streams were discarded. The teats were then dipped in a disinfectant and the teat ends were wiped with alcohol swabs and allowed to dry. Then 10 ml of the milk was collected into sterile tubes. The samples were cooled and immediately transported to the laboratory. The SCC were analysed in a commercial laboratory using a MilkoScan FT2 (Foss Electric, Hillerod, Denmark).

The bacteriological examinations were performed according to commonly accepted rules [6]. Milk samples (0.05 ml) were inoculated onto blood agar (Oxoid, UK) and cultivated at 37°C for 24 h. Based on the colony morphology and Gram staining, *Staphylococcus* spp. bacteria were selected for the tube coagulase test (Staphylo PK, ImunaPharm, Slovakia). Suspected colonies of *Staphylococcus* spp., *Streptococcus* spp. and *Enterobacteriaceae* spp. were isolated on blood agar, cultivated at 37°C for 24 h and identified biochemically using the STAPHY-test, STREPTO-test, or ENTERO-test, using software TNW Pro 7.0 (Erba-Lachema, Czechia).

Individual forms of mastitis (subclinical, subacute and acute) based on clinical signs, CMT scores, SCC and bacteriological examination of milk samples were classified according to Vasiľ et al. [14].

### Statistical analysis

The statistical analysis was performed using Graph-Pad PRISM 6.0 (GraphPad Software Inc., USA). The differences in incidence of mastitis among the herds were statistically analysed using the Chi-square test. The level of significance was set at  $P < 0.05$ .

### RESULTS

The results obtained by the California mastitis test (CMT) are presented in Table 1. The elevation of SCC to the level below 200 000 ml<sup>-1</sup> was detected in 63.2% quarters on average. The average score (>1) of CMT above 400 000 ml<sup>-1</sup> was detected in 13.1% of the quarters. The prevalence of mastitis in the herds of dairy cows (A and B) was 34.7% and 18.8%, respectively.

The differences in the prevalence of subclinical and clinical forms of mastitis in the quarters between herds were statistically significant ( $P < 0.05$ ). The prevalence of subclinical mastitis in the quarters of the two herds (A, B) reached 35.3% and 20.6% and of clinical mastitis 14.6% and 6.8%, respectively (Table 2).

The microorganisms isolated from mastitis in the herds are presented in Table 3. Pathogenic bacteria were isolated from 25.6% of the quarters with subclinical (14.2%), and (12.4%) with clinical mastitis. The aetiological agents of mastitis detected most frequently were CoNS, *Str. agalactiae*, *Str. uberis*, *Enterococcus* spp. and *Bacillus* spp. *Staphylococci* were the main aetiological agents of the intramammary infections (IMI) in the dairy herds and *Staph. Aureus*, *Str. uberis* and *Str. agalactiae* were the most frequent isolate from the clinical mastitis cases. In both herds, subclinical mastitis was caused mainly by *Enterococcus* spp., *Enterobacter aerogenes* and CoNS.

### DISCUSSION

Bovine mastitis, as a major disease affecting dairy cattle worldwide, involves inflammation of the mammary gland [1]. Mastitis affects the milk quality and production of the cow and may spread to other cows in the herd. The severity of the inflammation can be classified as subclinical, clinical and chronic forms, and its degree is dependent on the nature of the causative pathogen and on the age, breed, immunological health and lactational status of the animal [4, 5].

Over 135 different organisms have been identified as the causative agents of bovine mastitis, including bacteria, viruses, mycoplasma, yeasts and algae [10]. In the present study, most of the mastitis cases were caused by CoNS and *Streptococcus* spp. Similar results were obtained in Poland by Malinowski et al. [6] and in Finland by Taponen et al. [12].

In our study the CoNS belong among the organisms most commonly isolated from milk samples of dairy cows with subclinical mastitis as in other studies [1, 8, 9].

In the Netherlands, the prevalence of CoNS among bacterial isolates from milk samples increased from 16.2% in 1999 to 42.2% in 2004 for subclinical mastitis, and from 7.3% to 14.1% for clinical mastitis [10].

In New Zealand, as in the UK, *Str. uberis* was the most common pathogen associated with clinical mastitis, but in

contrast to the situation in the UK, *E. coli mastitis* was rarely observed [7]. In Norway, neither *Str. uberis* nor *E. coli* were commonly found. Rather, *S. aureus* and *Str. dysgalactiae* were the most common causes of clinical mastitis there [17]. The main pathogen associated with clinical mastitis in the Netherlands were CPS followed by *Str. dysgalactiae*, *Str. uberis* and *E. coli* [10]. IMI caused by *Strep. dysgalactiae* and mycoplasma were of major concern in the USA [3].

Coagulase-positive staphylococci (CPS) are permanently present in dairy herds. In our study, *S. aureus* and *S. hyicus* were isolated from 4.5% of the quarters with subacute and acute forms of mastitis. Similar results were obtained by Malinowski et al. [5], who found *Staph. aureus* in 5.1% of the cases of clinical and subclinical mastitis in the western part of Poland. This is in accordance with the data from other countries [11, 13].

## CONCLUSIONS

The results of our study showed that the average prevalence of mastitis in two dairy herds (A and B) situated in marginal parts of Slovakia reached 14.1% and 30.1%, respectively. The bacteria *Staph. aureus*, *Str. agalactiae* and *Str. uberis* were most frequently isolated from clinical mastitis. The CoNS were the pathogens most frequently isolated from subclinical mastitis cases. The pathogens *Str. agalactiae* and *Staph. aureus* played an important role in dairy herds in the marginal parts of Slovakia.

A successful mastitis control programme should focus on the management of dry and calving cows and heifers. A clean and comfortable environment, proper feeding and adequate supplementation of the diet with vitamins and trace elements are essential for maintaining good udder health.

## ACKNOWLEDGEMENT

*This study was supported by the project VEGA No. 1/0510/16.*

## REFERENCES

- Bradley, A. J., Leach, K. A., Breen, J. E. et al., 2007: Survey of the incidence and aetiology of mastitis on dairy farms in England and Wales. *Vet. Rec.*, 160, 253–257.
- Fox, L. K., Kirk, J. H., Britten, A., 2005: *Mycoplasma mastitis*: a review of transmission and control. *Jour. Vet. Med. Infect. Dis.*, 52, 153–60.
- Jackson, P., Cockcroft, P., 2002: *Clinical Examination of Farm Animals*. Oxford, UK, Blackwell Science Ltd, Wiley-Blackwell, 154–166.
- Malinowski, E., 2000: Mastitis prophylaxis and treatment during dry period – advantages and threats. *Medycyna Weterynaryjna*, 56, 759–763.
- Malinowski, E., Gajewski, Z., 2009: Characteristics of cows mastitis caused by human foodborne pathogens. *Życie Weterynaryjne*, 84, 290–294.
- Malinowski, E., Lassa, H., Kłossowska, A., Smulski, S., Markiewicz, H., Kaczmarowski, M., 2006: Etiological agents of dairy cows' mastitis in western part of Poland. *Pol. J. Vet. Sci.*, 9, 191–194.
- McDougall, S., 2003: Intramammary treatment of clinical mastitis of dairy cows with a combination of lincomycin and neomycin, or penicillin and dihydrostreptomycin. *N. Z. Vet. J.*, 51, 111–116.
- Østerås, O., Sølvørød, L., Reksen, O., 2006: Milk culture results in a large Norwegian survey-effects of season, parity, days in milk, resistance, and clustering. *J. Dairy Sci.*, 89, 1010–1023.
- Pyörälä, S., Taponen, S., 2009: Coagulase-negative staphylococci – emerging mastitis pathogens. *Vet. Microbiol.*, 134, 3–8.
- Sampimon, O. C., Vernooij, J. C., Mevius, D. J., et al., 2007: Sensitivity to various antibiotics of coagulase-negative staphylococci isolated from samples of milk from Dutch dairy cattle (In Dutch, English summary). *Tijdschr. Diergeneesk.*, 132, 200–204.
- Sumathi, B. R., Veeragowda, B., Amitha, R. G., 2008: Prevalence and antibiogram profile of bacterial isolates from clinical bovine mastitis. *Vet. World*, 1 237–238.
- Taponen, S., Koort, J., Björkroth, J., Saloniemä, H., Pyörälä, S., 2007: Bovine intramammary infections caused by coagulase-negative staphylococci may persist throughout lactation according to amplified fragment length polymorphism based analysis. *J. Dairy Sci.*, 90, 3301–3307.

13. Tenhagen, B. A., Koster, G., Wallmann, J., Heuwieser, W., 2006: Prevalence of mastitis pathogens and their resistance against antimicrobial agents in dairy cows in Brandenburg, Germany. *J. Dairy Sci.*, 89, 2542–2551.
14. Vasiľ, M., Elečko, J., Farkašová, Z., Bireš, J., 2009: The reduction on the occurrence of mastitis in dairy herd using the innovation of housing conditions, sanitary of milk storage and applying the therapy of mastitis during the lactation. *Folia Vet.*, 53, Suppl. II, 186–189.
15. Vasiľ, M., 2004: To know the etiology of mastitis in the herd (In Slovak, English summary). *Slovenský Chov*, 9, 20–22.
16. Vršková, M., Tančin, V., Kirchnerová, K., Sláma, P., 2015: Evaluation of daily milk production in Tsigai ewes by somatic cell count. *Potravinárstvo*, 9, 206–210.
17. Whist, A. C., Østerås, O., Sølvørød, L., 2007: *Streptococcus dysgalactiae* isolates at calving and lactation performance within the same lactation. *J. Dairy Sci.*, 90, 766–778.

*Received September 12, 2017*

*Accepted October 16, 2017*